AD_____

Award Number: W81XWH-10-1-0425

TITLE: Improve T Cell Therapy in Neuroblastoma

PRINCIPAL INVESTIGATOR: Gianpietro Dotti, M.D.

CONTRACTING ORGANIZATION: Baylor College of Medicine
Houston, TX 77030

REPORT DATE: July 2012

TYPE OF REPORT: Annual

PREPARED FOR: U.S. Army Medical Research and Materiel Command
Fort Detrick, Maryland 21702-5012

DISTRIBUTION STATEMENT: Approved for Public Release;
Distribution Unlimited

REPORT DOCUMENTATION PAGE

Form Approved
OMB No. 0704-0188

1. REPORT DATE	2. REPORT TYPE	3. DATES COVERED
July 2012	Annual	1 July 2011 – 30 June 2012

4. TITLE AND SUBTITLE

Improve T cell therapy in neuroblastoma

5a. CONTRACT NUMBER

5b. GRANT NUMBER
W81XWH-10-1-0425

5c. PROGRAM ELEMENT NUMBER

6. AUTHOR(S)

Dotti, Gianpietro, MD

E-Mail: gdotti@bcm.tmc.edu

5d. PROJECT NUMBER

5e. TASK NUMBER

5f. WORK UNIT NUMBER

7. PERFORMING ORGANIZATION NAME(S) AND ADDRESS(ES)

Baylor College of Medicine
One Baylor Plaza
Houston, TX 77030

8. PERFORMING ORGANIZATION REPORT NUMBER

9. SPONSORING / MONITORING AGENCY NAME(S) AND ADDRESS(ES)
U.S. Army Medical Research and Materiel Command
Fort Detrick, Maryland 21702-5012

10. SPONSOR/MONITOR'S ACRONYM(S)

11. SPONSOR/MONITOR'S REPORT NUMBER(S)

12. DISTRIBUTION / AVAILABILITY STATEMENT
Approved for Public Release; Distribution Unlimited

13. SUPPLEMENTARY NOTES

14. ABSTRACT

Neuroblastoma (NB) is the most common malignant extracranial tumor of childhood. Since NB appears susceptible to immunotherapies that include monoclonal antibodies and T-cell immune responses elicited by tumor vaccine, we have combined the beneficial effects of both humoral and cell-mediated components of the anti tumor response. We demonstrated indeed that adoptive transfer of Epstein-Barr-virus (EBV)-specific cytotoxic T lymphocytes (EBV-CTLs) genetically modified to express a chimeric antigen receptor (CAR-GD2) targeting the GD2 antigen expressed by neuroblasts persist in the peripheral blood and induce objective tumor responses (including complete remissions). We will now augment the expansion and survival of CAR-GD2 modified EBV-CTLs by coexpressing the IL-7Rα that restores their capacity to respond to homeostatic IL-7. We will also enhance the capacity of these cells to invade solid tumor masses by expressing heparanase (HPSE) that disrupts the non-cellular stromal elements of NB. Experiments will be conducted in vitro and in vivo in a xenograft mouse model.

15. SUBJECT TERMS
Neuroblastoma, immunotherapy, chiemric antigen receptor, GD2 antigen, heparanase, regulatory T cells, tumor stroma.

16. SECURITY CLASSIFICATION OF:			17. LIMITATION OF ABSTRACT	18. NUMBER OF PAGES	19a. NAME OF RESPONSIBLE PERSON
a. REPORT	b. ABSTRACT	c. THIS PAGE			USAMRMC
U	U	U	UU	40	19b. TELEPHONE NUMBER *(include area code)*

Table of Contents

Introduction. In our recent Phase I study we found that the adoptive transfer of Epstein-Barr-virus (EBV)-specific cytotoxic T lymphocytes (EBV-CTLs) genetically modified to express a chimeric antigen receptor (CAR-GD2) targeting the GD2 antigen expressed by neuroblasts, can persist in the peripheral blood for 6 weeks and induce objective tumor responses (including complete remission) or tumor necrosis in 4/8 subjects with refractory/relapsed NB[1]. Although encouraging, this study also revealed that the signal from the transgenic CTLs progressively declined over time in the majority of patients[1;2] suggesting that the anti tumor effects of these cells could be augmented by prolonging the survival and effector function of the transgenic CTLs, for example by restoring their responsiveness to homeostatic cytokines such as IL-7[3] and inducing a robust $CD8^+$ T cell memory response[4]. Our second approach aims to disrupt the non-cellular stromal elements of NB that may impede access to CAR-modified EBV-CTLs. The ability of tumor-specific CTLs to cross tumor blood vessels is crucial for reaching the tumor cells. Leukocyte extravasation is highly dependent upon the degradation of the components of the subendothelial basement membrane (SBM) and the extracellular matrix (ECM) such as heparan sulfate proteoglycans (HSPGs), fibronectin and collagen[5]. Heparanase (HPSE) is the only known mammalian endoglycosidase degrading HSPGs at distinct HS intra-chain sites[5;6]. Although HPSE is expressed in activated $CD4^+$ lymphocytes, neutrophils, monocytes and B lymphocytes[5;7;8] we have found it to be deficient in cultured T cells and EBV-CTLs.

Key research accomplishments

In Task 1 we proposed to co-express CAR-GD2 and IL-7Rα in EBV-CTLs to improve their expansion and anti tumor effects in response to IL-7, whilst avoiding the expansion of regulatory T cells (Treg) (time frame months 1-24).

- In this task we have optimized the condition to isolate and expand human Tregs. We found that although expanded Tregs preserve inhibitory function, *ex vivo* expanded Tregs have mutated chemokine receptor profile that affects their migration capacity. In particular, they retain CCR7 expression but lack the expression of CCR4 and CCR5 receptors. As a consequence expanded Tregs have impaired capacity to migrate towards the specific chemokine TARC (CCL17), RANTES (CCL5) and MIP-1α (CCL3). The results of this optimization have been published in Journal of Immunotherapy[9].

- We found that Tregs inhibits the anti-tumor activity of EBV-CTLs expressing the CAR-GD2. However, when CTLs are genetically modified to coexpress CAR-GD2 and IL-7Rα, these cells respond to IL-7 and became resistant to the inhibitory effects of Tregs unlike CTLs exposed to IL-2 (manuscript in preparation).

- Achievement of objective clinical responses in neuroblastoma patients receiving CAR-GD2-modified CTLs is strictly related to the *in vivo* survival of adoptively transferred CTLs. Experiments in mice and in nonhuman primates suggest that the infusions of tumor- or virus-specific T cells with T_N or T_{CM} phenotype have superior survival and anti-tumor or anti-viral effects as compared to effector-memory T cells (T_{EM})[10;11]. CAR^+ CTLs generated with our current protocol are mainly represented by T-effector cells (T_E) or T_{EM} cells, characterized by CD45RO expression and low or absent expression of the lymphoid trafficking molecules CD62L and CCR7[1;2]. Obtaining CAR^+ T cells enriched in T_N or T_{CM} cells remains of crucial importance to enhance their persistence *in vivo*. We have found that a significant fraction of human T lymphocytes preserve their naïve phenotype when activated *in vitro* in the presence of glycogen synthase kinase-3β inhibitor (TWS119) that activates the Wnt signaling. Importantly, these cells can be engineered to express a CAR using a lentivirus so that this approach can be exploited to generate CAR^+ T cells enriched in T_N or T_{CM} for clinical use. Thus the activation of Wnt signaling pathway by GSK3β inhibitor during the generation of CAR^+ CTLs will enrich them with T_N and/or T_{CM} cells and enhance their persistence *in vivo*. The results of the experiments performed in this task have been published in Journal of Immunology[12].

- In addition to CAR-GD2 modified CTLs, Vα24-invariant NKT cells inhibit neuroblastoma growth by targeting tumor-associated macrophages (TAMs). In collaboration with Dr Metelitsa we found that neuroblastoma cell lines and primary tumors expresses membrane-bound TNF-α (mbTNF-α) that induces the production of the chemokine CCL20 from TAMs via activation of the NF-κB signaling

pathway. Importantly this effect is amplified in hypoxia. We found that hypoxia impaired NKT cell viability and function, and that IL-15 protected antigen-activated NKT cells from hypoxia, and transgenic expression of IL-15 in adoptively transferred NKT cells dramatically enhanced their antimetastatic activity in mice. The results of the experiments performed in this task have been published in Journal of Clinical Investigation[13].

Task 2. To evaluate the contribution of IL-7Rα ligation and co-stimulation from viral-infected target cells on the development of long-lived memory CAR-GD2-mofied EBV-CTLs in a humanized SCID mouse model previously engrafted with human hematopoietic stem cells (time frame months 12-48).

- In the first set of experiments in vivo we found that the engraftment of CTLs in humanized mice is relatively poor. As mentioned in the potential problems and solution of the original application, we hypothesize that CTLs need to be restimulated *in vivo* to enhance the generation of central memory CTLs. For these reason, we generated artificial antigen presenting cells (aAPCs) expressing CD40L and OX40L to boost in vivo adoptively transferred CTLs.
- We found that aAPC can efficiently be used in vitro to boost virus-specific CTLs.
- Preliminary experiments in vivo also indicate that aAPC can boost virus-specific CTLs.

Task 3: To co-express CAR-GD2 and HPSE in EBV-CTLs and determine the consequent modulation of NB tissue infiltration and killing (time frame 1-48).

- Leukocyte extravasation in response to inflammation has been extensively studied. It is highly dependent upon the degradation of the components of the subendothelial basement membrane (SBM) and the extracellular matrix (ECM) such as heparan sulfate proteoglycans (HSPGs), fibronectin and collagen. Heparanase (HPSE) is the only known mammalian endoglycosidase degrading HSPGs at distinct HS intra-chain sites.
- We found that while freshly isolated CD4 and CD8 T lymphocytes express HPSE and efficiently invade the extracellular matrix, HPSE expression is lost in expanded T lymphocytes used for adoptive immunotherapy. As a consequence these cells show impaired capacity to invade the extracellular matrix.
- Expression of HPSE can be restored in expanded T lymphocytes by retroviral gene transfer.
- Genetically modified T cells and freshly isolated T cells equally invade the Matrigel layer.
- We have then generated a bicistronic vectors encoding both HPSE and CAR-GD2. We found that T cells genetically modified with this novel vector show enhanced invasion capacity and anti-tumor activity as compared to T cells expressing only the CAR-GD2 when the antitumor effects are measured against neuroblastoma cells surrounded by Matrigel.
- Preliminary experiments in vivo indicate that T cells coexpressing both HPSE and CAR-GD2 have enhanced anti-tumor activity.

Reportable outcomes

1 Muralidharan S, Hanley P, Liu E, Chakraborty R, Bollard C, Shpall E, Rooney C, Savoldo B, Rodgers J, **Dotti G**. Activation of Wnt Signaling Arrests Effector Differentiation in Human Peripheral and Cord Blood-Derived T Lymphocytes. J Immunol. 2011 Nov 15;187(10):5221-32.

2 Chakraborty R, Rooney C, **Dotti G**, Savoldo B. Changes in chemokine receptor expression of regulatory T cells after ex vivo culture. J Immunother. 2012 May;35(4):329-36.

3 Liu D, Song L, Wei J, Courtney AN, Gao X, Marinova E, Guo L, Heczey A, Asgharzadeh S, Kim E, **Dotti G**, Metelitsa LS. IL-15 protects NKT cells from inhibition by tumor-associated macrophages and enhances antimetastatic activity. J Clin Invest. 2012 Jun 1;122(6):2221-33.

Reference List

1. Pule MA, Savoldo B, Myers GD et al. Virus-specific T cells engineered to coexpress tumor-specific receptors: persistence and antitumor activity in individuals with neuroblastoma. Nat.Med. 2008;14:1264-1270.

2. Louis CU, Savoldo B, Dotti G et al. Antitumor activity and long-term fate of chimeric antigen receptor-positive T cells in patients with neuroblastoma. Blood 2011;118:6050-6056.

3. Vera J, Savoldo B, Vigouroux S et al. T lymphocytes redirected against the kappa light chain of human immunoglobulin efficiently kill mature B lymphocyte-derived malignant cells. Blood 2006;108:3890-3897.

4. Buentke E, Mathiot A, Tolaini M et al. Do CD8 effector cells need IL-7R expression to become resting memory cells? Blood 2006;108:1949-1956.

5. Parish CR. The role of heparan sulphate in inflammation. Nat.Rev.Immunol. 2006;6:633-643.

6. Edovitsky E, Elkin M, Zcharia E, Peretz T, Vlodavsky I. Heparanase gene silencing, tumor invasiveness, angiogenesis, and metastasis. J.Natl.Cancer Inst. 2004;96:1219-1230.

7. de Mestre AM, Staykova MA, Hornby JR, Willenborg DO, Hulett MD. Expression of the heparan sulfate-degrading enzyme heparanase is induced in infiltrating CD4+ T cells in experimental autoimmune encephalomyelitis and regulated at the level of transcription by early growth response gene 1. J.Leukoc.Biol. 2007;82:1289-1300.

8. de Mestre AM, Soe-Htwe T, Sutcliffe EL et al. Regulation of mouse Heparanase gene expression in T lymphocytes and tumor cells. Immunol.Cell Biol. 2007;85:205-214.

9. Chakraborty R, Rooney C, Dotti G, Savoldo B. Changes in chemokine receptor expression of regulatory T cells after ex vivo culture. J.Immunother. 2012;35:329-336.

10. Gattinoni L, Klebanoff CA, Palmer DC et al. Acquisition of full effector function in vitro paradoxically impairs the in vivo antitumor efficacy of adoptively transferred CD8+ T cells. J.Clin.Invest 2005;115:1616-1626.

11. Gattinoni L, Zhong XS, Palmer DC et al. Wnt signaling arrests effector T cell differentiation and generates CD8+ memory stem cells. Nat.Med. 2009;15:808-813.

12. Muralidharan S, Hanley PJ, Liu E et al. Activation of wnt signaling arrests effector differentiation in human peripheral and cord blood-derived T lymphocytes. J.Immunol. 2011;187:5221-5232.

13. Liu D, Song L, Wei J et al. IL-15 protects NKT cells from inhibition by tumor-associated macrophages and enhances antimetastatic activity. J.Clin.Invest 2012;122:2221-2233.

Changes in Chemokine Receptor Expression of Regulatory T Cells After Ex Vivo Culture

Rikhia Chakraborty, Cliona Rooney,*†‡ Gianpietro Dotti,*‡§ and Barbara Savoldo*†*

Summary: By controlling and limiting inflammatory conditions, naturally occurring regulatory T cells (Tregs), defined as circulating $CD4^+CD25^{bright}FoxP3^+$ cells, play critical roles in maintaining tolerance and preventing autoimmunity and thus have tremendous potential for adoptive immunotherapy. Because they represent a scanty subset of the $CD4^+$ T-lymphocyte subset, several approaches have been developed to isolate and expand ex vivo polyclonal Tregs. However, one limitation of the functional analyses performed on these cultured Tregs is the incomplete characterization of their tissue-trafficking properties. As this aspect provides crucial information for their therapeutic effects, we have here explored the chemokine receptor expression profile and function of Tregs cultured ex vivo with validated expansion protocols. Our data show that ex vivo cultured Tregs retained the expression of CCR7 but dramatically downregulated CCR5 as compared with freshly isolated Tregs. The differential chemokine receptors expression pattern corroborated with their respective steady state messenger RNA expression and also with their migration toward specific chemokines. Our analyses suggest that ex vivo cultured Tregs may display impaired or suboptimal migration to the inflamed tissues releasing RANTES and MIP-1α chemokines.

Key Words: Tregs, rapalog, chemokine

(*J Immunother* 2012;35:329–336)

$CD4^+CD25^+FoxP3^+$ regulatory T cells (Tregs) play a crucial role in controlling and limiting the inflammatory milieu[1] through suppression of cytokine production and inhibition of T-cell proliferation.[2] Transfer of T cells depleted of the $CD4^+CD25^+$ subset into neonatal thymectomized mice results in the onset of systemic autoimmune diseases, such as colitis, gastritis, insulin-dependent autoimmune diabetes, and thyroiditis.[3] These inflammatory conditions are then strongly attenuated when $CD4^+CD25^+$ Tregs are cotransferred with T-effector (Teff) cells.[3,4] Several evidences also correlate the emergence of human diseases such as multiple sclerosis, rheumatoid arthritis, type 1 diabetes, inflammatory bowel disease, and autoimmune lymphoproliferative syndrome with either decreased frequencies or defective suppressive function of Tregs.[5,6]

The central role of Tregs in modulating inflammatory processes has led to a quest for novel therapies based on the adoptive transfer of these cells to treat a variety of immunologic disorders, ranging from autoimmunity to transplantation, allergy, and asthma.[7] However, the clinical translation of the promising results obtained in preclinical models[8] requires the selection and ex vivo expansion of large numbers of Tregs, because this T-cell subset represents $<5\%$ of the $CD4^+$ T cells circulating in the peripheral blood of healthy subjects.[9]

Circulating naturally occurring Tregs (nTregs) can be isolated by using a 2-step magnetic cell separation that takes advantage of their constitutive coexpression of the CD25 and CD4 cell-surface markers.[10] These $CD25^{bright}$ $CD4^+$ cells can then be expanded ex vivo by stimulation through their T-cell receptor (TCR) using a variety of tools, including monoclonal antibodies or coated Xcyte beads,[11] irradiated $CD4^+CD25^-$ feeder cells,[12] and cytokines such as interleukin-2 (IL-2).[13] T-cell products obtained using these methodologies usually retain immunosuppressive capacity but are frequently contaminated with Teff cells expressing CD25 and expanding in response to TCR stimulation and IL-2. To overcome this limitation, rapamycin analogs (rapalogs) have been added to these cultures to inhibit the growth of contaminating Teff cells while preferentially promoting Treg expansion.[14]

Although the isolation and expansion of functional inhibitory Tregs is feasible, therapeutic strategies using Tregs have to take into account that these cells not only require potent suppressive function but also need appropriate tissue trafficking to enable contact with their target cells. A fraction of expanded Tregs must retain the expression of molecules such as CD62L and CCR7 that are crucial for their migration to the lymph nodes-draining inflamed tissues where they can block the activation and expansion of reactive or autoreactive Teff cells.[15] However, Tregs must also migrate directly to the inflammation sites to locally contain the inflammation.[16] Because distinct chemokine axis are involved in regulating the recruitment of T lymphocytes and Tregs to maintain tissue homeostasis,[17] we have investigated the chemokine receptor profile of freshly isolated nTregs and compared it with that of ex vivo cultured Tregs, in order to discover whether and how culture conditions affect this expression pattern. This analysis is vital, as modifications in Treg-migration properties would have important implications for their clinical use.

MATERIALS AND METHODS

Blood Samples

Peripheral blood was obtained from buffy coat preparations derived from 9 healthy volunteer donors (Gulf Coast Regional Blood Center, Houston, TX).

Cell Isolation and In Vitro Expansion Protocols

Peripheral blood mononuclear cells (PBMCs) were separated by density-gradient centrifugation over Lymphoprep (AXIS-SHIELD PoC AS, Oslo, Norway).

Received for publication August 29, 2011; accepted March 7, 2012.

From the *Center for Cell and Gene Therapy; Departments of †Pediatrics; ‡Immunology; and §Medicine, Baylor College of Medicine, Methodist Hospital and Texas Children's Hospital, Houston, TX.

Reprints: Barbara Savoldo, Center for Cell and Gene Therapy, Baylor College of Medicine, 6621 Fannin St./MC 3-3320, Houston, TX 77030 (e-mail: bsavoldo@bcm.tmc.edu).

Supplemental Digital Content is available for this article. Direct URL citations appear in the printed text and are provided in the HTML and PDF versions of this article on the journal's Website, www.immunotherapy-journal.com.

eTregs Expansion

nTregs ($CD4^+CD25^{bright}$) were isolated from PBMCs using positive selection, after labeling cells with CD25 magnetic beads (2 μL/10^7 cells; Miltenyi Biotec Inc., Auburn, CA), followed by selection of $CD4^+$ cells with CD4 MicroBeads (20 μL/10^7 cells; Miltenyi) as previously described (Fig. 1A).[18] Supplementary Figure 1A (Supplementary Digital Content 1, http://links.lww.com/JIT/A224) and Supplementary Table 1 (Supplementary Digital Content 2, http://links.lww.com/JIT/A225) illustrate the gating used to identify the $CD25^{bright}$ population during our purification step. The mean fluorescence intensity used to denote $CD25^{bright}$ cells was 99–110. The average purity of $CD4^+CD25^{bright}$ T cells was 97% ± 3.4% (n = 9). After selection, $CD4^+CD25^{bright}$ (10^6 cells/mL) were cultured in complete medium consisting of RPMI1640 (Hyclone, South Lorgan, UT), 10% AB-human serum (Valley Biomedical, Winchester, VA), 2 mM L-glutamine (BioWhittaker Inc., Walkersville, MD), and penicillin-streptamycin (BioWhittaker), in the presence of β-mercaptoethanol (Invitrogen, Carlsbad, CA). On day 0, the purified $CD4^+$ $CD25^{bright}$ T cells were activated in 24-well plates coated with anti-CD3 antibody (1 μg/mL) (OKT3, Orthoclone; Cilag Ag Int., Zug, Switzerland) and anti-CD28 mAb (1 μg/mL) (BD Biosciences PharMingen, San Diego, CA) in complete medium ± temsirolimus (LC Laboratories, Woburn, MA) at a final concentration of 1 μg/mL. On days 7 and 14, the cells were harvested, counted, and restimulated with anti-CD3, anti-CD28, ± temsirolimus, plus rIL-2 (50 IU/mL) (Proleukin; Chiron, Emeryville, CA). During the experiment, the cells were restimulated only when cell concentration was $\geq 5 \times 10^6$/mL. At the end of 3 weeks (day 21), cells were harvested, counted, and used for experiments. The expanded Tregs obtained through this protocol were named as eTregs to signify that they have been in vitro expanded from nTregs.

rTregs Expansion

$CD4^+$ T cells were purified from PBMCs by negative selection using the untouched $CD4^+$ T-cell isolation kit (Miltenyi), according to the manufacturer's instructions (Fig. 1B). The average purity of $CD4^+$ T cells was

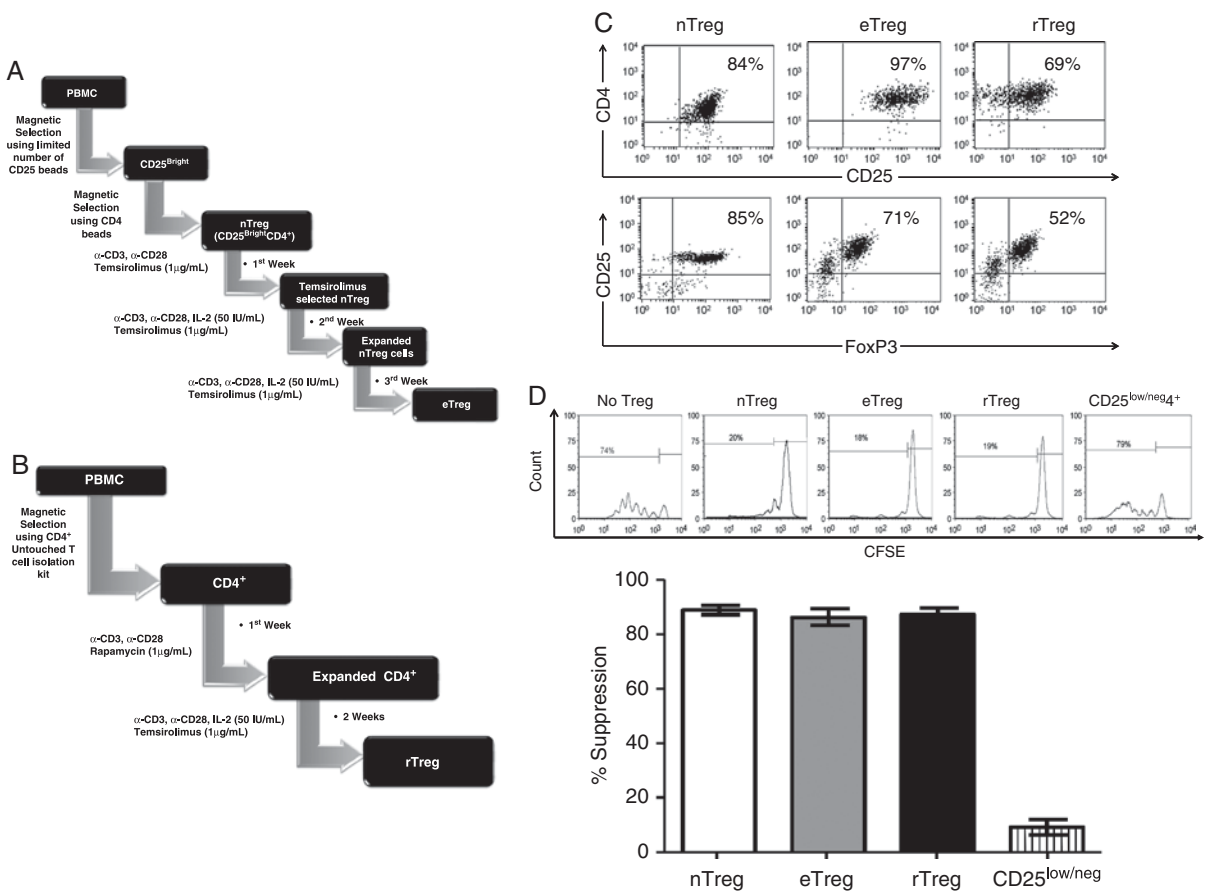

FIGURE 1. Ex vivo culture and functional characterization of freshly isolated and ex vivo expanded Tregs. A, Naturally occurring Tregs (nTregs; $CD4^+CD25^{bright}$) and (B) $CD4^+$ T cells were purified from PBMCs as schematically represented and cultured to obtain eTreg and rTreg, respectively. C, Flow cytometry dot plots of nTregs, eTregs, and rTregs from 1 representative donor, stained with anti-CD4, anti-CD25, and anti-FoxP3 fluorochrome-conjugated mAbs. D, The suppressive activities of nTregs, eTregs, rTregs, and control $CD25^{low/neg}4^+$ T cells were evaluated using a CFSE-based assay in which PBMCs labeled with CFSE were stimulated with irradiated allogeneic feeders and OKT3 in the presence or absence of Tregs. Upper panels illustrate the proliferation of T cells using a CFSE assay in the absence or in the presence of the different Tregs population and for a representative experiment, confirming the inhibitory activity of nTregs, eTregs, and rTregs. The lower graph illustrates the percentage of suppression of T cells in the presence of the different Tregs (n = 9 donors). Data show mean ± SD. CFSE indicates carboxyfluorescein succinimidyl ester; PBMC, peripheral blood mononuclear cell.

92% ± 4.2% (n = 9). Purified CD4$^+$ T cells were cultured in complete medium at 10^6 cells/mL. The in vitro expansion protocol was adapted from a previously described protocol,[19] with slight modification. Briefly, on day 0, the purified CD4$^+$ T cells were activated in 24-well plates coated with anti-OKT3 (1 μg/mL) and anti-CD28 mAb (1 μg/mL) in complete RPMI-1640 ± rapamycin (Sigma, St Louis, MO) at a final concentration of 100 nM. On days 7 and 14, the cells were harvested, counted, and restimulated with anti-OKT3, anti-CD28, ± rapamycin, and recombinant rIL-2 (50 IU/mL). During the experiment, the cells were passaged only when the medium was exhausted (turned yellow) or cell concentration was $\geq 5 \times 10^6$/mL. At the end of 3 weeks (day 21), cells were harvested, counted, and used for experiments. The expanded Tregs obtained through this protocol are named as rTregs to signify that in vitro expanded in the presence of rapamycin.

Phenotypic Analysis

Expression of cell-surface molecules was determined by flow cytometry using a FACSCalibur system (BD Biosciences), equipped with the filter set for quadruple fluorescence signals. The respective mAbs conjugated with phycoerythrin, fluorescein isothiocyanate, allophycocyanin, and/or peridinin chlorophyll proteins were used: CD3, CD4, CD25, CCR1, CCR3, CCR4, CCR5, CCR7, CCR9, CXCR3, and CXCR4. Staining for FoxP3 (eBioscience Inc., San Diego) was performed following manufacturer's instruction. Samples were analyzed using CellQuest Pro software (BD Biosciences). At least 10,000 positive events were measured for surface staining, and 50,000 events were collected for FoxP3 samples.

Suppression Assay

The assay was performed as described previously.[20] Briefly, PBMCs were labeled with 1.5 μM carboxyfluorescein succinimidyl ester (CFSE) (Invitrogen) following the manufacturer's instructions. PBMCs were then stimulated with irradiated (40 Gy) allogeneic PBMCs (at a 4:1 effector/feeders ratio) and 0.5 μg/mL OKT3. To assess their suppressive capacity, Tregs were added to the culture (at a 1:1 or 1:2 ratio). As positive control, we used freshly isolated nTregs. On day 7 of culture, cells were labeled with phycoerythrin-conjugated, peridinin chlorophyll protein-conjugated, or allophycocyanin-conjugated CD4 and CD8 mAbs, and CFSE dilution was analyzed using a FACSCalibur to assess cell proliferation. Suppression was expressed as the percentage of inhibition of T cells proliferation in the presence of the different Treg subsets.

Transwell Migration Assay

Transwell migration assay was performed using the 5-μm pore 24-transwell plates (Corning Life Sciences, Acton, MA), as previously described.[20] The chemoattractant ligands (R&D System) were added to the lower chamber, whereas ^{51}Cr (100 μCi)-labeled Tregs were loaded in the upper chamber. ^{51}Cr-labeled cells, loaded directly into the lower chamber, served as the positive control, whereas lower chambers without any recombinant ligands were used as negative controls. Plates were incubated at 37°C, 5% CO_2 for 4 hours before being assayed for migration. After incubation, the transwell inserts were disposed, and the cells from the lower compartment were recovered and lysed with Triton-X (Sigma-Aldrich). Chromium release was quantified in the lysates using a γ counter (PerkinElmer Life and Analytical Sciences, Waltham, MA). The percentage of migrating cells was calculated as follows: 100 × [cpm from experimental supernatant (cells migrated in the lower chamber) − cpm in the presence of media only (random migration)/cpm of positive control − cpm random migration]. Specificity of the observation was proved by blocking migration of Tregs by addition of the respective blocking antibodies (R&D Systems) or isotype controls (R&D Systems) to the lower chamber before the chemotactic assay.

RNA Isolation and Quantitative Real-time Polymerase Chain Reaction (RT-PCR) Analysis

Total RNA was isolated by extraction with Trizol (Invitrogen) and treated with DNase I (Invitrogen), following the manufacturer's protocols. RNAs were quantitated and checked for integrity and quality by 1% nondenaturing agarose (Sigma) gel. A total of 1 μg of total RNA was subjected to reverse transcription using a QuantiTect reverse transcription reagent kit (Qiagen, Valencia, CA). PCR amplification was carried out using iQ SYBR Green Supermix (Bio-Rad, Hercules, CA) and a C1000 Thermal Cycler (Bio-Rad CFX96 Real-Time System). Primers were designed so as to produce different amplicon sizes for each target gene. Before being used in RT-PCR, each primer pair was authenticated by standard reverse transcription-PCR and by checking the amplicons for the right size. The results were expressed after normalization to β-actin expression levels from 3 different experiments. Data have been represented as mean ± SD. The primer sequences for the different genes were as follows:

CCR1 forward (F), 5′-TGGAACCAGAGAGAAGC CGGGATG-3′;

CCR1 reverse (R), 5′-AAGGCAAACACGGCGTG GAC-3′;

CCR5 (F), 5′-TGTGTAGTGGGATGAGCAGAGA ACA-3′;

CCR5 (R), 5′-AGGCGGGCTGCGATTTGCTT-3′;

CCR7 (F), 5′-CCTTCTGGGCCTACAGCGCG-3′;

CCR7 (R), 5′-TGGTGGTGGTCTCGGCCTCC-3′;

CCR9 (F), 5′-ACACCCACAGACTTCACAAGCC CTA-3′;

CCR9 (R), 5′-TCATGGCCTGGGCAATGGCAAT-3′.

Statistical Analysis

All in vitro experiments were summarized as mean ± SD. Student t test was used to determine the statistical significant differences between samples, with $P < 0.05$ indicating a significant difference.

RESULTS AND DISCUSSION

Rapalog-selection Enriches Functional Tregs

For the current study, we generated Tregs according to 2 different approaches, as detailed in the Materials and Methods section and in the Figures 1A and B. For the first approach, the starting population was represented by naturally occurring CD4$^+$CD25^{bright} cells (nTregs) isolated from the PBMCs of 9 healthy donors, using immunomagnetic selection. Here, Tregs expanded using this protocol will be designated as eTregs (Fig. 1A). For the second approach, the starting cell population was instead represented by CD4$^+$ T cells, also obtained after immunomagnetic selection as previously described.[19] Here, Tregs expanded using this approach will be designated as rTregs (Fig. 1B). First, we identified the rapalog that provided the best expansion rate while preserving suppressive

capacity. As shown in Supplementary Figure 1B (Supplementary Digital Content 1, http://links.lww.com/JIT/A224, eTreg expanded best in the presence of temsirolimus, whereas rTregs had superior expansion in the presence of rapamycin. Next, IL-2 concentrations were determined by using a dose–response curve to evaluate the change in expansion rate. We found that an increase in IL-2 dose was paralleled by an expansion of the cells number (Supplementary Fig. 1C, top panel, Supplementary Digital Content 1, http://links.lww.com/JIT/A224). However, cells that were expanded with >100 IU/mL of IL-2 had significantly reduced suppressive functionality (Supplementary Fig. 1C, middle panel, Supplementary Digital Content 1, http://links.lww.com/JIT/A224) and FoxP3 expression (Supplementary Fig. 1C, bottom panel, Supplementary Digital Content 1, http://links.lww.com/JIT/A224). Similarly, titration experiments with different concentrations of temsirolimus were performed to determine the optimum concentration of the drugs providing expansion without compromising functionality or viability (Supplementary Fig. 2, Supplementary Digital Content 3, http://links.lww.com/JIT/A226). Of note, for rapamycin we used previously validated concentrations.[19]

At the end of the third week of culture, eTregs and rTregs expanded 5 ± 0.6 and 8 ± 0.7, respectively. Phenotypic analyses after 3 weeks of culture showed that 68% ± 4.3% of eTregs and 41% ± 0.3% of rTregs expressed FoxP3 as compared with 72% ± 0.3% of freshly isolated nTregs (Fig. 1C). In contrast, cells expanded using the same protocol in the absence of rapalogs, lost FoxP3 expression by 3 weeks of culture (4% ± 3%), suggesting that in the absence of rapalog, Teff cells preferentially expand (data not shown). The expression of FoxP3 by both eTregs and rTregs paralleled their inhibitory function as assessed in vitro using a CFSE-based suppression assay (Fig. 1D). As expected, proliferation of T lymphocytes in response to OKT3 antibody and allogeneic feeder cells (90% ± 2.5%) was significantly reduced when freshly isolated nTregs were added to the culture (16.4% ± 5.5%, $P < 0.01$), accounting for a suppression of 88.8% ± 1.5% for $CD8^+$ cells ($P < 0.0001$). Similarly, proliferation of T cells was reduced when either eTregs or rTregs were added to the cultures (16.7% ± 6.5% and 16.8% ± 5.8%, respectively, $P < 0.01$), accounting for a suppression of 86.3% ± 3% and 87% ± 2.3% for $CD8^+$ cells, respectively ($P < 0.0001$). In contrast, proliferation of T cells was not significantly changed in the presence of control T cells grown without rapalogs ($CD25^{low/neg}4^+$) (85.1% ± 4.3%), accounting for a suppression of 9% ± 2.8% (P = not significant). Of note, we observe similar suppressions irrespective of the Treg:Teff ratio used in the experiment (Supplementary Fig. 3, Supplementary Digital Content 4, http://links.lww.com/JIT/A227).

Ex Vivo eTregs Show Specific Pattern of Chemokine Receptor Expression

The tissue homing of Tregs is discretely regulated, which in turn dictate where the in vivo suppressive functions are exerted. Hence, we next determined the chemokine receptor expression profile of eTregs and rTregs as compared with freshly isolated nTregs, with the goals of characterizing their homing capacity and predicting their potential trafficking upon adoptive transfer in vivo. As shown in Figures 2A and B, ex vivo expanded Tregs upregulated or downregulated the expression of specific chemokine receptors when compared with freshly isolated nTregs. We found that CXCR4 was upregulated in both eTregs (19.3% ± 4.7%) and rTregs (21.5% ± 1.7%) as compared with nTregs (6.6% ± 1.5%) ($P < 0.05$). In contrast, CCR4 and CCR5 were both significantly downregulated in eTregs (36.3% ± 2.3% and 0.1% ± 0.1%, respectively) and rTregs (15.6% ± 0.7% and 2.3% ± 0.5%, respectively) as compared with nTregs (63% ± 7.2% and 56% ± 6.5%, respectively) ($P < 0.05$). No significant differences were observed in receptors such as CXCR3 (eTregs 11.3% ± 1.5%, rTregs 18.6% ± 1.6%, and nTregs 26.6% ± 2.0%, respectively), CCR1, CCR3, and CCR9 (< 1% in all 3 subsets). As previously described,[21] CCR7 expression (17% ± 4.3% on freshly isolated nTregs) was retained by rTregs (11.5% ± 1.7%) and upregulated by eTregs (37.6% ± 6.4%) ($P < 0.05$).

We next investigated if the observed downregulation of CCR5 expression in eTregs (Fig. 3A) and rTregs (data not shown) was associated with corresponding downregulation of its messenger RNA. As shown in Figure 3A, *CCR5* mRNA levels were significantly reduced (85% ± 0.01% reduction) at the end of week 3 of culture in rapalogs ($P < 0.05$). This indicates that the downregulation of CCR5 expression occurs either at the transcriptional level or at the posttranscriptional level through increased *CCR5* mRNA decay or decreased *CCR5* mRNA half-life. We also performed quantitative RT-PCR studies to monitor the mRNA expression of *CCR7*, *CCR1*, and *CCR9* (Figs. 3B–D, respectively) in nTregs cultured in the presence of rapalogs as compared with nTregs cultured without the rapalog. *CCR7* mRNA expression was 3.2 ± 0.03-fold higher at the end of week 3 of rapalogs treatment ($P < 0.05$). This finding is in line with the slightly enhanced CCR7 expression in eTregs (37.6% ± 6.4%) compared with nTregs (17.0% ± 4.3%) (Fig. 2). As expected, on the basis of phenotypic analyses, the levels of *CCR1* and *CCR9* mRNA were low in both rapalog treated and control cells (Figs. 3C–D). In summary, the overall chemokine receptor expression profile, except for CCR7, in both eTregs and rTregs was similar and showed some critical differences with that of nTregs.

Chemokine Receptor Expression by Tregs Correlates With Their Migratory Capacity

To determine whether the expression of specific chemokine receptors correlated with different functional migration capacity of Tregs, we tested their response to specific ligands with a transwell migration assay and compared it with that of freshly isolated nTregs (Fig. 4).

Expression of CCR7, which plays a crucial role for the homing of T lymphocytes to lymph nodes,[21] was not only retained by rTregs and eTregs (Figs. 2A, B) but was also functional. Indeed, freshly isolated and cultured Tregs migrated toward ELC (CCL19) gradient proportionally to their receptor expression (nTregs 11.6% ± 1.7%, rTregs 11.3% ± 0.7%, and eTregs 75.4% ± 12.8%) (Fig. 4A). As expected and anticipated by the lack of expression of both CCR3 and CCR9 receptors (Figs. 2, 3D), we did not observe significant migration of neither freshly isolated Tregs nor cultured Tregs in response to Eotaxin (CCL11) (nTregs 1.2% ± 0.5%, eTregs 1.4% ± 0.4%, and rTregs 5.9% ± 1.3%) (Fig. 4B) and TECK (CCL25) (nTreg 3.9% ± 0.9%, eTregs 3.1% ± 0.4%, and rTregs 3.2% ± 1.1%) (Fig. 4C). Modest migration was observed in response to I-TAC (CXCL11) (nTreg 14.7% ± 2.6%, eTregs 7.1% ± 1.4%, and rTregs 21.8% ± 2.7%) (Fig. 4D) and SDF-1 (CXCL12) (nTregs 4.4% ± 1%, eTregs 12.1% ± 1.7%, and rTregs 20.5% ± 2.9%) (Fig. 4E), and

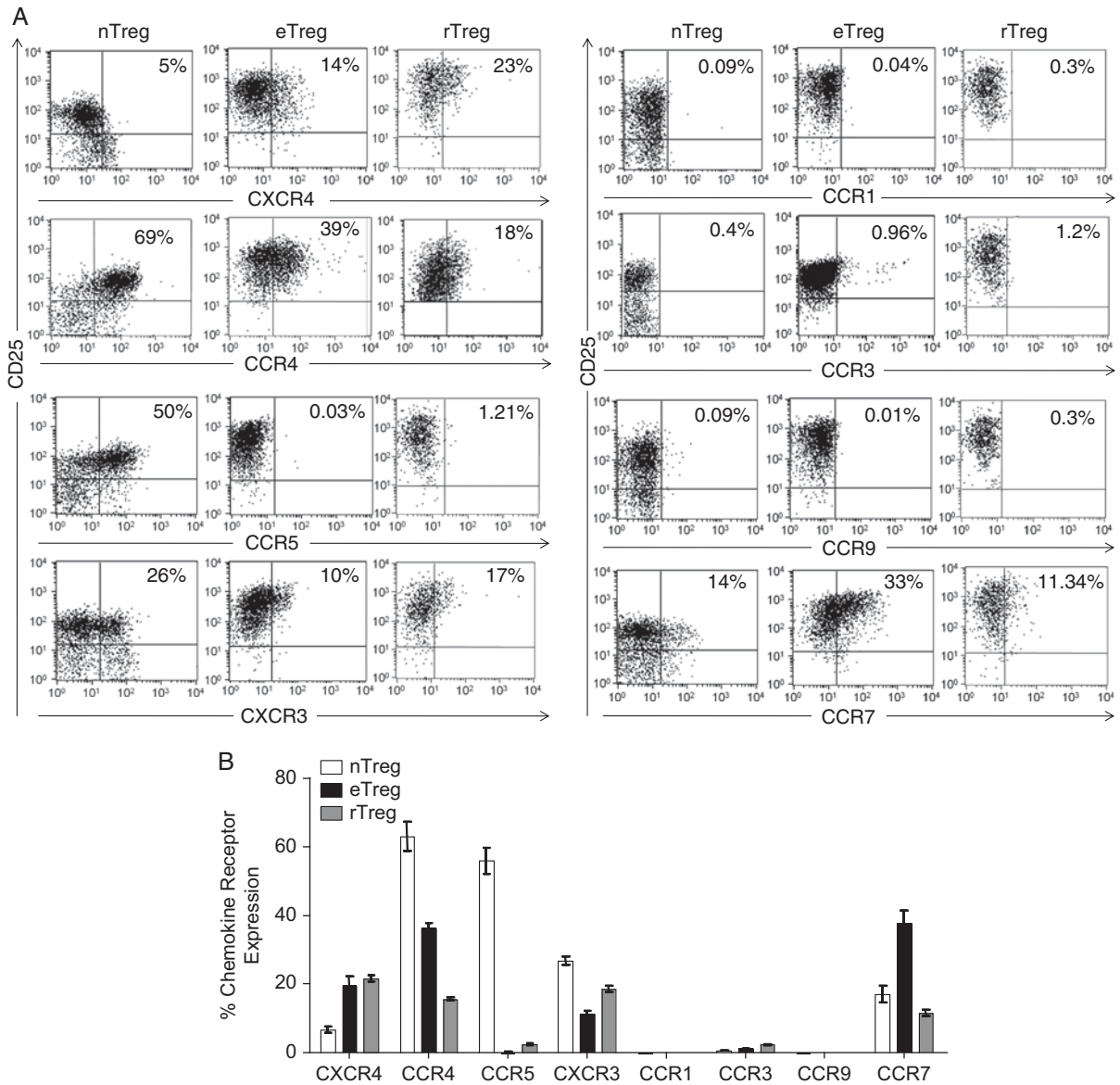

FIGURE 2. Expression profile of chemokine receptors by differentially cultured Tregs. A, Analysis of chemokine receptors in freshly isolated nTregs and ex vivo cultured eTregs and rTregs. Shown are flow cytometry dot plots for nTregs, eTregs, and rTregs, stained with anti-CXCR4, CCR4, CCR5, CXCR3, CCR1, CCR3, CCR9, and CCR7 fluorochrome-conjugated mAb from 1 representative donor. The percentages shown represent the double-positive cells (chemokine receptor and $CD25^+$). B, Comparative phenotypic analysis of chemokine receptors expression in freshly isolated nTregs and ex vivo cultured eTregs and rTregs. Bars (white for nTregs, black for eTregs, and gray for rTregs) represent mean ± SD of 5 different donors.

again this paralleled the modest expression of CXCR3 and CXCR4 by these cells (Fig. 2). In fact, the relative increase in migration in response to SDF-1 corroborated with the relative increase in CXCR4 expression in rTregs and eTregs. In sharp contrast, the migration of cultured Tregs against TARC (CCL17), RANTES (CCL5), and MIP-1α (CCL3) was reduced as compared with nTregs. The migration in response to TARC was significantly reduced in rTregs (12.8% ± 02.5%) as compared with eTregs (42.3% ± 9.5%) and nTregs (71.3% ± 10.2%) (Fig. 4F), reflecting the low expression of CCR4 by the former. More dramatically, although nTregs efficiently migrated in response to RANTES (63.7% ± 6.4%) (Fig. 4G) and MIP-1α (50.2% ± 7.3%) (Fig. 4H), both eTregs and rTregs completely lost their capacity to migrate toward these chemokines (RANTES: eTregs 1.8% ± 0.4% and rTregs 4.4% ± 1.6%; MIP-1α: eTregs 2.5% ± 0.7% and rTregs 2.7% ± 0.7%) (Figs. 4G, H), as these cells lacked the expression of both CCR5 and CCR1. Although freshly isolated nTregs lacked the expression of CCR1 (Fig. 2), their efficient migration toward MIP-1α can perhaps be explained by the fact that MIP-1α is also a ligand for CCR5,[22] which is expressed by nTregs but not by the cultured Tregs. Migration

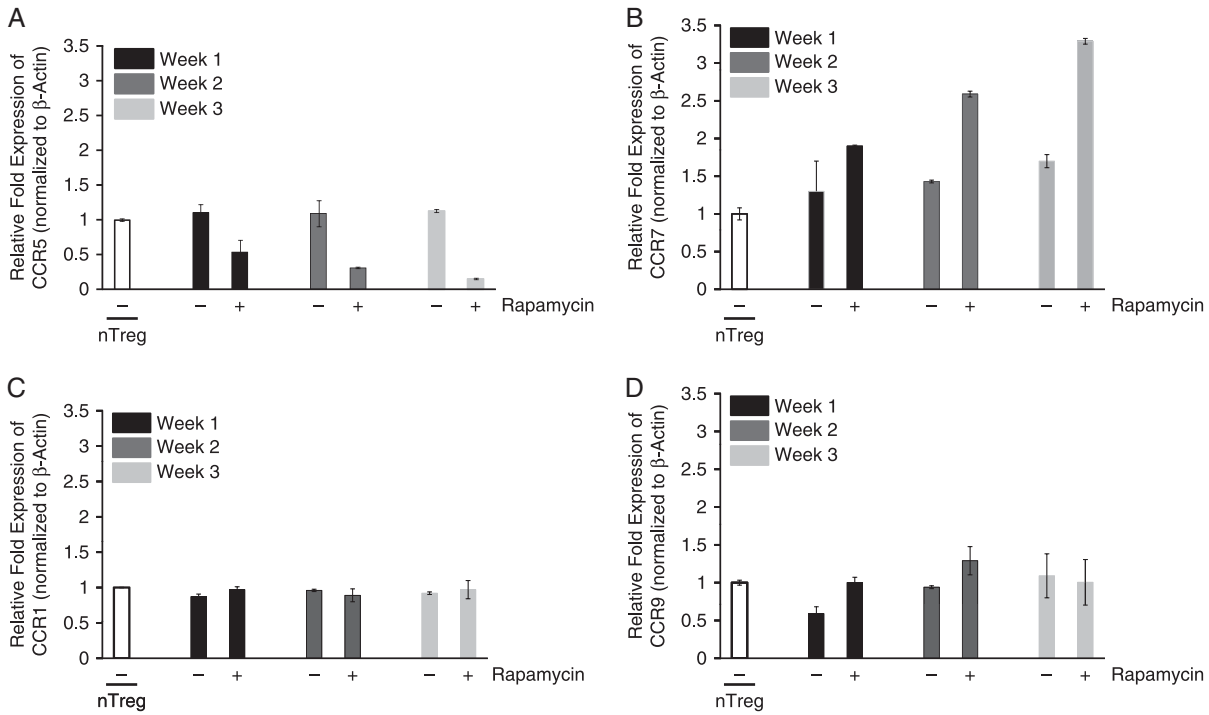

FIGURE 3. qRT-PCR analyses of chemokine receptors expression by eTregs. Total mRNAs, isolated from eTregs treated with rapalogs and nTregs maintained without rapalog selection for the indicated times, were subjected to qRT-PCR to assess steady state mRNA expression levels of CCR5 (A), CCR7 (B), CCR1 (C), and CCR9 (D). The values (mean ± SD) shown are representative of relative amount of test mRNA normalized to β-actin from 3 different experiments. qRT-PCR indicates quantitative real-time polymerase chain reaction.

evaluated in all these assays was specific, as it was significantly prevented by incubation with specific mAbs but not by the isotype controls.

The emergence of Tregs as an essential component of immune homeostasis provides a potential therapeutic opportunity for active immune regulation and induction of long-term tolerance. The optimization of culture conditions to expand T-cell subsets with regulatory function establishes a paradigm for the efficient generation of these cells to implement clinical trials based on the adoptive transfer of Tregs. Although Tregs cultured in vitro retain efficient inhibitory function, to our knowledge this report is the first one that discerns the chemokine receptor expression profile of ex vivo cultured Tregs and defines their migration capacity using in vitro assays. These data, in addition to functional inhibitory capacity, are crucial in determining the potential therapeutic effects of these cells.

Freshly isolated nTregs express CCR7, which is considered a crucial chemokine to drive T-cell homing to peripheral lymph nodes.[21] Our current analysis demonstrates that Tregs cultured ex vivo in presence of rapalogs and generated starting from $CD4^+CD25^{bright}$ cells (eTregs) or $CD4^+$ cells (rTregs) preserved the expression of CCR7. This indicates that these cells should be able to migrate to lymph nodes after adoptive transfer in vivo and thus inhibit the priming of Teff cells and autoreactive T cells.[21]

Freshly isolated Tregs are also characterized by the expression of CCR5, which determines their capacity to migrate toward RANTES and MIP-1α gradients, and chemokines often present in inflamed tissues.[22] In sharp contrast, we observed that ex vivo cultured Tregs lacked CCR5 receptor expression and had impaired migration toward both RANTES and MIP-1α as assessed by specific in vitro migration assays. This observation may have relevant implications for the use of these cultured Tregs in autoimmune diseases characterized by inflamed tissues in which RANTES and MIP-1α are abundantly secreted.[16,22] Cultured Tregs may poorly migrate to these tissues and thus be ineffective in controlling chronic inflammation at the local site. It has indeed been demonstrated that CCR5 downregulation in Tregs prevents their migration to the intestine in an inflammatory bowel disease disease model, with consequent significant increase in intestinal inflammation.[16] Our data suggest that the defective migration toward RANTES and MIP-1α gradients can be partially compensated by the expression of CXCR3, which is the receptor for I-TAC, a chemokine typically released in inflamed tissues.[17] However, because the expression of CXCR3 is moderate in cultured Tregs, we anticipate that this will provide only a marginal migration toward I-TAC.

It has been previously shown that expression and migration toward chemokine receptor is tightly coupled to IL-2 treatment.[23,24] However, activation of fully responsive T lymphocytes through TCR/CD3 complex and the CD28 antigen had an inverse effect on chemokine effect and IL-2 responsiveness.[24] Receptor expression and consequent migration were both downregulated in cultured Treg cells even after IL-2 treatment.[25] Cumulatively, it is believed that the chemokine receptor expression is transcriptionally regulated, as our data also show, whereas translation of the receptor transcripts and consequent ability to migrate to chemokine gradient depend on IL-2. It will be interesting

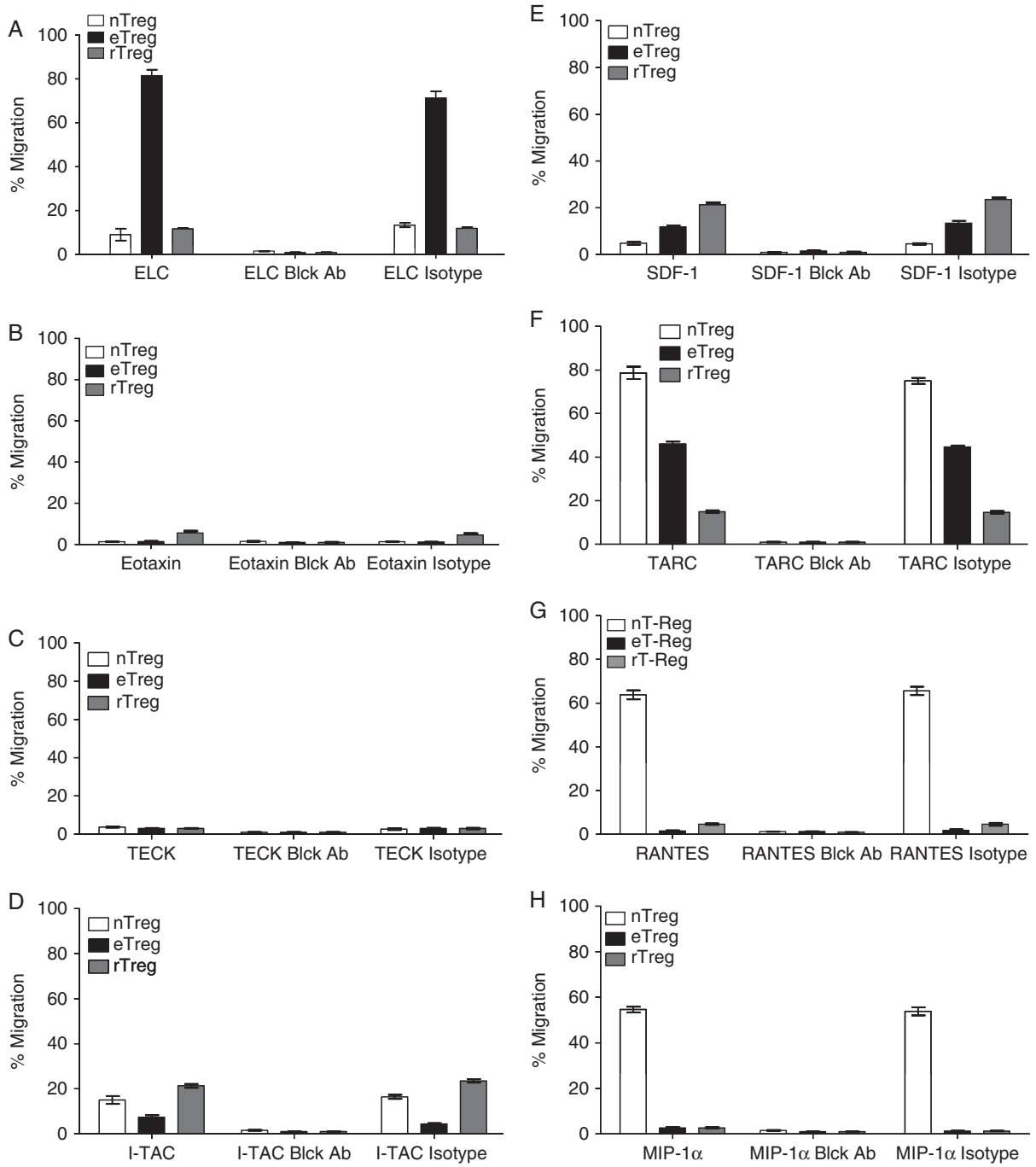

FIGURE 4. Differential migration capacity of ex vivo cultured Tregs. The migration of nTregs (white bars), eTregs (black bars), and rTregs (gray bars) toward (A) ELC (CCL19), (B) Eotaxin (CCL11), (C) TECK (CCL25), (D) I-TAC (CXCL11), (E) SDF-1 (CXCL2), (F) TARC (CCL17), (G) RANTES (CCL5), and (H) MIP-1α (CCL3) was evaluated using a transwell migration assay. Specificity of the migration assay was confirmed using blocking antibodies and isotype controls. The data are represented as mean ± SD for Tregs isolated or expanded from 9 healthy donors.

to further delineate the transcription machinery and its regulation by rapalogs, as it will provide additional handles to regulate specific chemokine receptor expression in the ex vivo expanded Tregs and usefully manipulate their migratory behavior as required under specific conditions. In conclusion, our analysis of chemokine receptor expression and function in cultured Tregs provides valuable information to predict their potential clinical activity in specific autoimmune diseases or off-target suppressive effects upon adoptive transfer. In addition, as previously described for antitumor specific cytotoxic T lymphocytes,[20] our data suggest that manipulation of cultured Tregs by

transgenic expression of appropriate chemokine receptors may be useful to optimize their tissue migration.

CONFLICTS OF INTEREST/ FINANCIAL DISCLOSURES

Supported in part by RO1 CA142636 NIH-NCI and by RO1CA131027 from NIH-NCI and by W81XWH-10-10425 Department of Defense, Technology/Therapeutic Development Award. The authors are grateful to Reshma Kulkarni for the phenotypic analysis and Rongfu Wang from Baylor College of Medicine for critical review of the manuscript.

All authors have declared that there are no financial conflicts of interest in regard to this work.

REFERENCES

1. Brusko TM, Putnam AL, Bluestone JA. Human regulatory T cells: role in autoimmune disease and therapeutic opportunities. *Immunol Rev*. 2008;223:371–390.
2. Zeiser R, Leveson-Gower DB, Zambricki EA, et al. Differential impact of mammalian target of rapamycin inhibition on $CD4^+CD25^+Foxp3^+$ regulatory T cells compared with conventional $CD4^+$ T cells. *Blood*. 2008;111:453–462.
3. Sakaguchi S, Takahashi T, Yamazaki S, et al. Immunologic self tolerance maintained by T-cell-mediated control of self-reactive T cells: implications for autoimmunity and tumor immunity. *Microbes Infect*. 2001;3:911–918.
4. Baecher-Allan C, Hafler DA. Suppressor T cells in human diseases. *J Exp Med*. 2004;200:273–276.
5. Lan RY, Ansari AA, Lian ZX, et al. Regulatory T cells: development, function and role in autoimmunity. *Autoimmun Rev*. 2005;4:351–363.
6. Kang SM, Tang Q, Bluestone JA. $CD4^+CD25^+$ regulatory T cells in transplantation: progress, challenges and prospects. *Am J Transplant*. 2007;7:1457–1463.
7. Bluestone JA, Tang Q. Therapeutic vaccination using $CD4^+CD25^+$ antigen-specific regulatory T cells. *Proc Natl Acad Sci U S A*. 2004;101(suppl 2):14622–14626.
8. Eghtesad S, Morel PA, Clemens PR. The companions: regulatory T cells and gene therapy. *Immunology*. 2009;127:1–7.
9. Yang Z-Z, Ansell SM. The role of Treg cells in the cancer immunological response. *Am J Immunol*. 2009;5:17–28.
10. Bresatz S, Sadlon T, Millard D, et al. Isolation, propagation and characterization of cord blood derived $CD4^+$ $CD25^+$ regulatory T cells. *J Immunol Methods*. 2007;327:53–62.
11. Earle KE, Tang Q, Zhou X, et al. In vitro expanded human $CD4^+CD25^+$ regulatory T cells suppress effector T cell proliferation. *Clin Immunol*. 2005;115:3–9.
12. Godfrey WR, Ge YG, Spoden DJ, et al. In vitro-expanded human CD4(+)CD25(+) T-regulatory cells can markedly inhibit allogeneic dendritic cell-stimulated MLR cultures. *Blood*. 2004;104:453–461.
13. Hoffmann P, Eder R, Kunz-Schughart LA, et al. Large-scale in vitro expansion of polyclonal human CD4(+)CD25high regulatory T cells. *Blood*. 2004;104:895–903.
14. Battaglia M, Stabilini A, Roncarolo MG. Rapamycin selectively expands $CD4^+CD25^+FoxP3^+$ regulatory T cells. *Blood*. 2005; 105:4743–4748.
15. Mahnke K, Ring S, Bedke T, et al. Interaction of regulatory T cells with antigen-presenting cells in health and disease. *Chem Immunol Allergy*. 2008;94:29–39.
16. Kang SG, Piniecki RJ, Hogenesch H, et al. Identification of a chemokine network that recruits FoxP3(+) regulatory T cells into chronically inflamed intestine. *Gastroenterology*. 2007;132:966–981.
17. Ebert LM, Schaerli P, Moser B. Chemokine-mediated control of T cell traffic in lymphoid and peripheral tissues. *Mol Immunol*. 2005;42:799–809.
18. Porter CM, Bloom ET. Human $CD4^+CD25^+$ regulatory T cells suppress anti-porcine xenogeneic responses. *Am J Transplant*. 2005;5:2052–2057.
19. Battaglia M, Stabilini A, Migliavacca B, et al. Rapamycin promotes expansion of functional $CD4^+CD25^+Foxp3^+$ regulatory T cells of both healthy subjects and Type 1 diabetic patients. *J Immunol*. 2006;177:8338–8347.
20. Di Stasi A, De Angelis B, Rooney CM, et al. T lymphocytes coexpressing CCR4 and a chimeric antigen receptor targeting CD30 have improved homing and antitumor activity in a Hodgkin tumor model. *Blood*. 2009;113:6392–6402.
21. Hirao M, Onai N, Hiroishi K, et al. CC chemokine receptor-7 on dendritic cells is induced after interaction with apoptotic tumor cells: critical role in migration from the tumor site to draining lymph nodes. *Cancer Res*. 2000;60:2209–2217.
22. Wang CR, Liu MF. Regulation of CCR5 expression and MIP-1α production in $CD4^+$ T cells from patients with rheumatoid arthritis. *Clin Exp Immunol*. 2003;132:371–378.
23. Olson TS, Ley K. Chemokines and chemokine receptors in leukocyte trafficking. *Am J Physiol Regul Integr Comp Physiol*. 2002;283:R7–R28.
24. Loetscher P, Seitz M, Baggiolini M, et al. Interleukin-2 regulates CC chemokine receptor expression and chemotactic responsiveness in T lymphocytes. *J Exp Med*. 1996;184:569–577.
25. Wuest TY, Willette-Brown J, Durum SK, et al. The influence of IL-2 family cytokines on activation and function of naturally occurring regulatory T cells. *J Leukoc Biol*. 2008;84:973–980.

Activation of Wnt Signaling Arrests Effector Differentiation in Human Peripheral and Cord Blood-Derived T Lymphocytes

Sujatha Muralidharan,* Patrick J. Hanley,† Enli Liu,† Rikhia Chakraborty,† Catherine Bollard,*,† Elizabeth Shpall,‡ Cliona Rooney,*,† Barbara Savoldo,† John Rodgers,* and Gianpietro Dotti*,†,§

The canonical Wnt/β-catenin signaling pathway plays an important role in thymocyte development and T cell migration, but little is known about its role in naive-to-effector differentiation in human peripheral T cells. We show that activation of Wnt/β-catenin signaling arrests human peripheral blood and cord blood T lymphocytes in the naive stage and blocks their transition into functional T effector cells. Wnt signaling was induced in polyclonally activated human T cells by treatment either with the glycogen synthase kinase 3β inhibitor TWS119 or the physiological Wnt agonist Wnt-3a, and these T cells preserved a naive CD45RA$^+$CD62L$^+$ phenotype compared with control-activated T cells that progressed to a CD45RO$^+$CD62L$^-$ effector phenotype, and this occurred in a TWS119 dose-dependent manner. TWS119-induced Wnt signaling reduced T cell expansion, as a result of a block in cell division, and impaired acquisition of T cell effector function, measured by degranulation and IFN-γ production in response to T cell activation. The block in T cell division may be attributed to the reduced IL-2Rα expression in TWS119-treated T cells that lowers their capacity to use autocrine IL-2 for expansion. Collectively, our data suggest that Wnt/β-catenin signaling is a negative regulator of naive-to-effector T cell differentiation in human T lymphocytes. The arrest in T cell differentiation induced by Wnt signaling might have relevant clinical applications such as to preserve the naive T cell compartment in Ag-specific T cells generated ex vivo for adoptive T cell immunotherapy. ***The Journal of Immunology*****, 2011, 187: 5221–5232.**

The canonical Wnt/β-catenin signaling pathway regulates the progression of thymocyte development at different stages (1–3). However, the role of this signaling pathway in postthymic peripheral T lymphocytes is less understood. Resting and effector peripheral T cells express components of the Wnt signaling pathway. Wnt proteins induce T cell production of matrix metalloproteinases, which are required for peripheral T cell transmigration (4). TCR activation also leads to changes in expression patterns of Wnt-targeted transcription factors in peripheral T cells (5). These results indicate that the Wnt signaling pathway is active in peripheral T cells and it may play a role during T cell activation and differentiation. We undertook this study to elucidate the role of the canonical Wnt signaling pathway in naive-to-effector differentiation of human peripheral blood and cord blood T lymphocytes. This question is relevant both to the fundamental understanding of human T cells and our practical ability to expand therapeutic T cells ex vivo for treating patients with cancer. In particular, human T cells expanded ex vivo almost invariably acquire an effector phenotype that may limit their ability to persist in vivo after adoptive transfer into the patient. Manipulation of the Wnt pathway might help preserve the naive phenotype of T cells during these ex vivo cultures.

In the canonical Wnt pathway, a destruction complex comprised of scaffold proteins (adenomatous polyposis coli, axis inhibition protein 1) and two kinases (glycogen synthase kinase 3β [GSK3β], casein kinase 1) phosphorylates and promotes βTRCP-mediated ubiquitination and degradation of the β-catenin molecule in the absence of Wnt ligand (6). Nineteen different Wnt ligands identified in humans are all lipid-modified glycoproteins. Engagement of cell surface Frizzled/LRP-5/6 receptor complexes by Wnt ligands including Wnt1 and Wnt3a recruits the protein Disheveled to the receptor complex inducing phosphorylation of LRP-5/6 by casein kinase 1 and GSK3β. This recruits axis inhibition protein 1 to the plasma membrane and disassembles the destruction complex, allowing accumulation of cytoplasmic β-catenin, which can then translocate to the nucleus. β-catenin associates with transcription factors from the T cell factor or lymphoid enhancer binding factor family, including Tcf-1, Tcf-3, Tcf-4, and Lef-1 and activates expression of target genes including *Tcf7* (7), *Lef1* (8), *Nlk* (9), and *Jun* (10).

Willinger et al. (5) reported that mature human CD8$^+$ T lymphocytes downregulate the expression of Wnt transcription factors Tcf-1 and Lef-1 upon activation but shift the pattern of splicing to favor the stimulatory isoforms of these transcription factors rather than the inhibitory isoforms, suggesting that Wnt signaling may

*Department of Pathology and Immunology, Baylor College of Medicine, Houston, TX 77030; †Center for Cell and Gene Therapy, Baylor College of Medicine, Houston, TX 77030; ‡Division of Cancer Medicine, Department of Stem Cell Transplantation, The University of Texas MD Anderson Cancer Center, Houston, TX 77030; and §Department of Medicine, Baylor College of Medicine, Houston, TX 77030

Received for publication May 31, 2011. Accepted for publication September 15, 2011.

This work was supported in part by National Institutes of Health/National Cancer Institute Grant R01 CA142636, Department of Defense Grant W81XWH-10-1-0425, a Technology/Therapeutic Development award, and Cancer Prevention and Research Institute of Texas Grant RP 100484.

Address correspondence and reprint requests to Dr. Gianpietro Dotti, Center for Cell and Gene Therapy, Baylor College of Medicine, 6621 Fannin Street, MC 3-3320, Houston, TX 77030. E-mail address: gdotti@bcm.tmc.edu

The online version of this article contains supplemental material.

Abbreviations used in this article: 7AAD, 7-aminoactinomycin D; CAR, chimeric Ag receptor; GSK3β, glycogen synthase kinase 3β; LAT, linker for activation of T cells; nTreg, natural regulatory T cell; PLC, phospholipase C; Treg, regulatory T cell; Tscm, T memory stem.

play a complex role in peripheral T cell differentiation. It has been reported that induction of canonical Wnt signaling in pmel-1 transgenic TCR mouse $CD8^+$ T cells in vitro arrests effector T cell differentiation and function (11). This observation agrees with another study in which activation of Wnt-β signaling in mouse T cells obtained by genetic modification to express a non-degradable β-catenin inhibited T cell activation at the proximal stages of TCR signaling and also arrested effector T cell proliferation and function (12). Importantly, Gattinoni et al. (11) found that in addition to arresting effector cell differentiation, induction of Wnt signaling in pmel-1 mouse T cells generated a distinct population that they called "T memory stem" (Tscm) cells. These Tscm cells expressed high levels of Sca-1, Bcl-2, and CD122, preserved a $CD44^{low}CD62L^{high}$ naive phenotype even after undergoing several cycles of cell division, rapidly released cytokines upon Ag encounter, and had superior proliferative and antitumor activity in vivo compared with central or effector memory T cells (11).

Successful translation of these findings in human T cells could lead to an important clinical application to maintain naive T cells in ex vivo cultures, using Wnt signaling, for adoptive transfer. Infusion of naive T cells that have a greater potential to persist and expand in vivo may improve the objective clinical responses in cancer patients as previously observed in mouse models (13, 14). We investigated the role of canonical Wnt signaling in naive-to-effector T cell differentiation in human T lymphocytes. We found that induction of Wnt signaling, using graded doses of synthetic GSK3β inhibitor TWS119 or the native agonist Wnt-3a, preserves a naive phenotype ($CD45RO^-CD45RA^+CD62L^+$) in activated $CD4^+$ and $CD8^+$ peripheral T cells. These Wnt-induced phenotypically naive cells also showed reduced effector T cell function in response to polyclonal stimulation and in Ag-specific redirected T cells. Additionally, Wnt signaling impaired T cell activation by inhibition of proximal TCR signaling and significantly blocked T cell division. Similar effects were observed in T cells derived from cord blood, which can be considered a better source of immature T cells compared with those circulating in peripheral blood (15). However, Wnt-induced T cells could be rescued from arrest in proliferation by exogenous γ-chain cytokines, allowing them to become effector T cells. We also found that Wnt signaling induced by TWS119 does not imprint on the T cell phenotype and functions, as these cells acquire proliferative and effector function when restimulated in the absence of TWS119. Therefore, our results using human T lymphocytes support a model in which Wnt signaling inhibits effector T cell differentiation and this observation may have relevant clinical implications in T cell-based immunotherapy.

Materials and Methods

Cell isolation and selection

Mononuclear cells were isolated using Ficoll gradient from peripheral blood collected from healthy donors at the Gulf Coast Regional Blood Center (Houston, TX) or from research cord blood units obtained from the MD Anderson Cord Blood Bank. Samples were collected according to local Institutional Review Board-approved protocols. T cells were positively selected from PBMCs or cord blood-derived mononuclear cells by MACS using CD3, CD4, or CD8 microbeads (Miltenyi Biotec). CD45RO- and CD45RA-expressing T cells were sorted by negative selection using appropriate microbeads (Miltenyi Biotec).

T cell activation and culture

T cells were activated with plate-coated OKT3 (Ortho Biotech; 1 μg/ml) and anti-CD28 (clone CD28.2, BD Biosciences; 1 μg/ml) Abs and cultured for 7 d. TWS119 (GSK3β inhibitor) (EMD Biosciences) and recombinant human Wnt-3a (R&D Systems) were used at the indicated concentrations in culture. TWS119 was resuspended in DMSO (Sigma-Aldrich). Human recombinant IL-15 (PeproTech), IL-7 (PeproTech), and IL-2 (Proleukin) were added to the cells at 5 ng/ml, 10 ng/ml, and 50 U/ml, respectively, for indicated experiments. PHA (Sigma-Aldrich) was used at 5 μg/ml to activate T cells polyclonally for selected experiments. Ag-redirected T cells were generated by transduction of primary human T cells with a chimeric Ag receptor (CAR) directed against CD19 as previously described (16). These cells were retrovirally transduced (~25% CAR^+) and cultured in the presence of DMSO or 3 μM TWS119 and cytokines IL-15 (5 ng/ml) and IL-7 (10 ng/ml).

Complete T cell medium contained 45% RPMI 1640 (Thermo Scientific) and 45% Click's medium (Irvine Scientific) supplemented with 10% heat-inactivated FCS (HyClone), 100 U/ml penicillin, 100 mg/ml streptomycin, and 2 mM GlutaMAX (Invitrogen). Cells were maintained in a humidified atmosphere containing 5% CO_2 at 37°C.

Flow cytometry

Cells were stained with Abs (BD Biosciences) coupled to FITC, PE, PerCP, or allophycocyanin against the indicated molecules. Routinely, 1×10^6 cells were stained with the indicated Ab or appropriate isotype controls for 20 min at 4°C, washed in PBS containing 1% FCS, and resuspended for FACS analysis.

To examine intracellular IFN-γ production and surface CD107 expression, T cells were collected after 7 d culture with control DMSO or TWS119 and restimulated overnight with 10 ng/ml PMA (Sigma-Aldrich) and 1 μM ionomycin (EMD Biosciences). For intracellular staining, cells were treated with protein transport inhibitor (brefeldin A), fixed, permeabilized, and stained in saponin-containing buffer (17).

The effector function of the CAR-redirected T cells was examined by coculturing them with Raji cells at a 5:1 E:T ratio in the presence or absence of DMSO or 3 μM TWS119 as indicated. After 5 d culture, the residual Raji and T cells in coculture were identified by their CD20 and CD3 expression, respectively, using flow cytometry. Nontransduced DMSO- or TWS119-treated T cells served as negative controls.

Cells were analyzed by CellQuest software on a BD FACSCalibur cytometer. For each sample, a minimum of 10,000 events was analyzed.

ELISA

T cells were collected after 7 d culture with control DMSO or TWS119 and restimulated with 10 ng/ml PMA (Sigma-Aldrich) and 1 μM ionomycin (EMD Biosciences). For Ag-specific cells, the DMSO- or TWS119-treated CAR-redirected T cells were cocultured with Raji cells at a 5:1 ratio. After 24 h, the supernatant of the cultures was collected and analyzed for IFN-γ, IL-2, or IL-17 using 96-well plates coated with the specific Abs by ELISA, according to the manufacturer's instructions (R&D Systems). Other cytokines such as TNF-α, IL-4, and IL-10 were analyzed using cytometric bead array for human Th1 and Th2 cytokines (BD Biosciences).

Cell proliferation and apoptosis

T cell proliferation was evaluated in a CFSE dilution assay. Briefly, freshly isolated T cells were labeled with 1.5 μM CFSE (Invitrogen) according to the manufacturer's instructions. After 7 d culture, the progressive dilution of CFSE corresponding to each cycle of cell division was evaluated by flow cytometry. T cell apoptosis was measured at the end of a week of culture by staining the cells for annexin V and 7-aminoactinomycin D (7AAD; BD Biosciences).

Immunoblot analysis

For Western blot analysis, complete cell lysates were prepared from T cells cultured with control DMSO or TWS119 for 6 or 24 h as indicated. Cell lysates were resolved by SDS-PAGE. Expression of β-catenin, phospholipase C (PLC)γ, linker for activation of T cells (LAT), pY783 PLCγ, and pY132 LAT were detected using Abs purchased from Cell Signaling Technology and Abcam. Immunoblots were developed using ECL detection reagents (Amersham Biosciences). As a loading control, the blots were probed with GAPDH-specific mAb (Santa Cruz Biotechnology).

Quantitative RT-PCR

T cells were activated and cultured with control DMSO or TWS119 for indicated times, washed, and total RNA was isolated using the RNeasy Mini column purification kit (Qiagen). cDNA was synthesized using a High Capacity RNA-to-cDNA kit (Applied Biosystems) according to the manufacturer's instructions. Expression of genes *Nlk, Fzd7, Tcf7, Jun*, and *Lef1* was evaluated by quantitative RT-PCR using specific primers/probes purchased from Applied Biosystems. The difference in cycles threshold values (ΔCT) of the gene was normalized to the ΔCT of GAPDH, and fold change in expression was expressed relative to untreated cells.

Statistics

Results are presented as means ± SD. Student *t* test was used to determine the statistical significance of differences between samples (p values calculated as 0 were depicted as $p < 0.001$).

Results

TWS119 activates the canonical Wnt/β-catenin signaling pathway

First we wanted to determine whether treatment with the GSK3β inhibitor, TWS119, induces the canonical Wnt signaling pathway in human T cells as has been observed in mouse T cells (11). As illustrated in Fig. 1*A*, resting and activated human $CD3^+$ T lymphocytes treated with TWS119 for 6 h showed a large increase in β-catenin accumulation relative to cells treated with DMSO, indicating that canonical Wnt signaling is activated upon TWS119 treatment in human T cells.

The expression of genes downstream of canonical Wnt signaling (*Fzd7*, *Lef1*, *Nlk*, *Tcf7*, and *Jun*) was examined by quantitative RT-PCR. Control DMSO-treated activated T cells downregulated expression of *Fzd7*, *Lef1*, and *Tcf7* relative to untreated cells, and this is consistent with previously published observations (5) (Fig. 1*B*, 1*C*). However, in the presence of TWS119, activated T cells showed upregulation of *Fzd7, Nlk*, and *Jun* genes or reduced downregulation of *Lef1* and *Tcf7* compared with DMSO-treated cells. This trend of higher expression of Wnt target genes in TWS119-treated cells compared with DMSO-treated cells was observed for all genes with statistically significant differences in the case of *Nlk*, *Jun*, and *Tcf7* (Fig. 1*B*). This further supports the claim that TWS119 activates the Wnt pathway in human T cells.

Induction of Wnt signaling by TWS119 preserves the subset of $CD45RA^+CD62L^+$ cells in polyclonally activated T cells

Previous reports have shown that Wnt signaling inhibits splenic T cell differentiation in mouse T cells (11). The difference in expression patterns of transcription factors and receptors of the Wnt signaling pathway between naive and effector human T cells indicates that this pathway plays a significant, if complex, role in naive-to-effector human T cell differentiation as well (4, 5). To test whether Wnt signaling inhibits differentiation of naive human T cells to effector cells, naive cells were polyclonally activated and cultured with graded doses of TWS119 for a week. Freshly isolated T cells consisted of both naive ($CD45RA^+CD62L^+$) and effector cells ($CD45RO^+CD62L^-$) (Fig. 2*A*). As expected, upon activation with OKT3 and anti-CD28 Abs, naive T cells progressed to Ag-experienced cells, showing decline in the expression of CD45RA and acquisition of the alternatively spliced variant, CD45RO (18). By day 7, the control cells possessed predominantly effector T cell characteristics such as elevated expression of CD45RO and low expression of CD62L (Fig. 2*A*). In contrast, activated T cells treated with TWS119 retained the subset of naive $CD45RA^+CD62L^+$ cells in a dose-dependent manner. We selected

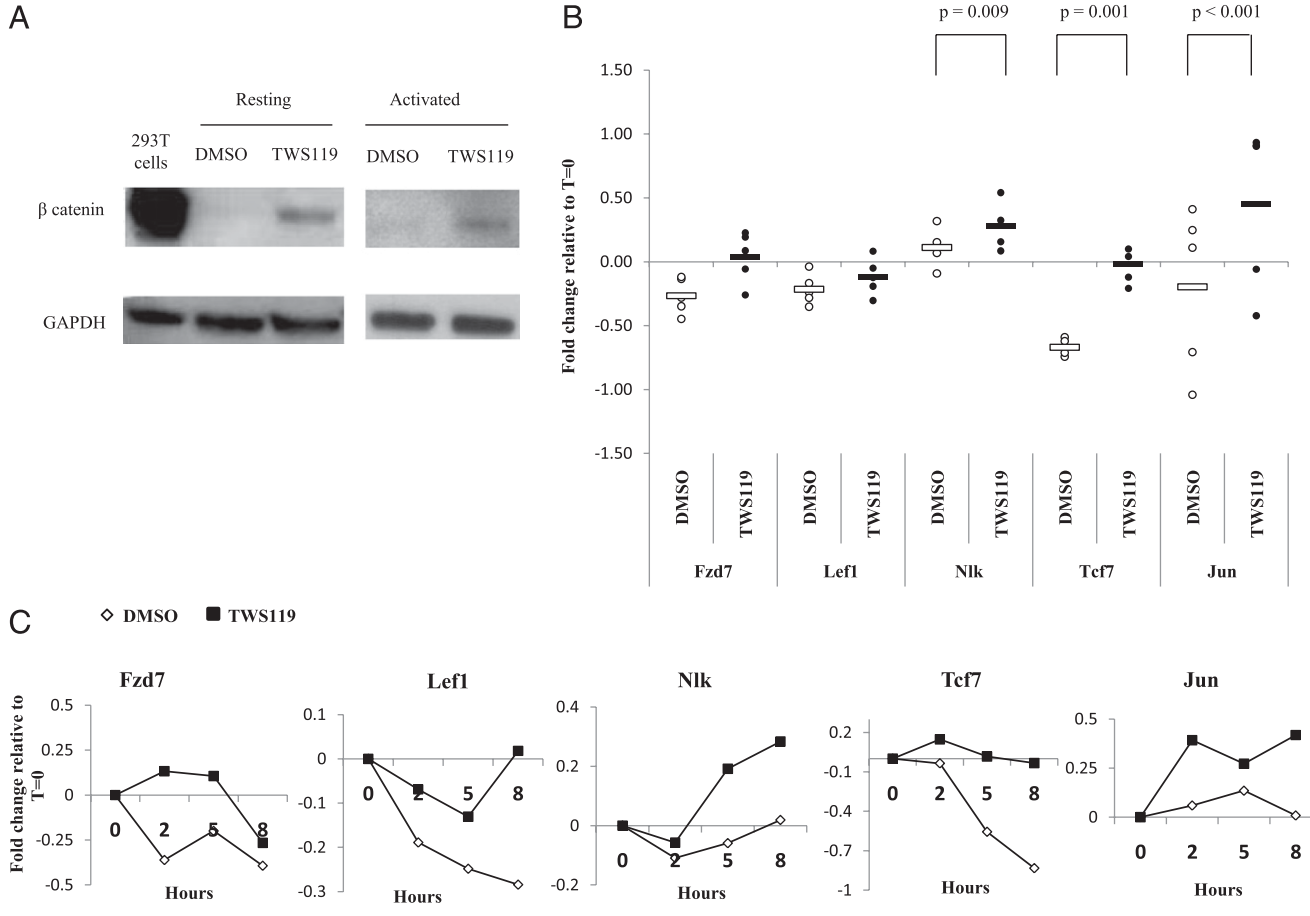

FIGURE 1. Treatment with TWS119 causes activation of canonical β-catenin/Wnt signaling. *A*, Western blot analysis of β-catenin expression in $CD3^+$ T cells cultured with DMSO or 7 μM TWS119 with or without activation for 6 h. 293T cells were used as a positive control for β-catenin expression, and GAPDH served as loading control. Immunoblot data are from one of two independent experiments. *B*, Quantitative RT-PCR analysis of Wnt target genes in activated $CD3^+$ T cells cultured with DMSO or 7 μM TWS119 for 8 h. Data summarize means ± SD of five independent experiments. *C*, Time course of Wnt target gene expression in activated T cells treated with DMSO or 7 μM TWS119 for 0, 2, 5, and 8 h analyzed by quantitative RT-PCR. Data are from one of two independent experiments. *B* and *C*, Fold change in expression of genes was calculated with respect to 0 h and the data are shown in a log scale.

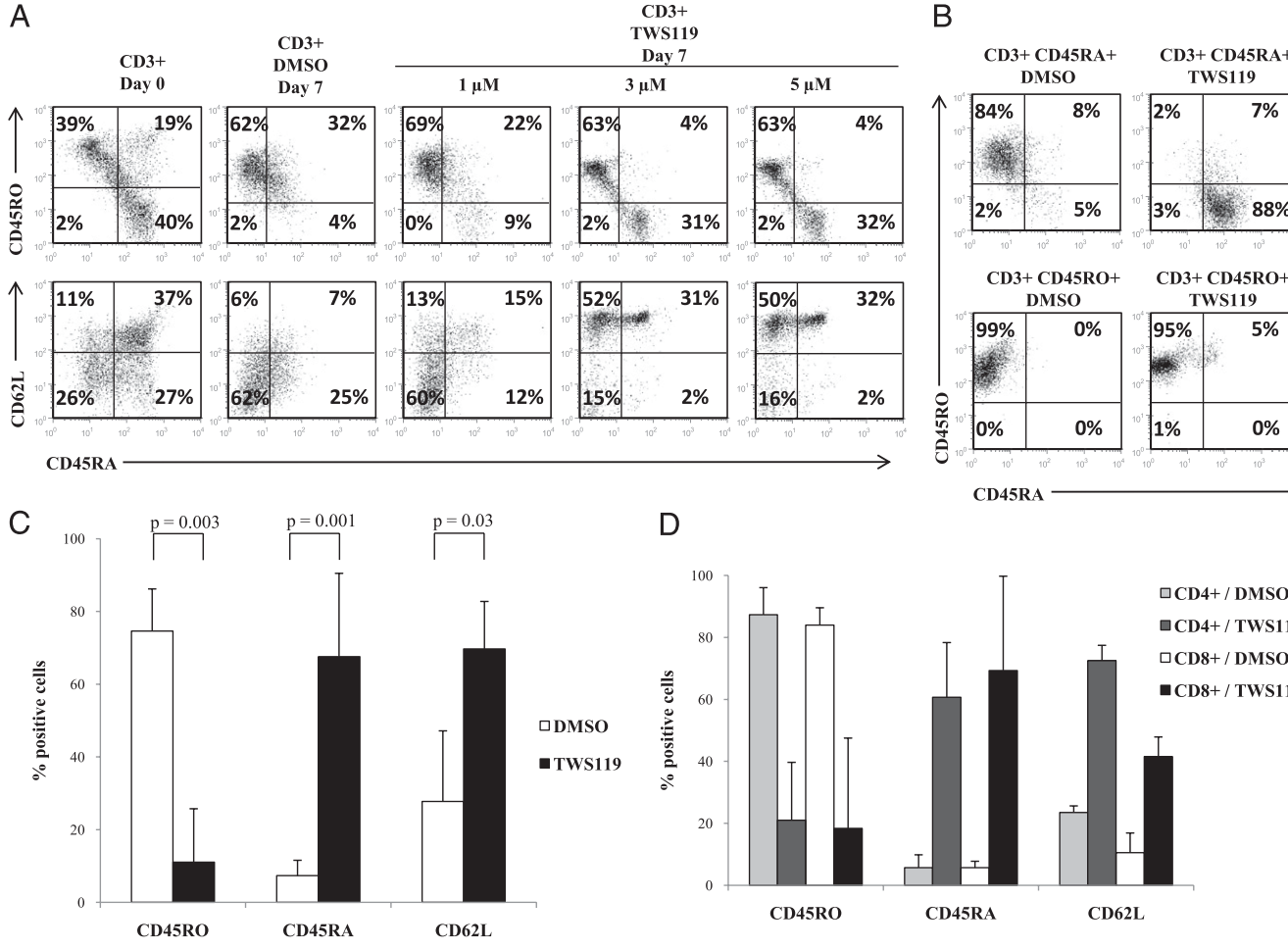

FIGURE 2. TWS119 treatment blocks transition of CD45RA$^+$ cells into CD45RO$^+$ cells and preserves a subset of phenotypically naive T cells. *A*, Flow cytometry analysis of naive and effector T cell markers (CD62L, CD45RA, and CD45RO) on freshly isolated CD3$^+$ T cells at baseline (*left panels*) and after activation and 7 d culture with DMSO or different doses of TWS119 (*right panels*). Plots are from one of three independent experiments. *B*, Analysis of CD45RO and CD45RA expression on CD3$^+$ T cells, further selected for CD45RA or CD45RO, activated and cultured with DMSO or 3 μM TWS119 for 7 d. Plots are from one of at least three independent experiments. *C*, Comparison of CD45RA, CD45RO, or CD62L expression on CD3$^+$CD45RA$^+$ selected cells after activation and culture with DMSO or 3 μM TWS119 for 7 d. Data summarize means ± SD of four independent experiments. *D*, Comparison of CD45RA, CD45RO, or CD62L expression on CD45RA$^+$ selected cells, further selected for CD4 or CD8, after activation and culture with DMSO or 3 μM TWS119 for 7 d. Data summarize means ± SD of three independent experiments.

3 μM TWS119 for our subsequent in vitro experiments because it was the lowest dose that produced an effect on T cell phenotype with minimal toxicity, whereas higher doses (>5 μM) resulted in substantial reduced viability of T cells by day 7 of culture (data not shown).

The increase in the CD45RA$^+$ subset after TWS119 treatment could be the result of a block in the transition of T cells from the naive CD45RA$^+$ to the effector CD45RO$^+$ phenotype or due to reversion of CD45RO$^+$ cells to CD45RA$^+$ cells (19). To determine whether TWS119 treatment blocks CD45RA–CD45RO transition, CD3-selected cells were purified based on the expression of CD45RA prior to treatment with TWS119. As expected, the great majority of CD45RA-selected cells lost CD45RA and expressed CD45RO after activation in the presence of DMSO (75 ± 12%). In contrast, most of the CD45RA$^+$ cells retained expression of CD45RA when activated in the presence of TWS119 (68 ± 23%) (Fig. 2*B*, *upper panels*). This indicates that induction of Wnt signaling blocked the transition of CD45RA-selected cells into effector CD45RO$^+$ cells. We wanted to test whether TWS119 treatment also causes reversion of CD45RO$^+$ cells to CD45RA$^+$ cells. CD45RO-selected T cells maintained CD45RO expression by day 7 after activation irrespective of treatment with DMSO (85 ± 21% CD45RO$^+$) or TWS119 (86 ± 10% CD45RO$^+$) (Fig. 2*B*, *lower panels*), indicating that TWS119 does not cause reversion of CD45RO-selected cells to CD45RA$^+$ cells. Fig. 2*C* summarizes the significant differences in CD62L, CD45RA, and CD45RO expression in naive CD45RA-selected T cells in response to TWS119 compared with DMSO-treated control cells. TWS119-treated cells showed higher expression of CD62L (70 ± 13% versus 28 ± 19%, $p = 0.03$) and CD45RA (68 ± 23% versus 7 ± 4%, $p = 0.001$) and low expression of CD45RO (11 ± 15% versus 75 ± 12%, $p = 0.003$) compared with control cells. We also examined the effect of Wnt signaling on the expression of other naive/memory markers such as CD127, activation markers such as 41BB and CD69, and costimulatory molecules such as CD27 and CD28 (Supplemental Fig. 1*A*). There was a significant decrease in the expression of CD28, 41BB, and CD69 on TWS119-treated T cells compared with control cells. TWS119 treatment also maintained high expression of naive markers CD127 and CD27.

These results were observed in CD3-selected T cells, which include both CD4$^+$ and CD8$^+$ T cells. To test whether Wnt signaling induced similar effects in both CD4$^+$ and CD8$^+$ T cells, CD4 and CD8-selected T cells were further purified based on CD45RA expression, then activated and treated with or without

TWS119 for 7 d. As illustrated in Fig. 2*D*, induction of Wnt signaling in CD4 and CD8-selected cells produced similar naive phenotypes. We also examined the expression of transcription factors, chemokine receptors, and cytokines associated with the Th1, Th2, Th17, and regulatory T cell (Treg) subsets (Supplemental Fig. 1*B*, 1*C*). TWS119-treated cells showed reduced expression of transcription factors, including T-bet, RORγ, Gata-3, and Foxp3, chemokine receptors such as CXCR3 and CCR4, and the cytokines TNF-α, IL-4, and IL-17. Expression of CCR6, which was downregulated by activation in DMSO control cells, was maintained by TWS119. These data suggest that TWS119 does not skew $CD4^+$ T cells to any specific subset (Th1, Th2, Th17, or Tregs), but rather it has a similar inhibitory effect on all the subsets. Our results demonstrate that TWS119 affected both $CD4^+$ and $CD8^+$ T cells equally, preserving a naive subset by blocking the transition of $CD45RA^+$ cells into $CD45RO^+$ cells.

TWS119-induced Wnt signaling impairs acquisition of effector function of T cells

Because TWS119 inhibited naive-to-effector T cell differentiation in terms of phenotype, we wanted to determine whether TWS119 treatment also inhibited the acquisition of effector function of T cells. CD3-selected T cells, activated and expanded for a week with or without TWS119, were stimulated overnight with PMA and ionomycin to elicit a polyclonal effector T cell response measured as IFN-γ and CD107 expression (a marker for degranulation). As shown in Fig. 3*A* and 3*B*, control cells that were stimulated with PMA/ionomycin expressed IFN-γ (41 ± 16%) and CD107 (53 ± 10%) compared with unstimulated cells. In contrast, fewer TWS119-treated cells expressed IFN-γ (17 ± 11%, $p = 0.004$) or CD107 (11 ± 10%, $p = 0.001$) in response to PMA/ionomycin. There was a significant decrease in the effector response of TWS119-treated cells in response to PMA/ionomycin compared with control cells (Fig. 3*B*). These results were further confirmed by ELISA detecting secreted IFN-γ from PMA/ionomycin-stimulated cells. TWS119-treated cells secreted significantly less IFN-γ (22,706 ± 5,815 pg/ml) than did control cells (41,306 ± 3,081 pg/ml, $p = 0.02$) (Fig. 3*C*).

To study the effect of Wnt signaling on effector function in an Ag-specific setting, CAR CD19-redirected T cells were cocultured with CD19-expressing Raji cells in the presence of DMSO or TWS119 for 5 d. Whereas the DMSO control CAR CD19 cells were able to eliminate the tumor cells from the culture, the TWS119-treated CAR CD19 cells were unable to eliminate the

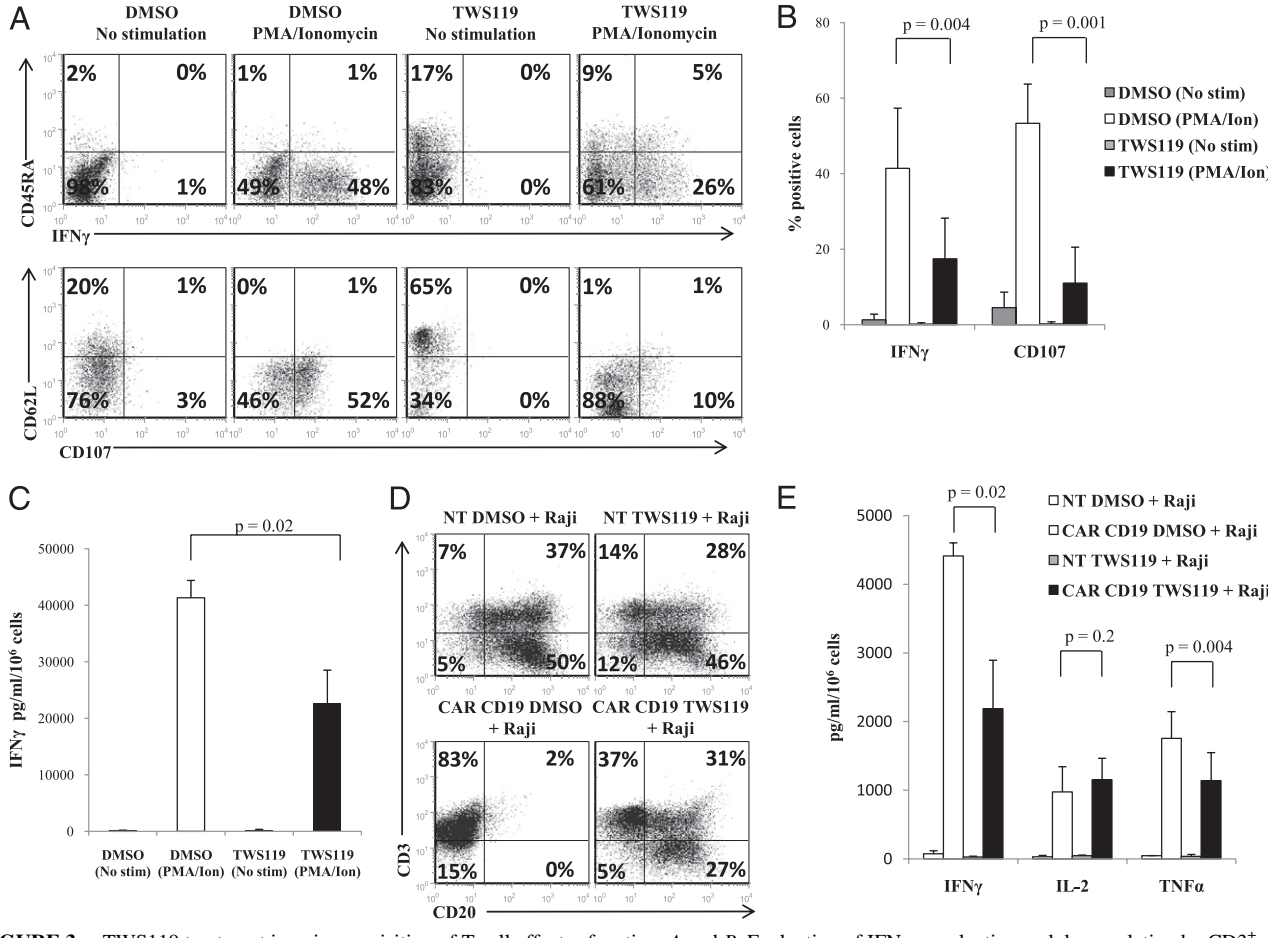

FIGURE 3. TWS119 treatment impairs acquisition of T cell effector function. *A* and *B*, Evaluation of IFN-γ production and degranulation by $CD3^+$ cells cultured for a week in DMSO or 3 μM TWS119 by flow cytometry. *A*, Representative plot and (*B*) percentages of DMSO- or TWS119-treated $CD3^+$ cells that express CD107 and intracellular IFN-γ in response to PMA/ionomycin stimulation. Data summarize means ± SD of at least four independent experiments. *C*, ELISA assessment of IFN-γ release in supernatant of PMA/ionomycin-stimulated T cells that had been treated for a week with DMSO or 3 μM TWS119. Data summarize means ± SD of three independent experiments. *D* and *E*, Evaluation of cytotoxic function and cytokine production of Ag-specific T cells cultured with DMSO or 3 μM TWS119 cells with $CD19^+$ Raji cells at 5:1 ratio for 5 d. Nontransduced (NT) DMSO- or TWS119-treated T cells served as negative controls. *D*, Representative plot of $CD20^+$ residual tumor cells in coculture of CAR CD19-redirected T cells with Raji cells. Data are from one of two independent experiments. *E*, Cytokines in the 24 h supernatant of coculture of CAR T cells with Raji cells assessed by cytometric bead array. Data summarize mean ± SD of three independent experiments.

tumor cells completely (Fig. 3*D*). The production of IFN-γ and TNF-α in the coculture of TWS119 CAR CD19 T cells and Raji cells was also significantly lower than in the control DMSO CAR CD19 T cells (Fig. 3*E*). Therefore, Wnt signaling induced by TWS119 inhibits full acquisition of effector function of T cells.

TWS119-induced Wnt signaling arrests the expansion of polyclonally activated T cells

The transition of naive into effector T cells induced by T cell activation is accompanied by cell proliferation. Because Wnt signaling inhibits naive-to-effector T cell differentiation, we wanted to determine whether Wnt signaling also arrests concomitant T cell expansion of naive or effector T cells. As shown in Fig. 4*A*, both $CD3^+CD45RA^+$ and $CD3^+CD45RO^+$ cells numerically expanded 2- to 3-fold in response to polyclonal activation by day 7 culture. In contrast, TWS119 treatment severely limited expansion of both T cell subsets. To discover whether this TWS119-mediated effect was the result of increased cell death induced by TWS119, impaired cell proliferation, or both, we analyzed apoptosis and cell division by annexin V/7AAD staining and CFSE dilution, respectively. As shown in Fig. 4*B*, TWS119 treatment did not cause a significant increase in cell death compared with control DMSO-treated cells in either $CD3^+CD45RO^+$ (78 ± 6% and 73 ± 6% annexin V^-7AAD^- for TWS119- and DMSO-treated cells, respectively; $p = 0.4$) or $CD3^+CD45RA^+$ cells (80 ± 10% and 52 ± 8% annexin V^-7AAD^- for TWS119- and DMSO-treated cells, respectively; $p = 0.08$). In contrast, in terms of proliferation, whereas control-activated $CD3^+CD45RA^+$ and $CD3^+CD45RO^+$ cells divided robustly (88 ± 7% and 90 ± 5% diluted CFSE), activated cells treated with TWS119 did not proliferate significantly (27 ± 29% and 6 ± 5% diluted CFSE, $p = 0.004$ and <0.001, respectively), similar to nonactivated cells (Fig. 4*C*, 4*D*). As expected, proliferating DMSO-treated $CD3^+CD45RA^+$ cells lost expression of CD45RA and CD62L, but TWS119-treated cells maintained their CD62L and CD45RA expression (Fig. 4*D*). Therefore, Wnt signaling reduced the expansion of T cells by causing an arrest in cell division.

To confirm that TWS119 treatment arrested cell division and blocked transition of $CD45RA^+$ to $CD45RO^+$ cells independently of the mode of T cell activation, PHA was used to activate the T cells instead of OKT3/anti-CD28. As expected, TWS119 treatment preserved the $CD45RA^+$ phenotype in PHA-activated T cells compared with control cells and also blocked cell division (Fig. 5*A*, 5*B*). We also confirmed that the observed effects on T cell phenotype were the result of induced Wnt signaling and not off-target effects of TWS119. Treatment of PHA-activated cells with physiological canonical Wnt ligand Wnt-3a recapitulated the results seen with TWS119 (Fig. 5*C*, 5*D*). In other words, Wnt signaling preserves the naive $CD62L^+CD45RA^+$ phenotype and limits cell expansion in activated T cells irrespective of the mode of induction of Wnt signaling or mode of T cell activation.

Based on the observed effect of Wnt signaling in arresting proliferation and naive-to-effector differentiation, we predicted that Wnt signaling impairs T cell activation, which induces proliferation

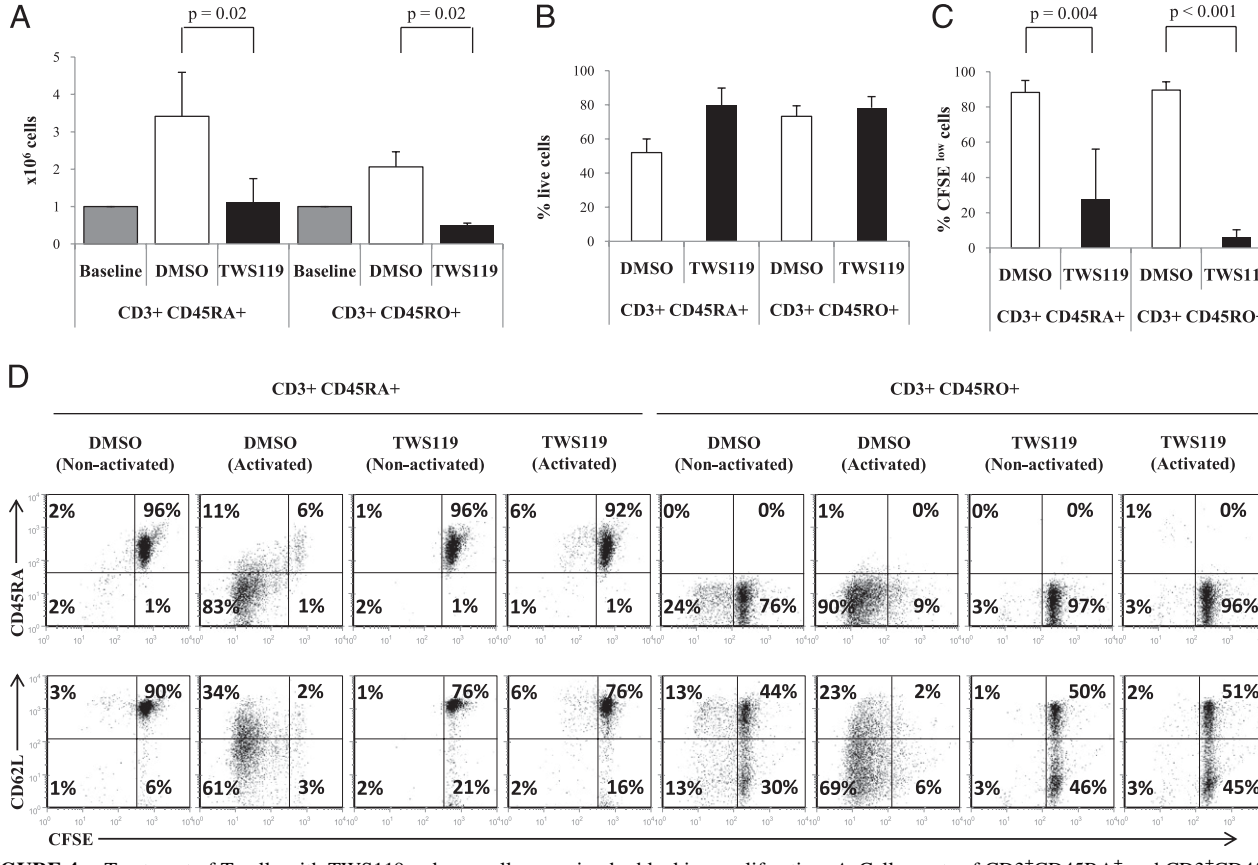

FIGURE 4. Treatment of T cells with TWS119 reduces cell expansion by blocking proliferation. *A*, Cell counts of $CD3^+CD45RA^+$ and $CD3^+CD45RO^+$ cells activated and cultured with DMSO or 3 μM TWS119 for 1 wk. Data summarize mean ± SD of at least three independent experiments. *B*, Assessment of live cell population, denoted by percentage of annexin V^-7AAD^- cells, at the end of 1 wk culture with DMSO or 3 μM TWS119. Data summarize mean ± SD of three independent experiments. *C* and *D*, Evaluation of T cell proliferation by CFSE dilution of $CD3^+CD45RO^+$ and $CD3^+CD45RA^+$ cells activated or left nonactivated and cultured with DMSO or 3 μM TWS119 for 7 d. Percentages of dividing cells after activation represent the $CFSE^{low}$ cells. Data summarize means ± SD of at least three independent experiments.

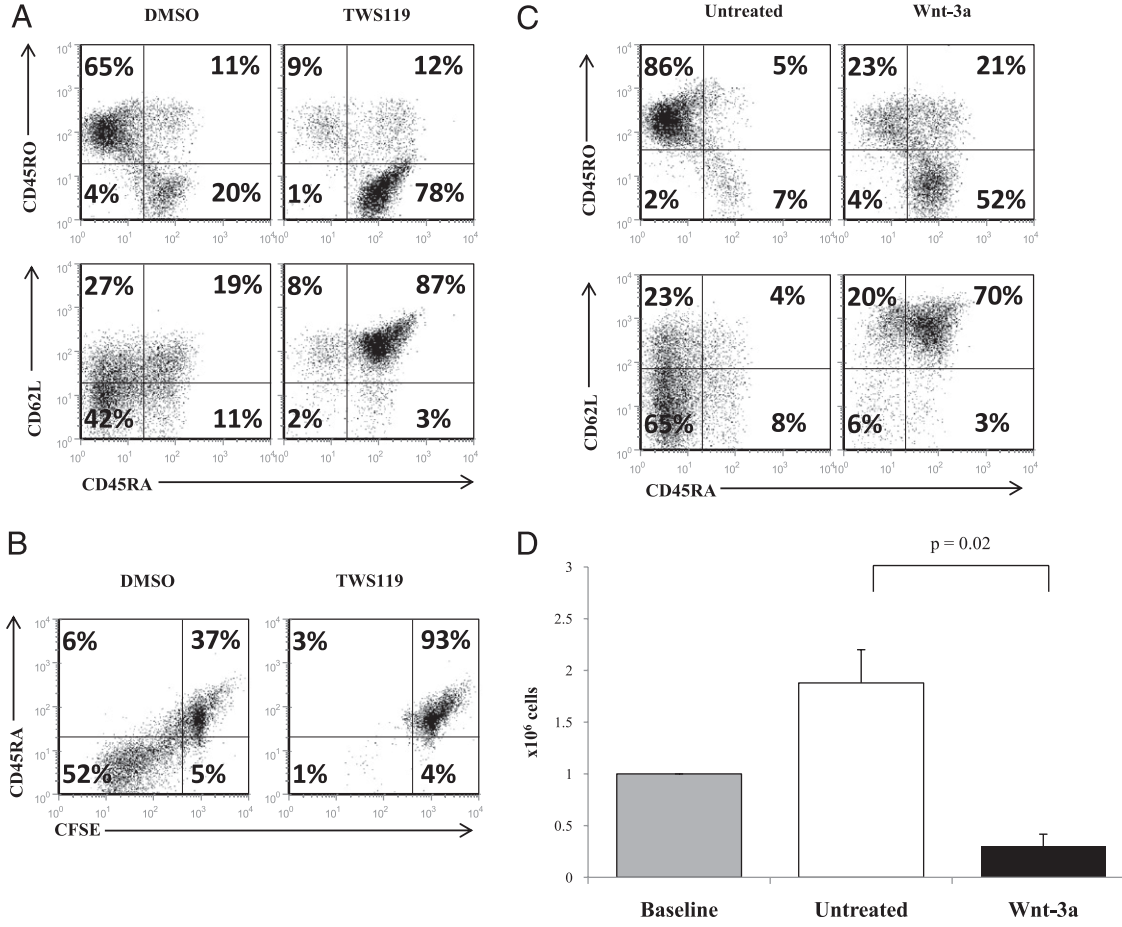

FIGURE 5. PHA activation of T cells or induction of Wnt signaling by Wnt-3a produces similar effects as OKT3/anti-CD28–activated, TWS119-treated T cells. *A*, Expression of CD62L, CD45RA, and CD45RO in T cells activated with 5 μg/ml PHA and cultured with DMSO or 3 μM TWS119 for 7 d. *B*, Cells were stained with CFSE and cultured with DMSO or 3 μM TWS119 and the extent of proliferation was measured in terms of CFSE dilution by day 7 of culture. *C*, Expression of CD62L, CD45RA, and CD45RO in T cells activated and cultured with or without Wnt-3a (5 μg/ml) for 7 d. *D*, Cell counts at the 7 d culture with or without Wnt-3a (5 μg/ml) were determined. Data summarize means ± SD of three independent experiments

and differentiation of T cells. The kinetics of expression of early and late T cell activation markers, CD69 and CD25 (20–23), was examined in cells treated with DMSO or TWS119. As expected, activated control cells rapidly upregulated both CD69 and CD25 (Fig. 6*A*). However, TWS119-treated cells continuously maintained low expression of CD69 and CD25, indicating that T cell activation is impaired in these cells (Fig. 6*A*). We also performed immunoblot analysis to examine the effect of TWS119 on the activation status of signaling molecules LAT and PLCγ, which are directly downstream of T cell activation. As illustrated in Supplemental Fig. 1*D*, the phosphorylation of Y783 in PLCγ and Y132 in LAT was severely impaired in TWS119-treated cells. This is consistent with published observations in mouse T cells in which proximal TCR signaling was inhibited by constitutively active β-catenin (12).

To begin to investigate the mechanism by which Wnt signaling arrests proliferation of T cells, we tested the ability of these cells to produce IL-2, a cytokine that supports T cell expansion upon activation. CD3-selected T cells activated and expanded for a week with or without TWS119 were stimulated overnight with PMA and ionomycin to induce IL-2 production. Intracellular staining showed comparable numbers of IL-2–producing cells in the TWS119 treatment group (22 ± 8%) and the control group (17 ± 11%, $p = 0.1$) (Fig. 6*B*, 6*C*). These results were confirmed by detection of secreted IL-2 in the supernatant of PMA/ionomycin-stimulated T cells by ELISA. There was no significant difference in the amount of IL-2 in the supernatants of DMSO-treated cells (1890 ± 736 pg/ml) and TWS119-treated cells (2554 ± 1466 pg/ml, $p = 0.7$) (Fig. 6*D*). Therefore, a difference in IL-2 production does not seem to account for the observed Wnt-induced arrest in proliferation. However, the ability of these TWS119-treated cells to use IL-2 would be affected by the expression of the IL-2R on activated T cells. As illustrated in Fig. 6*A*, the expression of the IL-2Rα-chain, CD25, was significantly lower in TWS119-treated cells (7 ± 4%) compared with control cells (99 ± 1%, $p < 0.001$) at day 7 (Fig. 6*A*, 6*E*). This indicates that although TWS119-treated cells are able to produce IL-2, they may have reduced ability to use this cytokine for expansion.

The effect of TWS119 on T cell proliferation and differentiation could also be cell-extrinsic. As shown in Fig. 6*E*, a small subset of T cells express CD25 after TWS119 treatment (7 ± 4%) and this could contain natural Tregs (nTregs), as Wnt signaling has been reported to enhance nTreg survival (24). Because the presence of Tregs may cause the observed arrest in T cell proliferation and differentiation, CD25-expressing cells were depleted prior to CD3 selection to eliminate nTregs. The cells were then activated and cultured in the presence of DMSO or 3 μM TWS119. At the end of 7 d culture, the subset of $CD4^+CD25^+$ cells was negligible but comparable in both $CD3^+$ and $CD3^+CD25^{depleted}$ cells after TWS119 treatment (Supplemental Fig. 2*A*). Furthermore, depletion of $CD25^+$ cells (containing nTregs) did not reverse the impaired expansion of T cells induced by TWS119 treatment (Sup-

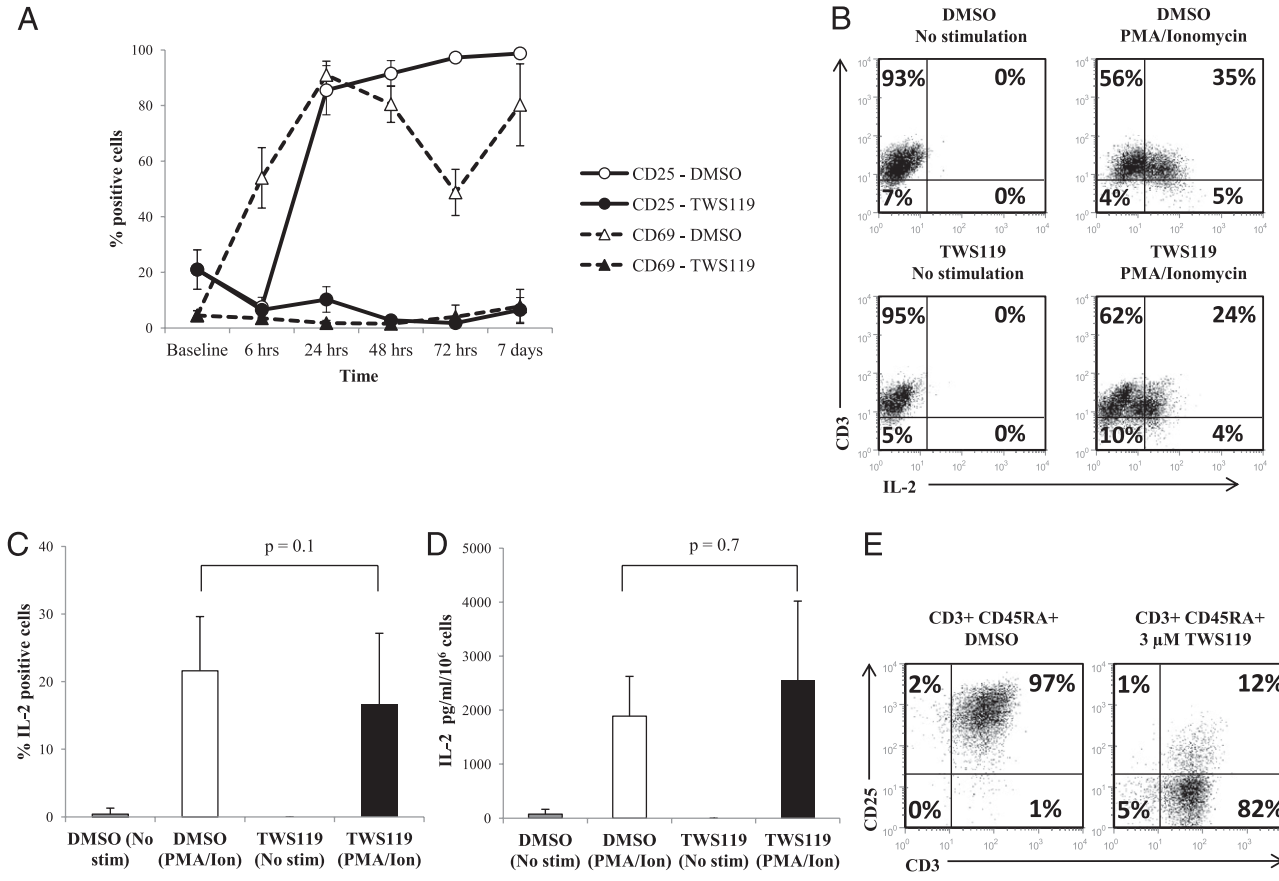

FIGURE 6. TWS119 treatment inhibits expression of activation markers CD25 and CD69 but not production of IL-2. *A*, Evaluation of CD25 and CD69 expression by $CD3^+$ cells treated for a week with DMSO (solid line; ○, △) or 3 μM TWS119 (dotted line; ●, ▲) by flow cytometry at the indicated time points. Data summarize means ± SD of three independent experiments. *B* and *C*, Evaluation of IL-2 production by $CD3^+$ cells cultured for a week in DMSO or 3 μM TWS119 by intracellular staining. *B*, Representative plot and (*C*) percentages of DMSO- or TWS119-treated $CD3^+$ cells that express intracellular IL-2 in response to PMA/ionomycin stimulation. Data summarize means ± SD of five independent experiments. *D*, ELISA assessment of IL-2 release in supernatant of PMA/ionomycin-stimulated T cells that had been cultured for a week with DMSO or 3 μM TWS119. Data summarize means ± SD of three independent experiments. *E*, Evaluation of CD25 expression on $CD3^+CD45RA^+$ cells treated with DMSO or 3 μM TWS119 for a week. Plots are from one of three independent experiments.

plemental Fig. 2*B*, 2*C*). This indicates that the Wnt-induced effects on T cell phenotype, proliferation, and effector differentiation are not mediated by an indirect effect of nTregs.

Cytokines overcome the block in T cell proliferation mediated by TWS119 but also cause a loss of the naive phenotype of T cells

Although reduced IL-2Rα expression may explain how TWS119 impairs T cell proliferation in the presence of physiological levels of IL-2 (25), we wanted to test whether pharmacological doses of growth factors can rescue the arrested expansion of Wnt-activated cells. Addition of exogenous γ-chain cytokines (IL-15, IL-7, or IL-2) in the presence of TWS119 overcame the block in cell proliferation, allowing T cell division as assessed by CFSE dilution assay (Fig. 7*A*) and numeric expansion similar to control cells (data not shown). However, cytokine-induced proliferation also led to a loss of the TWS119-induced naive phenotype (Fig. 7*B*). By day 7 culture, the naive $CD45RA^+CD62L^+$ subset was significantly reduced by the addition of cytokines IL-15, IL-7, or IL-2 to the TWS119-treated cells (from an average of 69 ± 12% to 15 ± 6%, 21 ± 12%, and 29 ± 16%; $p = 0.015$, 0.041 and 0.008, respectively) and was comparable to the DMSO-treated cells (6 ± 3%, $p > 0.1$). Therefore, addition of cytokines rescued the blocked proliferation of Wnt-arrested T cells and concomitantly led to a loss of the naive T cell phenotype.

Although Wnt signaling induced by TWS119 or Wnt-3a clearly arrests T cell proliferation and naive-to-effector cell differentiation in our in vitro cultures, we wanted to investigate whether these Wnt signaling effects imprint on T cell phenotype and function over a long term. Activated T cells cultured with TWS119 for a week were restimulated with OKT3 and anti-CD28 Abs and cultured for an additional week in the presence of DMSO or TWS119. As illustrated in Supplemental Fig. 3*A*, TWS119-treated cells that were deprived of the drug for the second week did not retain the naive phenotype and became activated effector cells similar to control DMSO-treated cells. The effector function of these cells as illustrated by production of IFN-γ and degranulation (CD107 expression) was slightly reduced or comparable to control DMSO cells (Supplemental Fig. 3*B*). In the case of Ag-redirected cells, TWS119-treated CAR CD19 cells that were deprived of this drug upon coculture with the Raji cells were able to recover their cytotoxic function and completely eliminate the tumor cells similar to DMSO-treated CAR CD19 T cells (Supplemental Fig. 3*C*). We also conducted experiments where the $CD3^+$ cells were transiently exposed to DMSO or TWS119 for 24 h following which the drug was washed out of the culture. As shown in Supplemental Fig. 3*D* and 3*E*, transient exposure to the TWS119 does not arrest the expansion and activation (CD25, CD69 expression) or preserve the naive phenotype (CD45RA expression) of these T cells. Therefore, the T cells are arrested in expansion and naive-to-

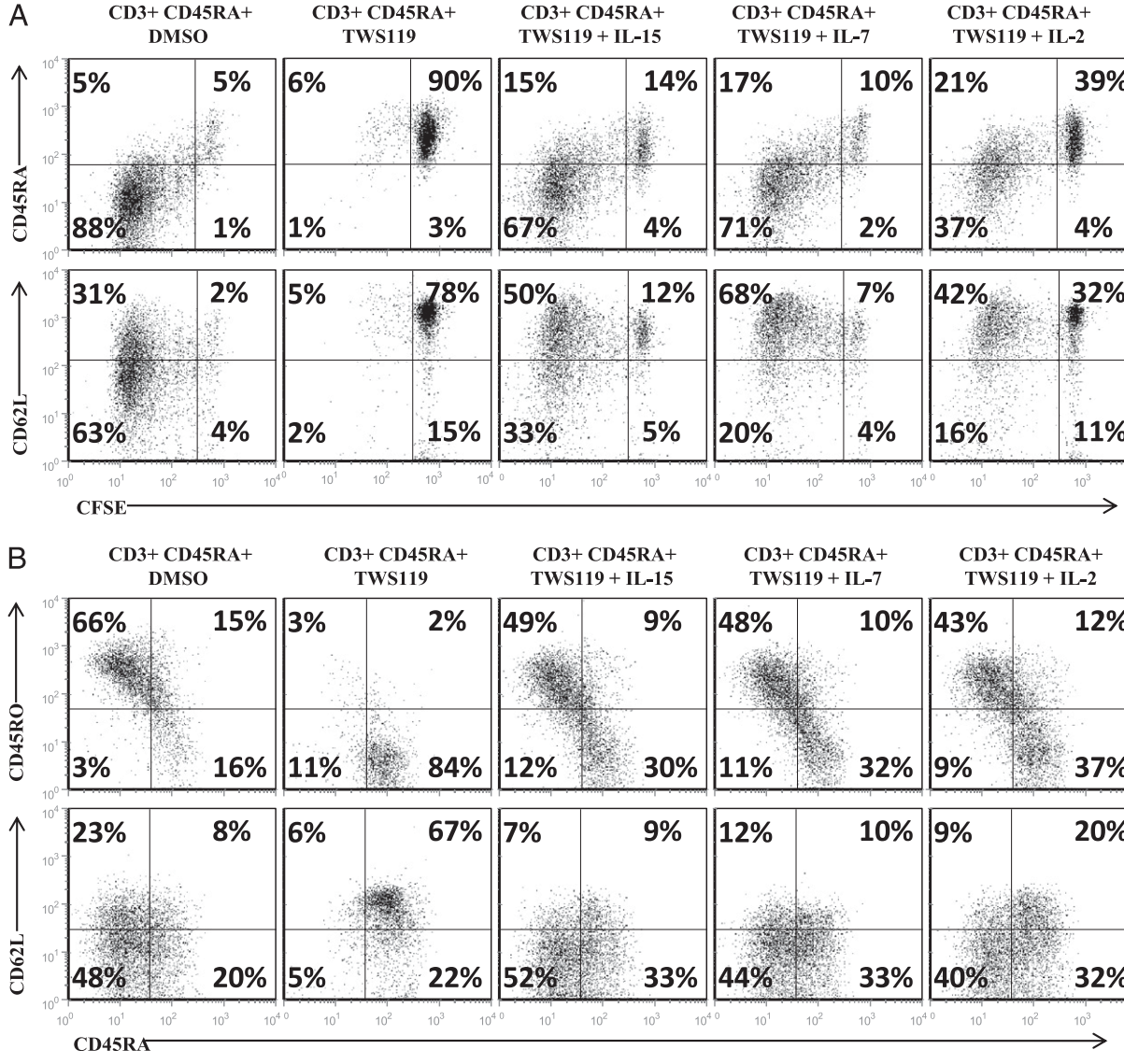

FIGURE 7. Cytokines can overcome the block in proliferation induced by TWS119 treatment but they lead to a concomitant loss of the naive T cell phenotype. *A*, Evaluation of proliferation of $CD3^+CD45RA^+$ cells cultured for a week with DMSO or 3 μM TWS119 in the absence or presence of IL-15 (5 ng/ml), IL-7 (10 ng/ml), or IL-2 (50 U/ml) using CFSE dilution assay. Plots show the extent of proliferation in terms of CFSE dilution by day 7 of culture. *B*, Analysis by flow cytometry of CD45RA, CD45RO, or CD62L expression by these cells at the end of 7 d culture in the absence or presence of the cytokines. Dot plots are from one of three independent experiments.

effector cell differentiation only in the continuous presence of the drug, and upon removal of the Wnt-signaling agonist, the T cells overcome this arrest and become effector cells. These results indicate that TWS119 treatment does not imprint on T cell phenotype and function.

TWS119 treatment of cord blood-derived T cells arrests proliferation and preserves the naive T cell phenotype

To determine whether Wnt signaling impairs proliferation and maintains a naive phenotype in peripheral T cells irrespective of the source of T cells, we repeated these experiments with umbilical cord blood-derived mononuclear cells, a source of phenotypically and functionally immature circulating T cells (15). As shown in Fig. 8*A* and 8*B*, activated T cells treated with TWS119 had increased expression of CD45RA (20 ± 11%) and CD62L (68 ± 21%) and reduced CD45RO expression (57 ± 7%) compared with control cells (3 ± 3%, 12 ± 16%, and 87 ± 7%; $p = 0.005$, 0.001, and <0.001, respectively) at the end of a week's culture. TWS119 also impaired proliferation of cord blood-derived T cells (Fig. 8*C*, 8*D*). Therefore, TWS119 treatment of T cells derived from umbilical cord blood recapitulated the results seen with T cells isolated from peripheral blood.

Discussion

Although Wnt signaling has been studied extensively in T cell development, its function in peripheral T cells has not been well defined and, to our knowledge, this is the first report evaluating the effects of induction of Wnt signaling on effector T cell differentiation in human T lymphocytes. We found that activation of Wnt signaling blocked the transition of naive T cells ($CD45RA^+$ $CD62L^+$) to effector T cells ($CD45RO^+CD62L^-$) but did not cause reversion of $CD45RO^+$ cells to CD45RA-expressing cells. Wnt signaling arrested T cell division and impaired the acquisition of effector function in response to polyclonal stimulation. Similar results were also observed in immature peripheral T cells derived from umbilical cord blood. Our phenotypic and functional in vitro data indicate that Wnt signaling inhibits the naive-to-effector differentiation of human T lymphocytes.

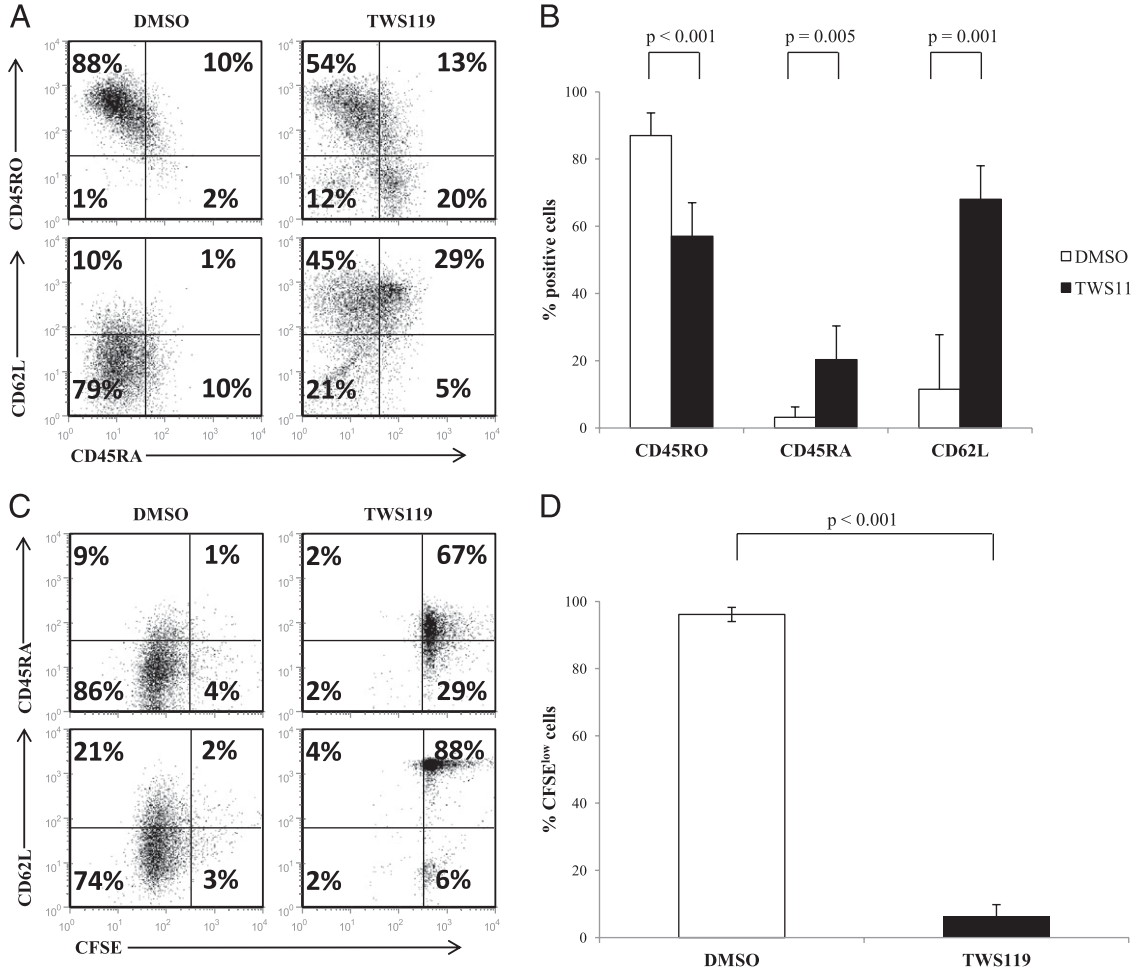

FIGURE 8. TWS119 treatment blocks transition of CD45RA$^+$ cells into CD45RO$^+$ cells in cord blood-derived T cells. *A*, Representative dot plots and (*B*) percentage of cells expressing CD45RA, CD62L, and CD45RO for CD3$^+$ T cells isolated from cord blood-derived mononuclear cells and cultured with DMSO or 3 μM TWS119 for 7 d. Data summarize means ± SD of five independent experiments. *C* and *D*, Assessment of cord blood-derived mononuclear cell-derived CD3$^+$ T cell proliferation using CFSE dilution assay after a week of culture with DMSO or 3 μM TWS119. Data summarize mean ± SD of three independent experiments.

Our findings are consistent with those of Driessens et al. (12) in mice who observed that genetically stabilized β-catenin inhibited mouse T cell activation and proliferation and impaired the function of Th1-, Th2-, and Th17-polarized cells. In particular, those authors demonstrated that β-catenin prevented the activation of the LAT/PLCγ1/Ca^{2+} pathway by diminishing phosphorylation of a specific residue in LAT, leading to defective recruitment of PLCγ1 to LAT. Consistent with these findings, we observed a similar impairment of phosphorylation in these TCR signaling molecules in TWS119-treated human T cells. We found that TWS119-treated cells had significantly reduced expression of IL-2Rα, and this may partially explain their impaired proliferation. Although the IL-2Rβ- and γ-chains are sufficient for IL-2R signaling in the presence of high levels of IL-2, the IL-2Rα is required to form the high-affinity IL-2R, which can use low physiological doses of IL-2 for expansion (25, 26). Because IL-2Rα is upregulated in T cells as a result of TCR activation (27, 28), and because inhibition of proximal TCR-induced IL-2Rα expression has been shown to be rescued by treatment with protein kinase C activator PMA and a Ca^{2+} ionophore (29), we speculate that the Wnt-induced inhibition of IL-2Rα expression illustrated in our experiments may be the consequence of inhibition of the LAT/PLCγ1/protein kinase C/Ca^{2+} pathway by Wnt signaling. Also note that TWS119-mediated inhibition of TCR activation would be expected to reduce IL-2 production (30). Although supernatants of TWS119-treated and control cells showed comparable levels of IL-2, a reduction in IL-2 production from TWS119-treated cells may be obscured due to the high consumption of IL-2 by CD25 expressing control-activated T cells. Further investigation will be required to fully identify the mechanisms by which Wnt signaling arrests T cell activation and proliferation in human cells.

Our results also agree in part with the findings of Gattinoni et al. (11) who reported that differentiation and production of IFN-γ of CD8$^+$ pmel-1 TCR transgenic mouse T cells in response to Ag stimulation were inhibited by TWS119-induced activation of Wnt signaling. Our data show that these inhibitory effects of Wnt signaling can be measured not only in CD8$^+$ T cells but also in CD4$^+$ naive T cells, indicating that this pathway is similar in both CD4$^+$ and CD8$^+$ T cells. However, we found that at the lowest dose of TWS119 (3 μM) that was required to obtain significant and consistent preservation of the naive T cell subset, T cell division was almost completely inhibited. Our experiments examining cell cycle show that most TWS119-treated cells are arrested at the G_0/G_1 phase in the cell cycle (data not shown). This observation is not in line with Gattinoni's study in which the CD8$^+$ pmel-1 TCR transgenic mouse T cells retained a significant proliferative capacity while maintaining a naive phenotype at similar TWS119 doses.

This discrepancy may arise from a number of factors including but not limited to differences in culture conditions of mouse versus human T cells, the intrinsic differences in T cells, namely, transgenic TCR T cells compared with polyclonal or CAR-redirected T lymphocytes, and also the magnitude of differences in Wnt target gene expression induced by TWS119 in both cases. The large induction of Wnt target genes such as *Fzd7* observed by Gattinoni et al. (11) may correlate with a higher level of Wnt signaling activity in the pmel-1 TCR transgenic mouse T cells compared with human T lymphocytes and may explain the divergence in the results. The authors also used APCs for activation of mouse T cells compared with our use of Abs for polyclonal activation of human T cells. However, our overall findings are consistent with conclusions from other studies that Wnt signaling inhibits T cell activation, expansion, and naive-to-effector differentiation.

The Wnt signaling-induced block in expansion and effector function of T cells may play a role in vivo in different situations. For instance, certain tumors, such as prostate cancer cells, secrete Wnt ligands into the tumor microenvironment (31). This could activate Wnt/β-catenin signaling in T cells targeting the tumor and inhibit their expansion and function. Because dysregulation of the Wnt signaling pathway has been implicated in various cancers, several studies are underway to target and inhibit this pathway in tumors (32, 33). Based on our data, inhibition of Wnt signaling at the tumor site may target the tumor in multiple ways—directly by inhibiting the signaling pathway in the tumor cells, and indirectly by reversing the inhibitory effects of Wnt signaling on T cells in the tumor microenvironment.

Another possibility is that activation of Wnt signaling in T cells may be induced in a tolerogenic setting. Macrophages and dendritic cells can produce canonical Wnt ligands (34, 35). It has been shown that constitutive expression of β-catenin in Tregs extends their survival and improves their suppressive function (24). Stable β-catenin expression also induced anergy in $CD4^+CD25^-$ cells in terms of reduced proliferation, increased expression of anergy-associated genes (Cblb, GRAIL, Itch), and reduced capacity to induce inflammatory disease in vivo (24). β-catenin signaling in intestinal dendritic cells induced tolerance via Treg induction and suppression of effector cells (36). Therefore, our data in conjunction with the literature support the hypothesis that Wnt signaling may induce a tolerogenic program in immune cells such as dendritic cells and T cells.

In addition to its role in effector T cell differentiation, Gattinoni et al. (11) also reported that Wnt signaling induced a subset of T memory stem cells that possessed a naive phenotype despite undergoing several cycles of cell division in vitro and that were characterized by self-renewal abilities, long-term persistence, and potent anti-tumor function in vivo. Recapitulating these results in Ag-specific human T cells using Wnt signaling would have a major impact on clinical applications of adoptive T cell therapy in cancer patients. A current limitation of this approach is indeed the short-term persistence of ex vivo-expanded Ag-specific T cells upon infusion into the patient, which is likely due to the presence of predominantly effector cells with limited life spans (37–39). The infusion of Ag-specific T cells with high renewal capacity would enhance clinical responses in cancer patients, as has been observed upon infusion of memory or naive T cells (13, 14, 40–42). We tested for the expression of Tscm markers including CD122 and Bcl-2, which were observed in Gattinoni et al. (11) on the TWS119-induced naive subset of T cells, and found no difference in expression of these markers compared with control-activated cells (data not shown). However, our results in vitro were obtained using polyclonally activated T cells, and this precludes us from evaluating whether Wnt signaling can be used to generate Ag-specific human T memory stem cells with potent anti-tumor effects in vivo.

Additionally, human Ag-specific T cells are expanded ex vivo by repeated stimulations of T cells with APCs (43–45), and thus Wnt signaling cannot be induced in this setting because it will inhibit T cell division. However, gene modification of the human T lymphocytes has been implemented to confer them with Ag specificity by the expression of transgenic TCRs or CARs (16, 46–48). Transduction of T cells in the presence of an optimal dose of TWS119 may preserve the naive status of these cells and could enhance their persistence in vivo after adoptive transfer. Examination of the effect of canonical Wnt signaling on Ag-specific human T cells in in vivo studies may also show more promising results in terms of generation of Tscm cells for adoptive T cell therapy.

In conclusion, we have identified the role of canonical Wnt signaling as a negative regulator in human peripheral T cell effector differentiation. In the presence of Wnt/β-catenin signaling, the T cells are arrested in their naive phenotype, impaired in the acquisition of effector function, and show inhibited cell proliferation. Because Wnt signaling does not imprint on the T cell phenotype and effector function, the cells should be able to expand and become effectors upon removal of the Wnt agonist. Therefore, Wnt signaling may be useful for the ex vivo maintenance of naive T cells for adoptive immunotherapy for cancer.

Acknowledgments

We are grateful to Reshma Kulkarni for the phenotypic analysis.

Disclosures

The authors have no financial conflicts of interest.

References

1. Mulroy, T., J. A. McMahon, S. J. Burakoff, A. P. McMahon, and J. Sen. 2002. Wnt-1 and Wnt-4 regulate thymic cellularity. *Eur. J. Immunol.* 32: 967–971.
2. Okamura, R. M., M. Sigvardsson, J. Galceran, S. Verbeek, H. Clevers, and R. Grosschedl. 1998. Redundant regulation of T cell differentiation and TCRα gene expression by the transcription factors LEF-1 and TCF-1. *Immunity* 8: 11–20.
3. Staal, F. J., J. Meeldijk, P. Moerer, P. Jay, B. C. van de Weerdt, S. Vainio, G. P. Nolan, and H. Clevers. 2001. Wnt signaling is required for thymocyte development and activates Tcf-1 mediated transcription. *Eur. J. Immunol.* 31: 285–293.
4. Wu, B., S. P. Crampton, and C. C. Hughes. 2007. Wnt signaling induces matrix metalloproteinase expression and regulates T cell transmigration. *Immunity* 26: 227–239.
5. Willinger, T., T. Freeman, M. Herbert, H. Hasegawa, A. J. McMichael, and M. F. Callan. 2006. Human naive CD8 T cells down-regulate expression of the WNT pathway transcription factors lymphoid enhancer binding factor 1 and transcription factor 7 (T cell factor-1) following antigen encounter in vitro and in vivo. *J. Immunol.* 176: 1439–1446.
6. Staal, F. J., T. C. Luis, and M. M. Tiemessen. 2008. WNT signalling in the immune system: WNT is spreading its wings. *Nat. Rev. Immunol.* 8: 581–593.
7. Roose, J., G. Huls, M. van Beest, P. Moerer, K. van der Horn, R. Goldschmeding, T. Logtenberg, and H. Clevers. 1999. Synergy between tumor suppressor *APC* and the β-catenin-Tcf4 target *Tcf1*. *Science* 285: 1923–1926.
8. Hovanes, K., T. W. Li, J. E. Munguia, T. Truong, T. Milovanovic, J. Lawrence Marsh, R. F. Holcombe, and M. L. Waterman. 2001. Beta-catenin-sensitive isoforms of lymphoid enhancer factor-1 are selectively expressed in colon cancer. *Nat. Genet.* 28: 53–57.
9. Zeng, Y. A., and E. M. Verheyen. 2004. Nemo is an inducible antagonist of Wingless signaling during *Drosophila* wing development. *Development* 131: 2911–2920.
10. Mann, B., M. Gelos, A. Siedow, M. L. Hanski, A. Gratchev, M. Ilyas, W. F. Bodmer, M. P. Moyer, E. O. Riecken, H. J. Buhr, and C. Hanski. 1999. Target genes of β-catenin-T cell-factor/lymphoid-enhancer-factor signaling in human colorectal carcinomas. *Proc. Natl. Acad. Sci. USA* 96: 1603–1608.
11. Gattinoni, L., X. S. Zhong, D. C. Palmer, Y. Ji, C. S. Hinrichs, Z. Yu, C. Wrzesinski, A. Boni, L. Cassard, L. M. Garvin, et al. 2009. Wnt signaling arrests effector T cell differentiation and generates $CD8^+$ memory stem cells. *Nat. Med.* 15: 808–813.
12. Driessens, G., Y. Zheng, F. Locke, J. L. Cannon, F. Gounari, and T. F. Gajewski. 2011. Beta-catenin inhibits T cell activation by selective interference with linker

for activation of T cells-phospholipase C-γ1 phosphorylation. *J. Immunol.* 186: 784–790.
13. Gattinoni, L., C. A. Klebanoff, D. C. Palmer, C. Wrzesinski, K. Kerstann, Z. Yu, S. E. Finkelstein, M. R. Theoret, S. A. Rosenberg, and N. P. Restifo. 2005. Acquisition of full effector function in vitro paradoxically impairs the in vivo antitumor efficacy of adoptively transferred $CD8^+$ T cells. *J. Clin. Invest.* 115: 1616–1626.
14. Hinrichs, C. S., Z. A. Borman, L. Cassard, L. Gattinoni, R. Spolski, Z. Yu, L. Sanchez-Perez, P. Muranski, S. J. Kern, C. Logun, et al. 2009. Adoptively transferred effector cells derived from naive rather than central memory $CD8^+$ T cells mediate superior antitumor immunity. *Proc. Natl. Acad. Sci. USA* 106: 17469–17474.
15. Harris, D. T., M. J. Schumacher, J. Locascio, F. J. Besencon, G. B. Olson, D. DeLuca, L. Shenker, J. Bard, and E. A. Boyse. 1992. Phenotypic and functional immaturity of human umbilical cord blood T lymphocytes. *Proc. Natl. Acad. Sci. USA* 89: 10006–10010.
16. Savoldo, B., C. A. Ramos, E. Liu, M. P. Mims, M. J. Keating, G. Carrum, R. T. Kamble, C. M. Bollard, A. P. Gee, Z. Mei, et al. 2011. CD28 costimulation improves expansion and persistence of chimeric antigen receptor-modified T cells in lymphoma patients. *J. Clin. Invest.* 121: 1822–1826.
17. Micklethwaite, K. P., B. Savoldo, P. J. Hanley, A. M. Leen, G. J. Demmler-Harrison, L. J. Cooper, H. Liu, A. P. Gee, E. J. Shpall, C. M. Rooney, et al. 2010. Derivation of human T lymphocytes from cord blood and peripheral blood with antiviral and antileukemic specificity from a single culture as protection against infection and relapse after stem cell transplantation. *Blood* 115: 2695–2703.
18. Lynch, K. W. 2004. Consequences of regulated pre-mRNA splicing in the immune system. *Nat. Rev. Immunol.* 4: 931–940.
19. Hargreaves, M., and E. B. Bell. 1997. Identical expression of CD45R isoforms by $CD45RC^+$ "revertant" memory and $CD45RC^+$ naive CD4 T cells. *Immunology* 91: 323–330.
20. Ziegler, S. F., F. Ramsdell, and M. R. Alderson. 1994. The activation antigen CD69. *Stem Cells* 12: 456–465.
21. Testi, R., J. H. Phillips, and L. L. Lanier. 1989. Leu 23 induction as an early marker of functional CD3/T cell antigen receptor triggering. Requirement for receptor cross-linking, prolonged elevation of intracellular $[Ca^{++}]$ and stimulation of protein kinase C. *J. Immunol.* 142: 1854–1860.
22. Zola, H. 2000. Markers of cell lineage, differentiation and activation. *J. Biol. Regul. Homeost. Agents* 14: 218–219.
23. Schuh, K., T. Twardzik, B. Kneitz, J. Heyer, A. Schimpl, and E. Serfling. 1998. The interleukin 2 receptor α chain/CD25 promoter is a target for nuclear factor of activated T cells. *J. Exp. Med.* 188: 1369–1373.
24. Graham, J. A., M. Fray, S. de Haseth, K. M. Lee, M. M. Lian, C. M. Chase, J. C. Madsen, J. Markmann, G. Benichou, R. B. Colvin, et al. 2010. Suppressive regulatory T cell activity is potentiated by glycogen synthase kinase 3β inhibition. *J. Biol. Chem.* 285: 32852–32859.
25. Nguyen, T., R. Wang, and J. H. Russell. 2000. IL-12 enhances IL-2 function by inducing CD25 expression through a p38 mitogen-activated protein kinase pathway. *Eur. J. Immunol.* 30: 1445–1452.
26. Johnston, J. A., C. M. Bacon, M. C. Riedy, and J. J. O'Shea. 1996. Signaling by IL-2 and related cytokines: JAKs, STATs, and relationship to immunodeficiency. *J. Leukoc. Biol.* 60: 441–452.
27. Gupta, S., M. Shimizu, K. Ohira, and B. Vayuvegula. 1991. T cell activation via the T cell receptor: a comparison between WT31 (defining α/β TcR)-induced and anti-CD3-induced activation of human T lymphocytes. *Cell. Immunol.* 132: 26–44.
28. Leonard, W. J., M. Krönke, N. J. Peffer, J. M. Depper, and W. C. Greene. 1985. Interleukin 2 receptor gene expression in normal human T lymphocytes. *Proc. Natl. Acad. Sci. USA* 82: 6281–6285.
29. Trevillyan, J. M., Y. L. Lu, D. Atluru, C. A. Phillips, and J. M. Bjorndahl. 1990. Differential inhibition of T cell receptor signal transduction and early activation events by a selective inhibitor of protein-tyrosine kinase. *J. Immunol.* 145: 3223–3230.
30. Isakov, N., and A. Altman. 2002. Protein kinase Cθ in T cell activation. *Annu. Rev. Immunol.* 20: 761–794.
31. Hall, C. L., S. Kang, O. A. MacDougald, and E. T. Keller. 2006. Role of Wnts in prostate cancer bone metastases. *J. Cell. Biochem.* 97: 661–672.
32. Luu, H. H., R. Zhang, R. C. Haydon, E. Rayburn, Q. Kang, W. Si, J. K. Park, H. Wang, Y. Peng, W. Jiang, and T. C. He. 2004. Wnt/β-catenin signaling pathway as a novel cancer drug target. *Curr. Cancer Drug Targets* 4: 653–671.
33. Garber, K. 2009. Drugging the Wnt pathway: problems and progress. *J. Natl. Cancer Inst.* 101: 548–550.
34. Lobov, I. B., S. Rao, T. J. Carroll, J. E. Vallance, M. Ito, J. K. Ondr, S. Kurup, D. A. Glass, M. S. Patel, W. Shu, et al. 2005. WNT7b mediates macrophage-induced programmed cell death in patterning of the vasculature. *Nature* 437: 417–421.
35. Lehtonen, A., H. Ahlfors, V. Veckman, M. Miettinen, R. Lahesmaa, and I. Julkunen. 2007. Gene expression profiling during differentiation of human monocytes to macrophages or dendritic cells. *J. Leukoc. Biol.* 82: 710–720.
36. Manicassamy, S., B. Reizis, R. Ravindran, H. Nakaya, R. M. Salazar-Gonzalez, Y. C. Wang, and B. Pulendran. 2010. Activation of β-catenin in dendritic cells regulates immunity versus tolerance in the intestine. *Science* 329: 849–853.
37. Dudley, M. E., J. Wunderlich, M. I. Nishimura, D. Yu, J. C. Yang, S. L. Topalian, D. J. Schwartzentruber, P. Hwu, F. M. Marincola, R. Sherry, et al. 2001. Adoptive transfer of cloned melanoma-reactive T lymphocytes for the treatment of patients with metastatic melanoma. *J. Immunother.* 24: 363–373.
38. Yee, C., J. A. Thompson, D. Byrd, S. R. Riddell, P. Roche, E. Celis, and P. D. Greenberg. 2002. Adoptive T cell therapy using antigen-specific $CD8^+$ T cell clones for the treatment of patients with metastatic melanoma: in vivo persistence, migration, and antitumor effect of transferred T cells. *Proc. Natl. Acad. Sci. USA* 99: 16168–16173.
39. Robbins, P. F., M. E. Dudley, J. Wunderlich, M. El-Gamil, Y. F. Li, J. Zhou, J. Huang, D. J. Powell, Jr., and S. A. Rosenberg. 2004. Cutting edge: persistence of transferred lymphocyte clonotypes correlates with cancer regression in patients receiving cell transfer therapy. *J. Immunol.* 173: 7125–7130.
40. Hinrichs, C. S., Z. A. Borman, L. Gattinoni, Z. Yu, W. R. Burns, J. Huang, C. A. Klebanoff, L. A. Johnson, S. P. Kerkar, S. Yang, et al. 2011. Human effector $CD8^+$ T cells derived from naive rather than memory subsets possess superior traits for adoptive immunotherapy. *Blood* 117: 808–814.
41. Berger, C., M. C. Jensen, P. M. Lansdorp, M. Gough, C. Elliott, and S. R. Riddell. 2008. Adoptive transfer of effector $CD8^+$ T cells derived from central memory cells establishes persistent T cell memory in primates. *J. Clin. Invest.* 118: 294–305.
42. Rolle, C. E., R. Carrio, and T. R. Malek. 2008. Modeling the $CD8^+$ T effector to memory transition in adoptive T-cell antitumor immunotherapy. *Cancer Res.* 68: 2984–2992.
43. Savoldo, B., M. L. Cubbage, A. G. Durett, J. Goss, M. H. Huls, Z. Liu, L. Teresita, A. P. Gee, P. D. Ling, M. K. Brenner, et al. 2002. Generation of EBV-specific $CD4^+$ cytotoxic T cells from virus naive individuals. *J. Immunol.* 168: 909–918.
44. Tsai, V., I. Kawashima, E. Keogh, K. Daly, A. Sette, and E. Celis. 1998. In vitro immunization and expansion of antigen-specific cytotoxic T lymphocytes for adoptive immunotherapy using peptide-pulsed dendritic cells. *Crit. Rev. Immunol.* 18: 65–75.
45. Heslop, H. E., C. Y. Ng, C. Li, C. A. Smith, S. K. Loftin, R. A. Krance, M. K. Brenner, and C. M. Rooney. 1996. Long-term restoration of immunity against Epstein-Barr virus infection by adoptive transfer of gene-modified virus-specific T lymphocytes. *Nat. Med.* 2: 551–555.
46. June, C. H., B. R. Blazar, and J. L. Riley. 2009. Engineering lymphocyte subsets: tools, trials and tribulations. *Nat. Rev. Immunol.* 9: 704–716.
47. Till, B. G., M. C. Jensen, J. Wang, E. Y. Chen, B. L. Wood, H. A. Greisman, X. Qian, S. E. James, A. Raubitschek, S. J. Forman, et al. 2008. Adoptive immunotherapy for indolent non-Hodgkin lymphoma and mantle cell lymphoma using genetically modified autologous CD20-specific T cells. *Blood* 112: 2261–2271.
48. Morgan, R. A., M. E. Dudley, J. R. Wunderlich, M. S. Hughes, J. C. Yang, R. M. Sherry, R. E. Royal, S. L. Topalian, U. S. Kammula, N. P. Restifo, et al. 2006. Cancer regression in patients after transfer of genetically engineered lymphocytes. *Science* 314: 126–129.

IL-15 protects NKT cells from inhibition by tumor-associated macrophages and enhances antimetastatic activity

Daofeng Liu,[1] Liping Song,[1] Jie Wei,[1] Amy N. Courtney,[1] Xiuhua Gao,[1] Ekaterina Marinova,[1] Linjie Guo,[1] Andras Heczey,[1] Shahab Asgharzadeh,[2] Eugene Kim,[1] Gianpietro Dotti,[3] and Leonid S. Metelitsa[1,3]

[1]Department of Pediatrics and Department of Pathology and Immunology, Texas Children's Cancer Center, Baylor College of Medicine, Houston, Texas, USA. [2]Division of Hematology-Oncology, Department of Pediatrics, Childrens Hospital Los Angeles and Keck School of Medicine, University of Southern California, Los Angeles, California, USA. [3]Center for Cell and Gene Therapy, Baylor College of Medicine, Houston, Texas, USA.

Vα24-invariant NKT cells inhibit tumor growth by targeting tumor-associated macrophages (TAMs). Tumor progression therefore requires that TAMs evade NKT cell activity through yet-unknown mechanisms. Here we report that a subset of cells in neuroblastoma (NB) cell lines and primary tumors expresses membrane-bound TNF-α (mbTNF-α). These proinflammatory tumor cells induced production of the chemokine CCL20 from TAMs via activation of the NF-κB signaling pathway, an effect that was amplified in hypoxia. Flow cytometry analyses of human primary NB tumors revealed selective accumulation of CCL20 in TAMs. Neutralization of the chemokine inhibited in vitro migration of NKT cells toward tumor-conditioned hypoxic monocytes and localization of NKT cells to NB grafts in mice. We also found that hypoxia impaired NKT cell viability and function. Thus, CCL20-producing TAMs served as a hypoxic trap for tumor-infiltrating NKT cells. IL-15 protected antigen-activated NKT cells from hypoxia, and transgenic expression of IL-15 in adoptively transferred NKT cells dramatically enhanced their antimetastatic activity in mice. Thus, tumor-induced chemokine production in hypoxic TAMs and consequent chemoattraction and inhibition of NKT cells represents a mechanism of immune escape that can be reversed by adoptive immunotherapy with IL-15–transduced NKT cells.

Introduction

Vα24-invariant NKT cells are an evolutionary conserved sublineage of T cells that are characterized by the expression of an invariant TCR α-chain, Vα24-Jα18, and reactivity to self- and microbial-derived glycolipids presented by the monomorphic HLA class I–like molecule CD1d (1). The antitumor potential of NKT cells has been demonstrated in numerous tumor models (2–4). Selective decreases in number and/or functional activity of NKT cells have been reported in patients with diverse types of cancer (5–7), which suggests that NKT cells may play an important role in the antitumor immune responses and, conversely, that an escape from NKT cells may contribute to tumor progression. Our group previously demonstrated that NKT cells infiltrate primary human tumors in a subset of children with neuroblastoma (NB) and that NKT cell infiltration is associated with improved long-term disease-free survival (8). NKT cell infiltration in primary tumors also served as a prognostic factor of favorable outcome in patients with colorectal cancers (9), while low levels of circulating NKT cells predicted a poor clinical outcome in patients with head and neck squamous cell carcinoma (10).

Because the majority of solid tumors are $CD1d^-$, tumor cells cannot be a direct target for NKT cell cytotoxicity (3, 11). Instead, tumor-associated macrophages (TAMs) are the only cells in primary NB tumors that have detectable CD1d expression (12). Moreover, upon recognition of tumor-derived glycolipids, NKT cells produce IFN-γ and kill monocytic cells in a CD1d-dependent manner. Since TAMs provide a critical stromal support for tumor cell growth in NB and many other types of cancer (13–15), NKT cell–mediated killing or inhibition of TAMs explains how NKT cells may indirectly impede tumor growth. Other recent reports have generated additional evidence for the importance of NKT cell interactions with monocytic cells and other myeloid cells in viral and tumor immunity (16, 17) and in the potential mechanism of antitumor activity of the NKT cell ligand β-manosylceramide (18).

Monocytes and other immature myelomonocytic precursors of TAMs localize to the tumor site in response to CCL2, the same chemokine that attracts NKT cells (8). Monocytic cells, however, respond to multiple other tumor-derived chemotactic signals that are not recognized by NKT or other T cells (19). The majority of these factors (e.g., VEGF, endothelin, and angiopoietin-2) are produced in hypoxic conditions and drive TAM migration to the hypoxic areas (13, 19, 20). Importantly, hypoxic signaling amplifies NF-κB activation in TAMs, leading to high levels of IL-6 production and sustained STAT3 activation in tumor cells that in turn promote inflammatory responses in TAMs, providing a positive feedback loop that plays an essential role in tumor progression (21).

Although NKT cells colocalize with IL-6–producing TAMs in primary NB tissues (12), the mechanism of this colocalization is not understood, nor is it clear how TAMs evade the inhibitory activities of NKT cells. An understanding of the NKT-TAM interaction in the context of tumor microenvironment is critically important for the development of rational cancer immunotherapy that targets tumor-supportive stroma, given that NKT cells are the only known immune effector cells that specifically recognize and negatively regulate TAMs. Here, we demonstrated that NKT cell localization to NB depended not only on tumor-derived CCL2,

Conflict of interest: The authors have declared that no conflict of interest exists.
Citation for this article: *J Clin Invest.* 2012;122(6):2221–2233. doi:10.1172/JCI59535.

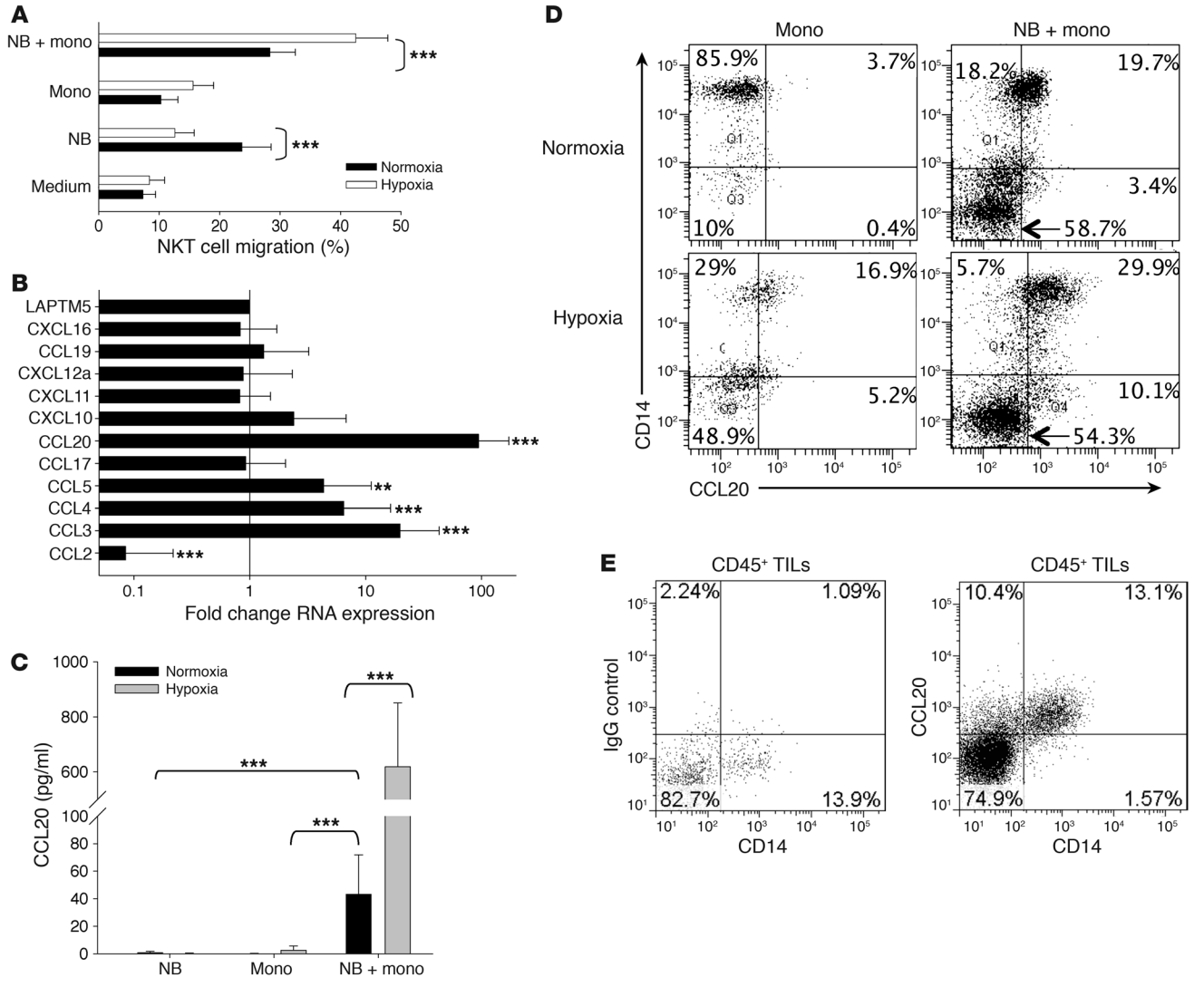

Figure 1

Contact with NB cells and hypoxia synergistically induce CCL20 in human monocytes. (**A**) Primary monocytes were cocultured with CHLA-255 NB cells (1:1 ratio) for 48 hours in normoxic (20% O_2) or hypoxic (1% O_2) conditions, and supernatants were placed in bottom chambers of dual-chambers plates with 5-μM pore membranes with or without addition of the indicated neutralizing antibodies or their isotype control. NKT cells were placed in the upper chambers and allowed to migrate for 3 hours, and the rate of NKT cell migration was quantified by FACS. Results are mean ± SD from 3 experiments in triplicate. (**B**) Monocytes were cocultured with or without CHLA-255 NB cells for 36 hours in normoxic or hypoxic conditions followed by mRNA isolation and quantitative real-time PCR analysis of 11 chemokine genes known to attract human NKT cells. Data are from a representative of 3 experiments in triplicate. (**C**) Monocytes and CHLA-255 NB cells were cultured alone or combined in hypoxic or normoxic conditions for 48 hours. CCL20 concentration was quantified in the supernatants using ELISA. Data are mean ± SD from experiments with monocytes from 6 donors in duplicate. (**D**) Cells were cultured as in **C** and analyzed for intracellular CCL20 accumulation in $CD14^+$ monocytes and $CD14^-$ NB cells. Regions were set using corresponding isotype controls. Data are from a representative of 3 experiments in duplicate. (**E**) Tumor-infiltrating leukocytes (TILs) were isolated from a cell suspension of freshly resected primary NB by gradient centrifugation and cultured with GolgiStop for 4 hours followed by FACS. After gating on $CD45^+$ events, CCL20 accumulation was examined in $CD14^+$ TAMs and compared with the corresponding isotype control. Data are from a representative of 3 experiments. $^{**}P < 0.01$; $^{***}P < 0.001$.

but also on CCL20, which was produced by TAMs in response to tumor-induced inflammation and hypoxia and in turn inhibited NKT cell viability and function. We also showed that IL-15 protected antigen-activated NKT cells from hypoxia and that transgenic expression of IL-15 in NKT cells strongly enhanced their antitumor efficacy in a metastatic NB model in humanized NOD/SCID/IL-2Rγ–null (hu-NSG) mice.

Results

Contact with NB cells and hypoxia synergistically induce CCL20 in human monocytes. To explain the observed colocalization of NKT cells with TAMs in primary human NB (12), we hypothesized that TAMs upon the influence of tumor cells and/or hypoxic environment actively chemoattract NKT cells. To test this hypothesis, we performed an in vitro migration experiment using dual-chamber wells

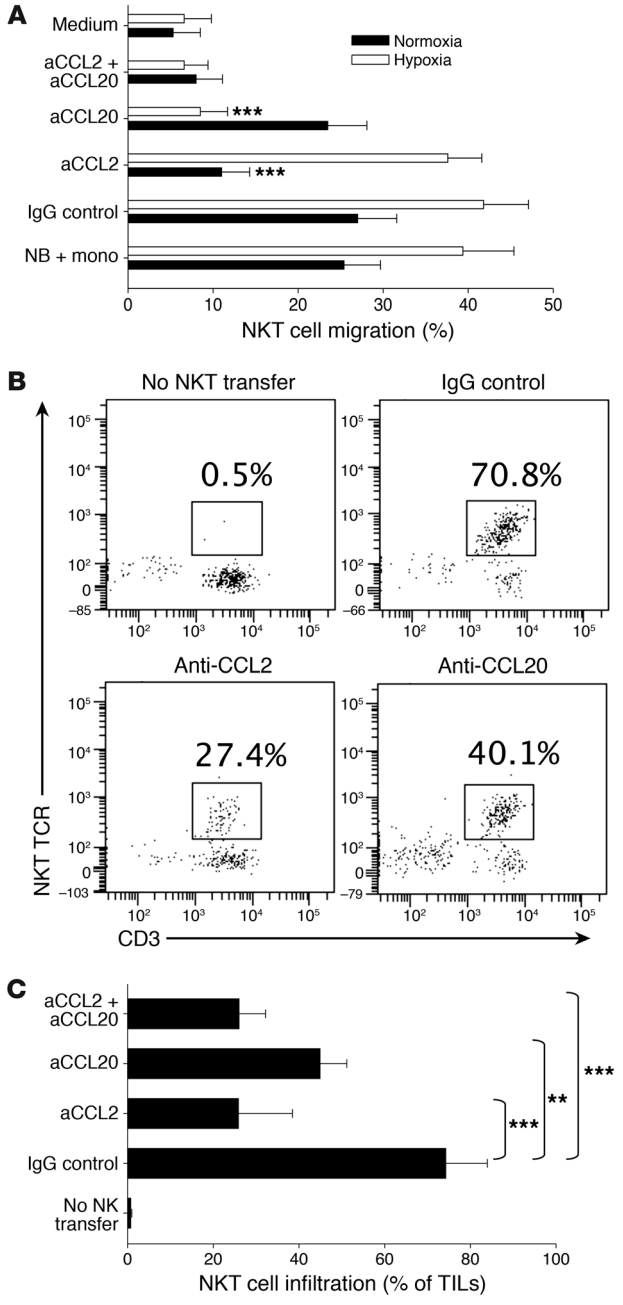

Figure 2
CCL20 is required for NKT cell migration toward hypoxic NB and monocyte culture and NB tumors in hu-NSG mice. (**A**) Monocytes were cocultured with CHLA-255 NB cells for 48 hours in normoxic or hypoxic conditions, followed by analysis of NKT cell in vitro migration with or without neutralizing antibodies (a-) or their isotype control, as in Figure 1A. Results are mean ± SD from 3 experiments in triplicate. (**B**) Xenografts of CHLA-255/luc cells were established under renal capsule of hu-NSG mice followed by i.v. transfer of ex vivo–expanded human NKT cells (5×10^7 per mouse) or PBS (control). Just before NKT cell transfer, mice received i.p. injections of neutralizing antibodies or their isotype control. The tumor-infiltrating leukocytes were analyzed by FACS on day 3 after NKT cell transfer. After gating on $hCD45^+$ cells, NKT cells were identified as $CD3^+Va24\text{-}Ja18^+$ events. Data are from a representative of 5 mice per group. (**C**) Tumor-infiltrating NKT cell frequency (mean ± SD) from **B**. $^{**}P < 0.01$; $^{***}P < 0.001$.

separated by 5-μM pore membrane. Human ex vivo–expanded NKT cells were added to the upper chambers and allowed to migrate for 3 hours into the lower wells, which contained CHLA-255 NB cells, freshly isolated (negative selection) human monocytes from peripheral blood, or 1:1 mixture of NB cells and monocytes. Before adding NKT cells, the plates with NB cells and monocytes were incubated in normoxic (20% O_2) or hypoxic (1% O_2) conditions for 48 hours. Consistent with our previous observations, NB cells were chemoattractive for NKT cells in normoxic conditions (8). Surprisingly, NKT cell migration to NB cells was nearly abrogated in hypoxia ($P < 0.001$; Figure 1A). In contrast, the rate of NKT cell migration toward the coculture of NB cells with monocytes nearly doubled under hypoxic conditions ($P < 0.001$), whereas monocytes alone had little chemoattractive activity in either normoxia or hypoxia. These data suggest that an interaction between NB cells and monocytes under hypoxia results in induction (upregulation) of chemokines that chemoattract NKT cells.

To examine the overall effect of hypoxia on the chemokine gene expression profile of NB cells and monocytes, we incubated monocytes and CHLA-255 NB cells in normoxic or hypoxic conditions for 36 hours followed by RNA isolation and quantitative RT-PCR for 11 CC and CXC chemokine genes that are known to have corresponding receptors on human NKT cells (8, 22–25). mRNA expression of CCL20, CCL5, CCL4, and CCL3 was upregulated, whereas that of CCL2 was downregulated, in hypoxia compared with normoxia ($P < 0.001$; Figure 1B). We previously reported that, unlike other chemokines, CCL2 is expressed at high levels in NB cells, and additional experiments with NB cells alone confirmed that hypoxia downregulated CCL2 expression in NB cells at both RNA and protein levels (data not shown). This finding explains the observed loss of NB cell chemoattraction for NKT cells in hypoxia. To examine whether the upregulation of mRNA expression of CCL20, CCL5, CCL4, and CCL3 results in increased production of the corresponding proteins, we analyzed supernatants from the same experimental conditions by ELISA. Only CCL20 production was significantly upregulated in the coculture of monocytes with NB cells compared with monocytes alone (NB cells do not produce detectable CCL20). Moreover, the effect of the coculture on CCL20 upregulation was amplified up to 70-fold in hypoxic compared with normoxic conditions ($P < 0.001$; Figure 1C and Supplemental Figure 1A; supplemental material available online with this article; doi:10.1172/JCI59535DS1). Despite the observed variability in the magnitude of CCL20 production by monocytes from 13 different individuals, hypoxia invariably increased it in all cases. The kinetics analysis demonstrated that upregulation of CCL20 reached maximum levels after 36 hours of coculture in normoxia, but continued to rise for at least 48 hours in hypoxia (Supplemental Figure 1B).

To unambiguously determine the cellular source of CCL20, we cultured monocytes alone or with NB cells in normoxic or hypoxic conditions and analyzed intracellular CCL20 accumulation by fluorescence-activated cell sorting (FACS) using surface staining for CD14 to discriminate monocytes from NB cells. Either contact with NB cells or hypoxia alone could upregulate CCL20 production in monocytes (Figure 1D). The highest level of CCL20 expression was achieved when monocytes were cocultured with

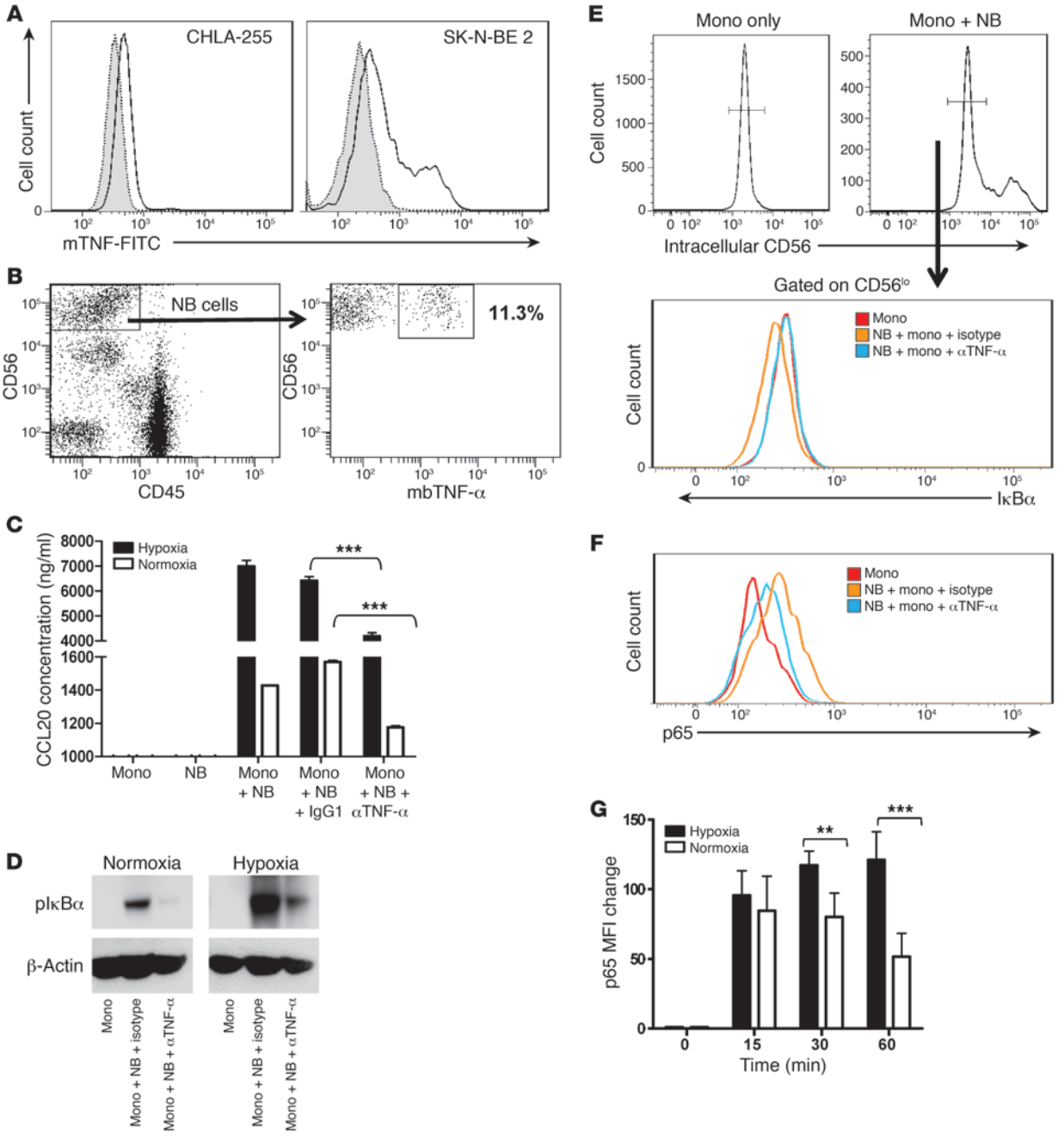

Figure 3

mbTNF-α on NB cells induces NF-κB activation in monocytes. (**A**) Cultured NB cells were suspended using 2% EDTA without trypsin and analyzed by FACS for cell surface expression of mbTNF-α in 2 representative NB cell lines (shaded, isotype control; open, anti–mbTNF-α). (**B**) Cell suspensions from freshly resected primary NB tumors were stained for surface markers. mbTNF-α expression on NB cells was analyzed after gating on $CD56^{hi}CD45^{-}$ events. (**C**) NB cells were preincubated with 50 ng/ml anti-human TNF-α or isotype control mAb for 1 hour before addition of monocytes; NB and monocytes alone were used as controls. CCL20 concentration in the culture supernatant was determined by ELISA after 36 hours. Results are mean ± SD from 3 experiments in triplicate. ***$P < 0.001$, 1-way ANOVA. (**D**) Monocytes were cultured alone in nonadherent plates or on top of NB cell monolayer, with addition of anti–TNF-α or isotype control mAb, in normoxia or hypoxia for 16 hours followed by monocyte detachment and Western blotting for phospho-IκBα using β-actin as a loading control. Data are from a representative of 3 experiments. (**E** and **F**) The same experiment as in **D** was followed by intracellular staining for (**E**) IκBα or (**F**) phospho-p65 in monocytes after gating out NB cells as $CD56^{hi}$ events. (**G**) Kinetics of phospho-p65 expression in monocytes upon coculture with NB cells in normoxic and hypoxic conditions. Results are mean ± SD from 2 experiments in triplicate. **$P < 0.01$; ***$P < 0.001$.

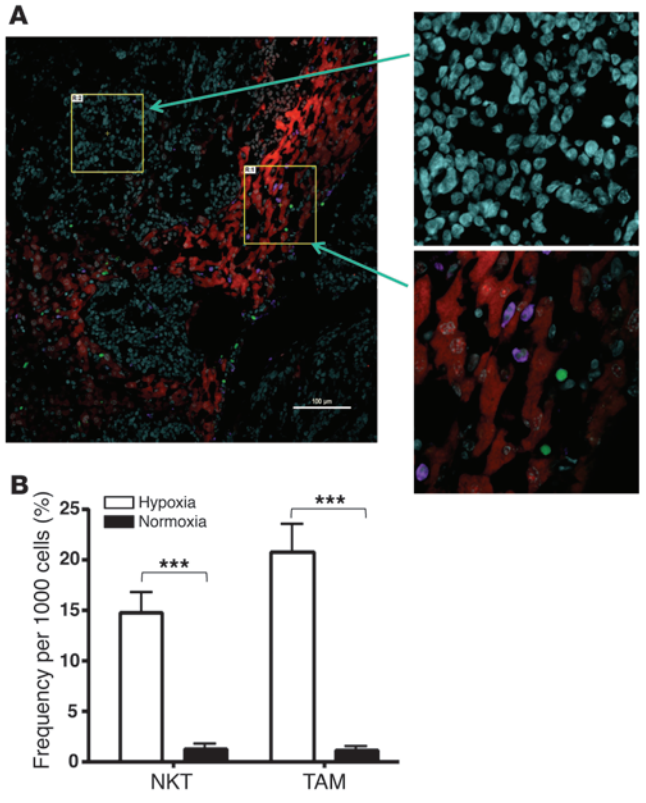

Figure 4
NKT cells preferentially localize to hypoxic areas within tumor tissues. At 3 months after SCT, hu-NSG mice (see Methods) received i.v. injection of 10^6 CHLA-255/luc NB cells; 3 weeks later, mice were injected with CFSE-labeled NKT cells. For labeling hypoxic tissues, mice were i.v. injected with EF5 3 hours before being euthanized. (**A**) Immunofluorescent analysis of liver metastasis for hypoxia (Cy3–anti-EF5; red), NKT cells (CFSE; green), and human myeloid cells (hCD11b; violet). Magnified images (left, ×20; right, ×60) show typical areas of normoxic and hypoxic tissues. Shown are representative of 10 100-μm fields analyzed per mouse, 5 mice per experiment, 2 independent experiments. Scale bar: 100 μm. (**B**) Image analysis (see Methods). Regions with mean Cy3 intensity lower than 200 and higher than 550 were defined as normoxic and hypoxic, respectively. Absolute numbers of NKT cells and hCD11b$^+$ cells in normoxic and hypoxic regions were counted in 10 100-μm fields per mouse, 5 mice per group. Shown are number of tumor-infiltrating NKT and CD11b$^+$ cells per 1,000 cells (mean ± SD) in 1 of 2 experiments with similar results. ***$P < 0.001$.

NB cells in hypoxia, consistent with the ELISA results in Figure 1C. NB cells did not express detectable CCL20 in any tested condition. To examine the requirement of cell-cell contact between monocytes and NB cells for CCL20 induction in monocytes, we cultured NB cells with monocytes in the same wells or in the dual-chamber wells, separated by a 400-nM semipermeable membrane. Monocytes failed to produce CCL20 in the absence of direct contact with NB cells (Supplemental Figure 1C). To determine whether the induction of CCL20 in monocytes that we observed in the described in vitro experimental system occurs at the tumor site in NB patients, we performed FACS on cell suspensions prepared from freshly resected primary NB tumors at diagnosis. We found that all tumor-derived monocytic cells expressed CCL20, whereas tumor cells and the majority of nonmonocytic CD45$^+$ tumor-infiltrating leukocytes were negative (Figure 1E). Therefore, TAMs in primary NB tumors produced CCL20, expression of which was selectively induced in monocytic cells upon direct contact with NB cells and enhanced by hypoxia.

CCL20 is required for NKT cell migration toward hypoxic NB-monocyte culture and NB xenografts in hu-NSG mice. CCL20 has been reported to be one of the most potent chemokines for human NKT cells (23, 24). Our analysis confirmed that the majority of primary NKT cells from peripheral blood expressed CCR6, the only receptor for CCL20. Moreover, CCR6 expression was preserved in ex vivo–expanded NKT cells (Supplemental Figure 2). To determine the requirement of the CCL20/CCR6 axis for the observed enhanced migration of NKT cells toward the coculture of NB cells with monocytes in hypoxia (Figure 1A), we repeated the in vitro migration experiment in the presence of chemokine-neutralizing mAbs. Consistent with our previous report (8), anti-CCL2 mAb effectively inhibited NKT cell migration to NB cells or NB-monocyte coculture under normoxia, but not under hypoxia. Only anti-CCL20 neutralizing mAb strongly inhibited NKT cell migration in hypoxia ($P < 0.001$; Figure 2A).

To examine the relative contribution of CCL2 and CCL20 to the mechanism of NKT cell in vivo localization to the tumor site, we adapted a previously described CHLA-255/luc human NB model in immunodeficient mice (12) and, instead of NOD/SCID, used hu-NSG mice (Supplemental Figure 3A). As has been observed by others (26, 27), hu-NSG mice had stable reconstitution of human myelomonocytic cells as well as B and T lymphocytes 3 months after stem cell transplantation (SCT) with human cord blood CD34$^+$ hematopoietic stem cells (Supplemental Figure 3, B and C). We injected CHLA-255/luc NB cells under the renal capsule 3.5 months after SCT. Like in human NB tissues (12), TAMs represented a major subset of tumor-infiltrating leukocytes (Supplemental Figure 3, D and E) and were enriched in a subset with M2 phenotype, as determined by the downregulation of HLA-DR expression compared with CD14$^+$ peripheral blood monocytes in the same mice (Supplemental Figure 3F). Importantly, similar HLA-DR^{lo}CD14$^+$ cells were the dominant subset of TAMs in primary tumors from NB patients (Supplemental Figure 3G). At 3 weeks after NB cell injection and clear evidence of tumor growth by bioluminescent imaging, mice were injected with human ex-vivo–expanded NKT cells and divided into groups to receive anti-human CCL2, anti-human CCL20 neutralizing mAb, both mAbs combined, or isotype control mAb. A control group did not receive NKT cells. On day 3 after NKT cell transfer, mice were euthanized and examined for NKT cell localization to the tumor tissues. Animals treated with anti-CCL2 or anti-CCL20 mAb had lower frequency of tumor-infiltrating NKT cells among the tumor-infiltrating human CD45$^+$ (hCD45$^+$) leukocytes (25.9% ± 12.6% and 44.9% ± 6.3%, respectively) compared with the

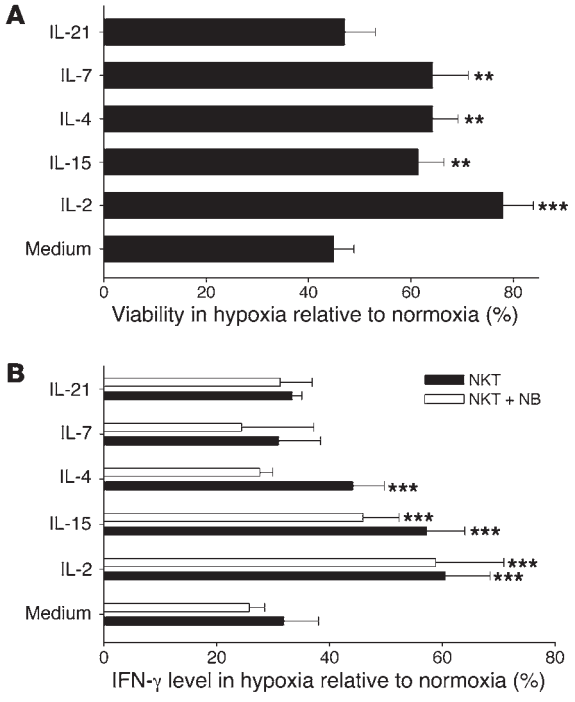

Figure 5
NKT cell viability and function are inhibited by hypoxia and protected by cytokines. (**A**) NKT cells were expanded from PBMCs of 4 donors using stimulation with αGalCer and cultured under hypoxia or normoxia in the presence or absence of the indicated cytokines at 200 U/ml for 24 hours. The number of viable cells was quantified using hemocytometer and trypan blue staining. (**B**) NKT cells were cultured for 24 hours as in **A**, followed by TCR stimulation with 6B11 mAb. Cytokine release was quantified by CBAPlex assay from 24-hour supernatants. The cytokine amount was normalized by percent viable cells in the corresponding conditions. Results are mean ± SD from 3 experiments in triplicate. $^{**}P < 0.01$; $^{***}P < 0.001$.

IgG control group (74.3% ± 9.7%, $P < 0.01$; Figure 2, B and C). The neutralization of both chemokines did not increase inhibition of NKT cell migration more than the neutralization of CCL2 alone (26% ± 6.2%, $P < 0.001$; Figure 2C), which suggests that the chemokines act along the same axis. While confirming the previously established role of NB-derived CCL2, these data also established the requirement of CCL20 for NKT cell localization to the tumor site, even though the latter chemokine was not produced by tumor cells, but induced in TAMs. Thus, NKT cells effectively localized to NB tumors in hu-NSG mice and migrated toward TAMs in a CCL20-dependent manner.

mbTNF-α on NB cells induces NF-κB activation in monocytes that results in CCL20 upregulation. The observed requirement for cell-cell contact between NB cells and monocytes for CCL20 induction in monocytes and the known requirement of NF-κB activation for CCL20 expression (28) prompted us to search for candidate cell surface molecules on NB cells with proinflammatory properties. Goillot et al. observed expression of TNF-α protein in 2 NB cell lines by immunohistochemistry (29). We here examined 3 MYCN-amplified (SK-N-BE2, IMR32, LA-N1) and 3 non–MYCN-amplified (CHLA-255, CHLA-15, LA-N-2) NB cell lines by FACS and found that the majority of cells in all lines expressed TNF-α intracellularly (Supplemental Figure 4), as well as on the cell surface as a membrane-bound cytokine (Figure 3A). No soluble TNF-α was detected by ELISA in the supernatants of all examined cell lines. Importantly, we found the presence of the membrane-bound TNF-α–positive (mbTNF-α$^+$) subset in all 7 examined primary NB tumors, with the frequency ranging from 1.1% to 38.2% (12.2% ± 14%; Figure 3B). The level of MYCN expression did not correlate with the frequency of mbTNF-α$^+$ cells, either in cell lines or in primary tumors (data not shown). The function blocking experiments demonstrated that preincubation of NB cells with an anti–TNF-α blocking mAb significantly inhibited their ability to induce CCL20 production in monocytes under both normoxic and hypoxic conditions ($P < 0.001$; Figure 3C). Neither the frequency of TNF-α$^+$ cells nor the level of TNF-α expression in NB cells was affected by hypoxia (data not shown). To examine the requirement of mbTNF-α for the activation of NF-κB signaling in monocytes, we cultured monocytes alone (in nonadherent plates) or on the monolayer of NB cells (because monocytes only loosely adhere to the NB cell monolayer) in the presence of an isotype control or anti–TNF-α blocking mAb in normoxic or hypoxic conditions. IκBα, an IκB inhibitor, was phosphorylated (a required upstream event in NF-κB activation by extracellular stimuli) in monocytes upon contact with NB cells, and the IκBα phosphorylation was almost completely prevented in the presence of anti–TNF-α blocking mAb (Figure 3D). The hypoxic condition enhanced IκBα phosphorylation, and this was also strongly inhibited by the anti–TNF-α blocking mAb. Since contaminating NB cells could not be excluded as a source of phospho-IκBα in the above-described monocyte preparations, we repeated this experiment and performed intracellular FACS analysis of IκBα and phosphorylated p65. After gating on CD56^{lo} cells (monocytes), we observed a decrease of IκBα expression (degradation upon phosphorylation) within 30 minutes of contact with NB cells, and the effect was abrogated in the presence of anti–TNF-α blocking mAb (Figure 3E). Consistent with the decreased IκBα expression, we observed increased phospho-p65 expression in monocytes, and this was inhibited by anti–TNF-α blocking mAb in normoxic (Figure 3F) and hypoxic (data not shown) conditions. Coculture of monocytes with NB cells under hypoxia resulted in higher levels and more sustained p65 expression compared with normoxia ($P < 0.01$; Figure 3G). We conclude that NB contains a subset of proinflammatory tumor cells that express mbTNF-α, which is required at least in part for the induction of CCL20 production in TAMs via activation of NF-κB signaling, which is stabilized and enhanced by tumor-induced hypoxia.

NKT cells preferentially localize to hypoxic areas within tumor tissues. To examine the relative distribution of NKT cells in hypoxic and normoxic areas of the tumor, we used a metastatic model of NB in hu-NSG mice. In this model, CHLA-255/luc cells were injected i.v. to produce metastatic growth in liver and bone/bone marrow (see below), the major metastatic sites in NB patients (30). On day 21, tumor-bearing mice were injected with CFSE-labeled NKT cells, and their localization in liver metastases was examined 3 days later. The areas of hypoxia in both primary and metastatic sites were visualized using intravital injection of EF5 followed by staining with anti-EF5 fluorochrom-conjugated mAb (31). The same tissues were costained with anti-CD11b mAb, so that distribution of both NKT cells and myeloid cells in normoxic and hypoxic tumor tissues was analyzed and quantified using 4-color confocal microscopy. In con-

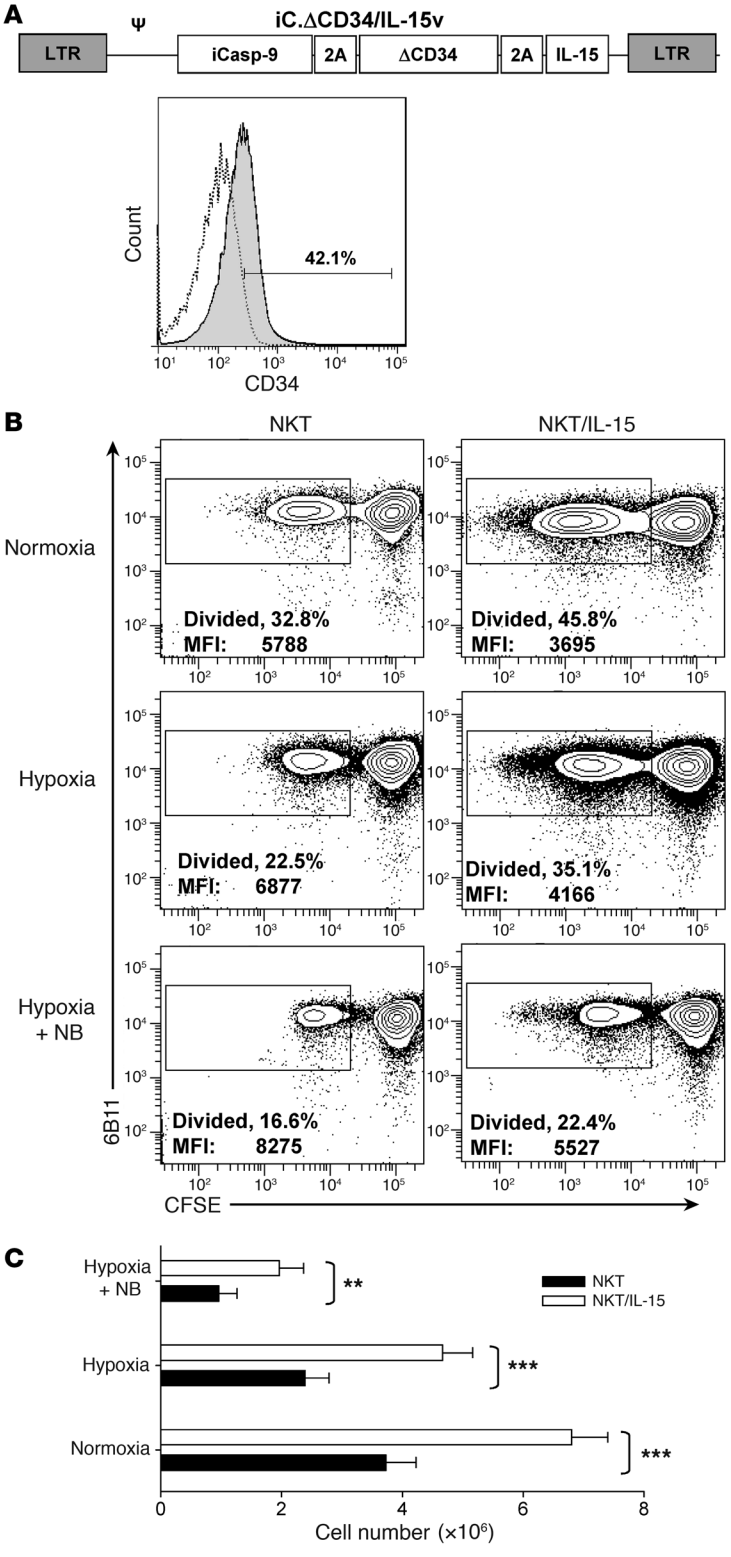

Figure 6

Transgenic expression of IL-15 in NKT cells protects them from hypoxia. (**A**) Retroviral construct used to transduce NKT cells. Proliferating NKT cells were transduced with the IL-15–containing retroviral vector (see Methods), and the transduced cells were identified by FACS using ΔCD34 tag. (**B**) NKT and NKT/IL-15 cells were labeled with CFSE and TCR-stimulated with OKT3 mAb in the absence or presence of NB cells (1:1 ratio) in normoxia or hypoxia (10^6 cells/well). The percent of proliferated cells (loss of CFSE expression) was quantified by FACS after 5-day culture with IL-2 (50 U/ml). Data are from a representative of 4 experiments with NKT cells from 4 donors. (**C**) Absolute number of viable NKT cells was quantified after 5-day culture using hemocytometer and trypan blue staining. Shown are mean ± SD of cells per condition from 4 experiments. $^{**}P < 0.01$; $^{***}P < 0.001$.

trast to normal liver tissues in tumor-free hu-NSG mice, in which no staining for hypoxia was detected (data not shown), metastatic tissues contained both normoxic and hypoxic areas, and more than 90% of NKT cells and myelomonocytic cells were found in the latter (Figure 4A). Quantitative analysis demonstrated that the frequency of NKT cells per 1,000 cells was 14.8% ± 6.3% in hypoxic versus 1.3% ± 1.6% in normoxic areas, and $CD11b^+$ cell frequency was 20.8% ± 8.9% versus 1.1% ± 1.2% ($P < 0.001$ for both; Figure 4B). Therefore, NKT cells colocalize with TAMs in the hypoxic tumor tissues.

NKT cells are inhibited by contact with NB cells and hypoxia. Since NKT cell–mediated killing or inhibition of TAMs is important for their antitumor activity against $CD1d^-$ tumors (12), we asked how the hypoxic tumor environment that is at least in part responsible for NKT cell trafficking toward TAMs affects their viability and function. NKT cells expanded from PBMCs of 4 donors using antigenic stimulation with α-galactosylceramide (αGalCer) were cultured in normoxic and hypoxic conditions for 24 hours, and NKT cell viability was examined by trypan blue exclusion at different time intervals. We found that in the absence of exogenous cytokines, the number of viable NKT cells in hypoxia was only half of that in normoxia. IL-2 and other cytokines that shared common γ chain (IL-15, IL-4, IL-7), with the exception of IL-21, significantly improved NKT cell survival in hypoxia ($P < 0.01$; Figure 5A). While both IL-2 and IL-15 significantly reduced the rate of NKT cell apoptosis in normoxia, neither cytokine significantly protected NKT cells from apoptosis in hypoxia conditions ($P < 0.05$), as measured by annexin V/7-AAD staining (Supplemental Figure 5 and data not shown), which suggests that the observed effect on the absolute number of viable cells was mostly due to cytokine-supported NKT cell proliferation — as we also showed for IL-15–transduced NKT cells (see below) — and is consistent with the metabolic switch of prolifereating lymphocytes to glycolysis with reduced dependence on oxygen (32–35).

To examine the effect of hypoxia on the functional activity of NKT cells, we activated NKT cell TCR by adding agonistic 6B11 mAb and measured cytokine production in cell supernatants by ELISA. After 24 hours of exposure to hypoxia, IFN-γ production by NKT cells cultured alone or with NB cells fell to 31.9% ± 6.1% and 25.7% ± 2.7%, respectively, of that produced in normoxia ($P < 0.001$; Figure 5B). To examine the potential of IL-2Rγ family cytokines to protect NKT cell function from hypoxia, we added saturating concentrations of these cytokines to NKT cell cultures. IL-2 and IL-15, but not other

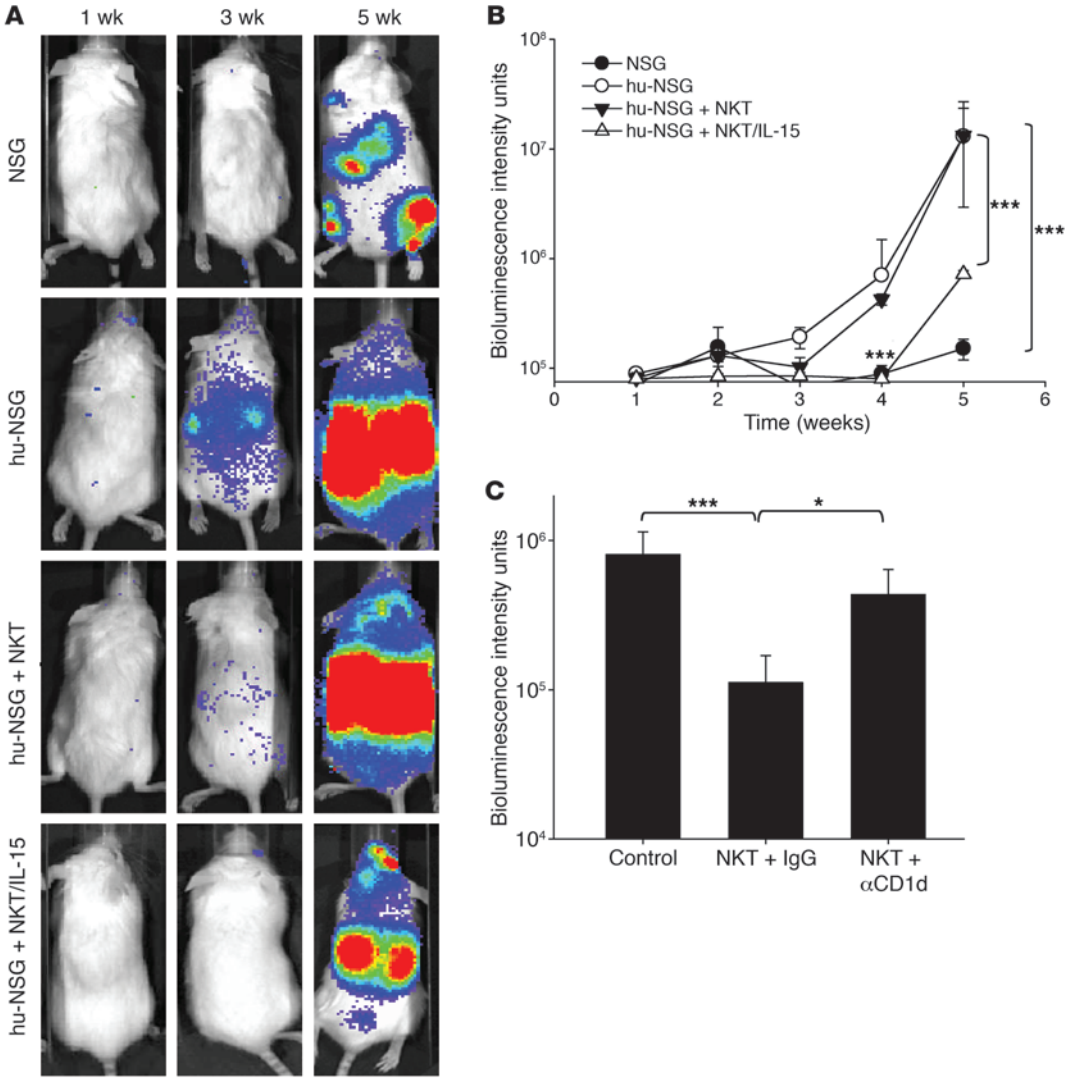

Figure 7

NKT/IL-15 cells have potent antitumor activity in a metastatic NB model in hu-NSG mice. At 3 months after SCT, hu-NSG or control NSG mice received i.v. injection of 10^6 CHLA-255/luc NB cells alone or followed by 10^7 NKT or NKT/IL-15 cells. Metastatic tumor growth was monitored by weekly bioluminescence imaging. (**A**) Representative bioluminescent images at the indicated times after tumor cell injection. (**B**) Mean ± SD values from of 1 of 2 experiments with 5 mice per group. ***$P < 0.001$. (**C**) Mice were pretreated with anti-CD1d blocking or isotype control mAb before transfer of NKT/IL-15 cells. Shown are mean ± SD values at week 5 from of 1 of 2 experiments with 5 mice per group. *$P < 0.05$; ***$P < 0.001$.

cytokines, rescued the IFN-γ response of NKT cells to TCR stimulation in the presence and absence of NB cells ($P < 0.001$; Figure 5B). Therefore, CCL20-mediated chemoattraction of NKT cells toward hypoxic TAMs may lead to the inhibition of NKT cell functional activity that could be reversed by IL-2 or IL-15.

Several recent reports demonstrated that NKT cells play a key role in liver and kidney ischemia-reperfusion injury (36, 37) and in the genesis of the vaso-occlusive crisis in sickle cell disease (38–40). The acute ischemia and inflammation in these conditions have been associated with spontaneous IFN-γ production by NKT cells both in mice and in humans. However, the direct effect of hypoxia on IFN-γ expression in NKT cells has not been evaluated. To examine the effect of hypoxia on spontaneous cytokine production by human NKT cells, we cultured quiescent NKT cells from 4 donors under normoxic or hypoxic conditions for different time intervals (2, 4, 6, 12, 24, and 48 hours) and measured IFN-γ and IL-4 production by ELISA. In the absence of antigenic stimulation, cytokines remained undetectable either in normoxia or hypoxia at all times examined (data not shown), which suggests that hypoxia does not directly stimulate human NKT cells.

IL-15 protects NKT cells and restores their antitumor potential. Our group and others have demonstrated that IL-15 plays a critical role in NKT cell development and homeostatic maintenance (41–43). The results of the present study (Figure 5B) suggest that IL-15 can also protect NKT cells from the inhibitory effect of the hypoxic tumor microenvironment. Therefore, we hypothesized that transgenic expression of IL-15 in adoptively transferred NKT cells would enhance their antitumor potential as a result of improved in vivo persistence and functionality at the tumor site. To test this hypothesis, we transduced NKT cells with a previously described

retroviral construct, containing cDNA of human IL-15, inducible caspase-9 suicide gene (iCasp-9), and CD34 tag (44), to create transgenic IL-15–expressing NKT cells (referred to herein as NKT/IL-15 cells). Ex vivo–expanded human NKT cells were stably transduced with the IL-15–containing vector (Figure 6A). We also confirmed IL-15 production by the transduced NKT cells by ELISA (data not shown). To examine the protective potential of transgenic IL-15 on NKT cell function under hypoxia and in the presence of tumor cells, we used in vitro settings similar to those described for Figure 4B and measured TCR-induced NKT cell proliferation using CFSE dilution assay and apoptosis rate using annexin V staining. Consistent with the observed protective properties of the exogenous recombinant human IL-15, we found that NKT cells/IL-15 had a significantly higher rate of proliferation upon hypoxia alone and in the presence of NB cells than did parental NKT cells ($P < 0.01$; Figure 6B). The antiapoptotic effect of transgenic IL-15 was significant only in normoxic conditions (data not shown), as was the antiapoptotic effect of exogenous IL-15 (Supplemental Figure 5). The absolute cell count at the end of 5-day culture conclusively demonstrated that NKT/IL-15 cells expanded significantly better than did NKT cells in all tested conditions (Figure 6C). Therefore, NKT/IL-15 cells will likely be protected upon antigen recognition in the hypoxic tumor microenvironment.

NKT/IL-15 cells have potent antitumor activity in a metastatic NB model in hu-NSG mice. To examine whether NKT/IL-15 cells have a therapeutic advantage, we used a metastatic NB model in hu-NSG mice. At 3.5 months after SCT and upon confirmation of human hematopoietic reconstitution (Supplemental Figure 4, B and C), mice were i.v. injected with luciferase-transduced human NB cells (CHLA-255/luc). The therapeutic groups also received a single injection of either NKT cells or NKT/IL-15 cells. NSG mice (which did not receive human $CD34^+$ stem cells) were used as a control group to assess the overall effect of human hematopoietic cells on the tumor growth. Metastatic growth in hu-NSG mice was dramatically enhanced compared with NSG mice ($P < 0.001$; Figure 7, A and B), providing further support for the prominent role of BM-derived cells in enhancing NB growth. Whereas immunotherapy with NKT cells had a significant ($P < 0.05$), but short-lived, inhibitory effect on metastatic growth, a single injection of NKT/IL-15 cells completely abrogated the tumor-promoting effect of the human hematopoietic environment ($P < 0.001$ at weeks 4 and 5; Figure 7, A and B). To determine whether the enhanced antitumor activity of NKT/IL-15 cells remains CD1d restricted, we repeated the treatment of NB metastases in hu-NSG mice with NKT/IL-15 cells after pretreatment with anti-CD1d blocking or isotype control mAb. Antitumor efficacy of NKT/IL-15 cells was inhibited by anti-CD1d mAb ($P < 0.05$; Figure 7C), which indicates that the effect of IL-15 depends, at least in part, on the function of CD1d-restricted NKT cells. However, due to incomplete inhibition, a contribution of NKT-independent effects of IL-15, such as activation of NK cells, cannot be excluded. These data suggest that immunotherapy with NKT/IL-15 cells may be effective in patients with metastatic NB and other types of cancer. For the maximum therapeutic benefit, this form of immunotherapy targeting tumor-supportive stroma could be combined with other forms of immunotherapy or chemotherapy that target tumor cells directly.

Discussion

Our present study reveals what we believe to be a novel mechanism of tumor escape from immune control by NKT cells and provides mechanistic insight into the development of NKT cell–based cancer immunotherapy. Because NKT cell antitumor activity against $CD1d^-$ tumors depends on their documented ability to colocalize and interact with $CD1d^+$ TAMs (12), elucidation of the mechanism by which NKT cells traffic toward TAMs and understanding of this process's effect on NKT cell function are critically important for the rational design of NKT cell–based immunotherapy. We show that, besides the previously described requirement for NB cell–derived CCL2 (8), NKT cell migration to the tumor site depended on CCL20, which was produced by TAMs inside the tumor tissues. CCL20 expression was induced in monocytic cells upon contact with NB cells and it was at least partly dependent on mbTNF-α, which was expressed on the surface of NB cells. Moreover, NB cell–induced CCL20 expression in monocytic cells was greatly amplified by hypoxia, which is known to attract TAMs (13, 19, 20). This suggests that the CCL20 gradient directs NKT cell trafficking toward hypoxic tumor tissues. Indeed, we found that more than 90% of tumor-infiltrating NKT cells were colocalized with macrophages in hypoxic areas of NB xenografts in hu-NSG mice. Hypoxia, in turn, inhibited the ability of NKT cells to respond to an antigenic stimulation, which explains how growing tumors can neutralize NKT cell function and rescue tumor-supportive TAMs from NKT cell attack. Importantly, we found that IL-15 protected antigen-activated NKT cells from hypoxia, and NKT/IL-15 cells had potent and long-lasting antitumor activity in a hu-NSG model of metastatic NB.

We found that TAMs in primary NB tumors produced CCL20, expression of which was selectively induced in monocytic cells upon direct contact with NB cells and enhanced by hypoxia. Our quest for the initiating inflammatory signal that triggers induction of CCL20 expression in monocytes upon their contact with tumor cells revealed expression of mbTNF-α on the cell surface in all tested NB cell lines regardless of their MYCN status and the existence of a $mbTNF\text{-}\alpha^+$ NB cell subset, which we believe to be previously unknown, in primary tumors. We demonstrated that NB cells had potent proinflammatory properties, TNF-α–dependently activating the NF-κB signaling pathway in monocytic cells that resulted not only in CCL20 expression, but also in the activation of a defined gene expression program, which is known to be a hallmark of tumor-promoting chronic inflammation (45, 46). For example, NF-κB activated gene expression of IL-6 — a known growth factor for non–MYCN-amplified NB cells — in monocytic cells, and the level of IL-6 mRNA expression negatively correlates with long-term disease-free survival in high-risk NB patients (12). The tumor-promoting role of the TNF-α/NF-κB axis is well-described in epithelial tumors both in mouse models of cancer and in cancer patients (21, 46–48). These are common tumors in adults that can often be etiologically or pathogenetically linked to preexisting chronic inflammatory conditions, such as hepatitis (45) or colitis (46). In contrast, NB as well as other pediatric tumors arises during embryogenesis or early postnatal development in the absence of preexisting chronic inflammation (49). The identification of a subset of NB cells in primary tumors that express mbTNF-α suggests that these cells may initiate tumor-supportive inflammation and could be targeted for therapy with TNF-α antagonists, which are currently being tested in clinical trials in adults with epithelial cancers and hematologic malignancies (50–52). However, incomplete inhibition of CCL20 production in the coculture of monocytes with NB cells by anti–TNF-α mAb suggests that other as-yet unidentified tumor-derived signals may contribute to macrophage activation in NB.

We observed a differential requirement for CCL2 and CCL20 for NKT cell in vitro migration toward a coculture of NB cells with monocytes in normoxic and hypoxic conditions. Whereas CCL2 was required for NKT cell migration in normoxia, CCL20 was largely responsible for their migration in hypoxia. The observed downregulation of CCL2 expression in NB cells under hypoxia combined with CCL20 induction in hypoxic monocytes suggests a 2-step mode of NKT cell migration in the tumor tissues: CCR2- or CCR4-mediated exit from circulation toward CCL2-producing NB cells in the oxygenated areas around blood vessels, and then CCR6-mediated trafficking toward CCL20-producing TAMs in the hypoxic areas. The in vivo blocking experiments with anti-CCL20 neutralizing mAb further support the importance of CCL20 for NKT cell localization to the tumor site. Furthermore, visualization of hypoxic areas within tumor xenografts using intravital staining with EF5 revealed that the vast majority of adoptively transferred NKT cells colocalized with TAMs in the hypoxic areas of the tumor tissues. Therefore, NKT cells may colocalize with TAMs as a component of a novel innate response to tumor-induced hypoxia. Moreover, this mechanism could reflect an evolutionary conserved role of NKT cells in linking tissue hypoxia with inflammation. This concept is supported by several recent reports demonstrating that NKT cells play a key role in the inflammatory response in liver and kidney ischemia-reperfusion injury (36, 37) and in the genesis of the vaso-occlusive crisis in sickle cell disease (38–40). Both in mice with experimental ischemia-reperfusion injury and in humans with sickle cell disease, NKT cells have increased IFN-γ production. However, to our knowledge, the direct effect of hypoxia on NKT cell IFN-γ expression had not previously been examined. We found that hypoxia did not have a direct stimulatory effect on human NKT cells, which suggests that increased IFN-γ production by NKT cells in patients with sickle cell disease could be due to a combined action of hypoxia and inflammatory mediators, in which hypoxia directs NKT cell localization to the site of inflammation rather than directly activating these cells. The ability of NKT cells to recognize and respond to hypoxia could be essential for their control of TAMs at the early stages of tumor progression, when TAMs play a major role in tumor vascularization and tumor cell survival (13–15, 53). However, growing tumor may also use the same phenomenon for the immune escape by trapping NKT cells in the hypoxic tissues and disabling their function.

We found that NKT cell viability and function were affected by hypoxia and that antigen-dependent proliferation and cytokine production was protected by IL-2 or IL-15. The protective effect of these cytokines on proliferating rather than quiescent NKT cells was consistent with similar observations in T cells, which have previously been shown to switch to glycolysis upon antigenic stimulation and to require less oxygen (34, 35). Studies in mice have demonstrated that NKT cell development, homeostatic maintenance, and survival largely depend on IL-15 (42, 43). Our group previously reported that IL-15 also stimulates proliferation and enhances survival of human NKT cells (41). Human $CD4^-$ NKT cells, which are mostly $CD8^-CD4^-$ double-negative (DN), express much higher levels of IL-2Rβ than do $CD4^+$ cells, so that IL-15 preferentially expands DN NKT cells (41). Importantly, DN NKT cells are more cytotoxic than are $CD4^+$ NKT cells, and a recent report demonstrated that only DN NKT cells are required for antitumor responses in vivo (54). This suggests that the expression of IL-15 in NKT cells for therapeutic purposes would support expansion, persistence, and antitumor activity of DN NKT cells in cancer patients. We indeed found that transduction of NKT cells with IL-15 cDNA protected them from the inhibitory effects of NB cells and hypoxia. Importantly, NKT/IL-15 cells demonstrated a potent therapeutic activity against NB metastases in hu-NSG mice, and this effect was at least in part CD1d dependent. Besides acting directly on NKT cells and enhancing their activity against TAMs, locally produced IL-15 is expected to activate other antitumor immune effector cells, such as NK and tumor-specific $CD8^+$ T cells (55). In contrast to IL-2, IL-15 does not fully activate Tregs (56), which are known to have an inhibitory effect on NKT cells (57) and could counteract their antitumor activity. To ensure the safety of the potential clinical use of NKT/IL-15 cells, we incorporated a suicide gene, iCasp-9, which allows the elimination of transgeneic cells upon its pharmacologic activation with a nontoxic small molecular drug, AP20187 (58–60). We previously demonstrated that T cells expressing the iCasp-9 molecule are efficiently eliminated upon pharmacologic activation of the suicide gene both in vitro and in vivo (59, 60), not only in a mouse model, but also in lymphoma patients (61). Therefore, NKT/IL-15 cell therapy under iCasp-9 control is expected to be safe and needs to be tested in patients with recurrent/resistant NB.

In summary, we have identified the mechanism by which NKT cells are attracted toward TAMs in tumor tissues. This mechanism could reflect a broader role of NKT cells in the regulation of inflammation and will need to be further investigated, not only in the context of tumor-associated inflammation, but also in chronic infectious and autoimmune diseases. The enabling NKT cell tumor localization and functional activity at the tumor site via pharmacological modulation or/and genetic engineering of NKT cells, as demonstrated herein, may lead to the development of effective and broadly applicable cancer immunotherapies.

Methods

Human specimens. 7 primary NB specimens were obtained from surgery of biopsy at diagnosis at Texas Childrens Cancer Center, Baylor College of Medicine. For FACS analysis, tissues were homogenized and digested with dispase II (Roche), collagenase (Sigma-Aldrich), and DNase I into single cell suspensions. The remaining tissues were embedded in OCT and maintained at –80°C. Cord blood was obtained from a cord blood bank at the MD Anderson Cancer Center.

Cell lines. CHLA-15, CHLA-255, CHLA-255/luc, LA-N-1, SK-N-BE(2), CHLA-90, and IMR32 NB cell lines were established and maintained as previously described (8, 25, 62). 293T cells were purchased from ATCC and maintained in IMDM plus 10% FBS (Hyclone) and 2 mM GlutaMAX-I (Gibco-BRL, Invitrogen).

Plasmids and retrovirus production. 2 SFG retroviral vectors, SFG.iCasp-9.2A.ΔCD34.2A.IL-15 and SFG.eGFP.FFluc, were constructed as previously described (44) and used to transduce NKT cells. To produce retroviral supernatants, 293T cells were cotransfected with 3 plasmids (Peg-Pam-e encoding for gag-pol, DRF encoding for the RDF114 viral envelope, and the retroviral construct) using the Genejuice transfection reagent (Merck KGaA), and viral supernatants were collected 48 and 72 hours later.

RNA isolation and real-time RT-PCR. Total RNA from cell pellets was isolated using TRIzol (Invitrogen). The RNA quality was assessed with gel electrophoresis prior to reverse transcription into cDNA using M-MLV reverse transcriptase with oligo dT priming (Invitrogen). qRT-PCR was performed with iQ Sybr green supermix assay using the iCycler iQ multicolor real-time PCR detection system (Bio-Rad). Primers were ordered from Sigma (Supplemental Table 1). The relative change in gene expression was

calculated based on the ΔCt method using housekeeping gene lysosomal-associated transmembrane protein 5 (*LAPTM5*) as the control.

NKT cell expansion, culture, and transduction. NKT cell lines were expanded from PBMCs of healthy volunteers as previously described (8), with modifications. Briefly, PBMCs were isolated by buffy coats by Ficoll-Hypaque gradient density centrifugation. NKT cells were purified by anti-iNKT microbeads (Miltenyi Biotec). The negative PBMC fraction was irradiated (150 Gy) and aliquoted. NKT cells were stimulated with an aliquot of autologous PBMCs pulsed with αGalCer (100 ng/ml; Funakoshi Co.). rhIL-2 (50 U/ml, BDP, NCI-Frederick) was added at the second day and then every other day. NKT cells were restimulated every 2 weeks with the remaining PBMC aliquots. The phenotype and purity of NKT cells were assessed using mAbs for CD3, Vα24-Jα18 (6B11), and CD4. Proliferating NKT cells were transduced with retroviral supernatants on day 5 after restimulation in non–culture-treated 24-well plates precoated with recombinant fibronectin fragment (FN CH-296; Retronectin, Takara Shuzo). The rate of NKT cell transduction was measured by FACS with anti-CD34–PE mAb. The transduced NKT cells then continued expansion in the presence of rhIL-2.

Expanded NKT cells (7 days after restimulation) were cultured under normoxic (20% O_2) or hypoxic (1% O_2 in a Hearcell 240i tri-gas incubator; Thermo Scientific) conditions for 24 or 48 hours in the absence or presence of one of the following cytokines: rhIL-2 (NIH), IL-15, IL-4, IL-7 (10 ng/ml each; Peprotech), or IL-21 (eBiosciences) at 200 U/ml each. The absolute number of viable cells was quantified using the trypan blue exclusion method.

Monocyte isolation and coculture experiments. PBMCs were isolated by gradient centrifugation from buffy coats purchased from Gulf Cost Regional Blood Center. Monocytes were isolated by negative selection using Monocyte Isolation kit II (Miltenyi Biotec) according to the manufacturer's instructions. In coculture experiments, monocytes were added directly to NB cells or to the inserts separated by 0.4 μm membrane (Costar Corning) from NB cells. Where indicated, NB cells were preincubated with anti-human TNF-α neutralizing antibody (clone 1825; R&D Systems) or isotype control IgG1 (clone 11711; R&D Systems) for 1 hour before coculture with monocytes. We then cultured cells under hypoxic (1% O_2) or normoxic (20% O_2) conditions and collected supernatants at the indicated time points.

Multiplex cytokine quantification assay and ELISA. Cytokines released by NKT cells were assessed by CBAPlex beads (BD Biosciences) on FACS-Array analyzer according to the manufacture's manual and as previously described (8). CCL20 level in the coculture supernatants was determined using human CCL20/MIP-3 alpha Quantikine ELISA Kit (R&D Systems).

In vitro migration assay. NKT cell in vitro migration was assessed using permeable Transwell inserts (5 μm; Corning Costar). Where indicated, supernatants from monocyte and NB cells in bottom chambers were preincubated with isotype control (clone 11711) or neutralizing antibody against CCL20 (clone 67310) or CCL2 (clone 24822) (R&D Systems) for 1 hour before adding NKT cells in the upper chambers. Quantitative analysis of NKT cell migration was performed by FACS, as previous described (25).

Flow cytometry (FACS). To analyze the expression of CCL20 in monocytes, cells were first incubated with GolgiStop (BD Biosciences) for 4 hours and then stained with the following surface markers: CD56-APC, CD14-APC.Cy7, CD33-PE.Cy7, and CD45-PerCP (BD Biosciences). Cells were then fixed and permebalized with a Perm/Fix Kit (BD Biosciences) and intracellularly stained with CCL20-PE (BD Biosciences). To determine the level of CCR6 expression on NKT cells, cells were surface stained with CD3-APC, 6B11-FITC, CD4-PE.Cy7, and CCR6-PE (BD Biosciences).

To monitor the development of human hematopoiesis in hu-NSG mice, the following set of antibodies was used: anti-human CD45-FITC, anti-mouse CD45-PerCP, CD14-PE, CD33-PE.Cy7, CD3-APC (BD Biosciences), and CD20-APC.Cy7 (Biolegend). The antibody set CD45-PerCP, CD3-APC, and CD34-PE (BD Biosciences) was used to assess purity of the human $CD34^+$ stem cells. The antibodies CD45-PerCP, CD3-APC, 6B11-FITC, CD14-APC.Cy7, HLADR-PE.Cy7, and CD1d-PE (all BD Biosciences) were used to identify tumor-infiltrating leukocytes in human primary NB tumor and tumor xenografts from hu-NSG mice. Additionally, primary NBs were analyzed for NB surface marker expression using the antibodies CD45-PerCP, CD56-APC (BD Biosciences), and TNF-α–FITC (clone 6401; R&D Systems).

To determine NKT cell proliferation, cells were first labeled with CFSE (Invitrogen) and then restimulated by anti-TCR agonistic mAb (6B11 or OKT3) followed by a 5-day culture with or without NB cells under hypoxic or normoxic conditions. Cells were then surface stained with 6B11-PE and CD3-APC mAbs and analyzed by flow cytometry to determine CFSE dilution in $CD3^+6B11^+$ cells.

The expression levels of IκBα and phosphorylated NF-κB p65 were determined by FACS in monocytes according to the manufacturer's protocols (BD PhosFlow). Briefly, $1–2 \times 10^6$ ml^{-1} monocytes were cultured with or without CHLA-255 NB cell line (~70%–80% confluence) in the presence of neutralizing anti–TNF-α or suitable isotype control for the indicated times. After incubation, cells were fixed immediately by adding an equal volume of prewarmed to 37C BD PhosFlow Cytofix fixation buffer; plates were incubated for an additional 10 minutes at 37°C, and then the cells were harvested. For permeabilization, BD Phosflow Perm Buffer IV, precooled at –20°C, was added drop by drop to the cell pellet and incubated for an additional 15–20 minutes at room temperature. The tubes were stored at –20°C until stained with Alexa Fluor 488 phosphospecific anti–NF-κB p65 mAb (or PE-labeled IκBα) and PE- or APC-labeled anti-CD56 mAb to identify NBs and monocytes in coculture. Analysis was performed on a LSR-II 4-laser flow cytometer (BD Biosciences) using BD FACDiva software version 6.0 and FlowJo 7.2.5 (Tree Star Inc.).

4-color immunofluorescent microscopy. Mouse livers were removed and cut into workable sizes. The tissues were then frozen in OCT and kept at –80°C until use. 10-μm frozen sections were made using Cryostat (HM550; Thermo Scientific) and immediately fixed in 4% paraformaldehyde for 1 hour at room temperature. The fixed sections were treated twice with 0.1% sodium borohydrite for 5 minutes and then rinsed 3 times in PBS containing 0.013% sodium azide and 0.004% thimerosal. Slides were blocked with 5% normal mouse serum plus 1.5% BSA and 0.3% skim milk in ttPBS (PBS containing 0.3% Tween 20, 0.013% azide, and 0.004% thimerosal) for 1 hour at room temperature. After blocking, tissue sections were incubated with mouse anti-human CD11b (Mac-1) antibody (PN IM0190; Beckman Coulter) diluted at 1:400 in ttPBS supplemented with 1.5% BSA at 4°C overnight. The tissue sections were then washed twice with ttPBS and once with 1× PBS, 15 minutes each time. The fluorescent Alexa Fluor 647–conjugated goat anti-mouse secondary antibody (A31517, 1:800; Invitrogen) was incubated with the sections for 1 hour at room temperature and rinsed 3 times as described above. The slides were refixed in 4% paraformaldehyde for 25 minutes and blocked again for 1 hour at room temperature before proceeding to the next step. The above-stained slides were incubated with Cy3-conjugated anti-EF5 antibody (ELK-351; Hypoxia-Imaging, Department of Radiation Oncology, University of Pennsylvania) overnight at 4°C, followed by 2 rinses in ttPBS and 1 rinse in 1× PBS, 45 minutes each time. The slides were then counterstained with ProLong Gold antifade reagent (P36930; Invitrogen) and coverslipped. The 4-color fluorescent images of the stained sections were acquired on a Nikon A1-Rs inverted Laser Scanning (Confocal) Microscope. For the quantification of CFSE-labeled NKT cells and Alexa Fluor–labeled CD11b cells in either normoxic or hypoxic regions, all the images were captured using the same setting, i.e., at the same PMT HV for each channel. The images were analyzed by Annotation and Measurement feature of the NIS Elements AR3.2 software. In each imaged region, the expression of EF5 was quantified as the intensity of Cy3

(shown as red), and the absolute numbers of NKT cells (shown as green) and the CD11b$^+$ cells (shown as purple) were counted. The regions for which the mean intensity of Cy3 was lower than 200 were defined as normoxia, whereas those areas for which the mean intensity of Cy3 was at least 2-fold higher were defined as hypoxia. 10 images from either normoxic or hypoxic regions were compared.

In vivo experiments. NOD/SCID/IL-2Rγ–null (NSG) mice were bred in the Texas Children's Hospital animal facility. 4-week-old mice were irradiated with 225 cGy and injected with human cord blood–derived CD34$^+$ stem cells, as previously described (26, 27), to generate hu-NSG mice. The frequency of CD34$^+$ cells was >95%, and the contamination by CD3$^+$ cells was <0.1% in the stem cell transplants. 3 months after SCT, reconstitution of human hematopoiesis was confirmed in peripheral blood by FACS, and mice were i.v. injected with human CHLA-255/luc cells, either under the renal capsule (localization experiments), as previously described (63), or i.v. (therapeutic experiments). Tumor growth was indirectly assessed by weekly bioluminescent imaging (Small Animal Imaging Core facility, Texas Children's Hospital). Where indicated, mice were injected i.p. with 100 μg/mouse of neutralizing anti-CCL2 (clone 24822), anti-CCL20 (clone 67310), both, or isotype control (clone 11711) mAb (R&D Systems). Some animals received i.v. injections of ex vivo–expanded human NKT cells (1–5 × 10^7 cells). Before injection into animals, NKT cells had been cultured with IL-2 (50 U/ml; Peprotech) for 7–10 days without TCR stimulation to achieve resting phase, when their trafficking pattern more closely resembled that of primary NKT cells, as we determined previously (8). When indicated, mice received i.p. injection of anti-hCD1d blocking mAb, 42.1 or isotype control (50 μg/ml; BD Biosciences). Mice were euthanized, and cell suspensions prepared from tumors were analyzed by multicolor flow cytometry as described in *Flow cytometry (FACS)*. When indicated, NKT cell antitumor efficacy was determined by bioluminescent imaging. To determine NKT cell distribution in normoxic versus hypoxic tumor tissues, NKT cells were labeled with CellTrace CFSE cell proliferation kit according to the manufacturer's protocol (Invitrogen) before injection. For labeling hypoxic tissues, mice were i.v. injected with 250 μl EF5 (100 mM solution, produced at NCI at no cost and provided by C.J. Koch, University of Pennsylvania, Philadelphia, Pennsylvania, USA). After 3 hours, mice were euthanized, and parts of their tumors were excised and immediately embedded in OCT medium to be used for immunofluorescent staining of EF5, NKT, and TAMs.

Statistics. Statistical analysis was performed using GraphPad Prism 5.0 software (GraphPad). Comparisons between groups were based on 1- or 2-way ANOVA, depending on whether 1 (e.g., CCL20 concentration) or 2 (e.g., CCL20 concentration in normoxic and hypoxic conditions) independent variables were measured. We also used the Bonferroni post-test to compare selected experimental groups according to the experimental design. All statistical tests were 2-sided, and a P value less than 0.05 was considered statistically significant.

Study approval. Primary NBs specimens were used in accordance with Baylor College of Medicine IRB-approved protocols H-26691 and H-6650. Cord blood was used in accordance with MD Anderson Cancer Center IRB-approved protocol H-20911. Informed consent was obtained in accordance with institutional review board policies and procedures for research dealing with human specimens. Animal experiments were performed according to IACUC-approved protocols at Baylor College of Medicine.

Acknowledgments

We thank Malcolm Brenner (Center for Cell and Gene Therapy, BCM, Houston, Texas, USA) for helpful discussions and James Broughman (Integrated Microscopy Core, Department of Molecular and Cellular Biology, BCM, Houston, Texas, USA) for excellent technical assistance. This work was supported by NIH grants (2RO1 CA116548 to L.S. Metelitsa; R01 CA142636 to G. Dotti), U.S. Department of Defense (W81XWH-10-10425 to G. Dotti), Cancer Prevention and Research Institute of Texas grants (RP1 100528 and RP1 110129 to L.S. Metelitsa), and The Caroline Wiess Law Scholar Award (to L.S. Metelitsa).

Received for publication June 17, 2011, and accepted in revised form March 21, 2012.

Address correspondence to: Leonid S. Metelitsa, Department of Pediatrics, Baylor College of Medicine, 1102 Bates Ave., C.1760.06, Houston, Texas 77030, USA. Phone: 832.824.4395; Fax: 832.825.4846; E-mail: lsmeteli@txch.org.

1. Kronenberg M, Gapin L. The unconventional lifestyle of NKT cells. *Nat Rev Immunol*. 2002;2(8):557–568.
2. Swann J, Crowe NY, Hayakawa Y, Godfrey DI, Smyth MJ. Regulation of antitumour immunity by CD1d-restricted NKT cells. *Immunol Cell Biol*. 2004; 82(3):323–331.
3. Swann JB, Coquet JM, Smyth MJ, Godfrey DI. CD1-restricted T cells and tumor immunity. *Curr Top Microbiol Immunol*. 2007;314:293–323.
4. Berzofsky JA, Terabe M. The contrasting roles of NKT cells in tumor immunity. *Curr Mol Med*. 2009; 9(6):667–672.
5. Yanagisawa K, Seino K, Ishikawa Y, Nozue M, Todoroki T, Fukao K. Impaired proliferative response of V alpha 24 NKT cells from cancer patients against alpha-galactosylceramide. *J Immunol*. 2002; 168(12):6494–6499.
6. Tahir SM, et al. Loss of IFN-gamma production by invariant NK T cells in advanced cancer. *J Immunol*. 2001;167(7):4046–4050.
7. Dhodapkar MV, et al. A reversible defect in natural killer T cell function characterizes the progression of premalignant to malignant multiple myeloma. *J Exp Med*. 2003;197(12):1667–1676.
8. Metelitsa LS, et al. Natural killer T cells infiltrate neuroblastomas expressing the chemokine CCL2. *J Exp Med*. 2004;199(9):1213–1221.
9. Tachibana T, et al. Increased intratumor Valpha24-positive natural killer T cells: a prognostic factor for primary colorectal carcinomas. *Clin Cancer Res*. 2005;11(20):7322–7327.
10. Molling JW, et al. Low levels of circulating invariant natural killer T cells predict poor clinical outcome in patients with head and neck squamous cell carcinoma. *J Clin Oncol*. 2007;25(7):862–868.
11. Metelitsa LS, et al. Human NKT cells mediate antitumor cytotoxicity directly by recognizing target cell CD1d with bound ligand or indirectly by producing IL-2 to activate NK cells. *J Immunol*. 2001; 167(6):3114–3122.
12. Song L, et al. Valpha24-invariant NKT cells mediate antitumor activity via killing of tumor-associated macrophages. *J Clin Invest*. 2009;119(6):1524–1536.
13. Mantovani A, Allavena P, Sica A, Balkwill F. Cancer-related inflammation. *Nature*. 2008; 454(7203):436–444.
14. Sica A, et al. Macrophage polarization in tumour progression. *Semin Cancer Biol*. 2008;18(5):349–355.
15. Sica A, Bronte V. Altered macrophage differentiation and immune dysfunction in tumor development. *J Clin Invest*. 2007;117(5):1155–1166.
16. De Santo C, et al. Invariant NKT cells reduce the immunosuppressive activity of influenza A virus-induced myeloid-derived suppressor cells in mice and humans. *J Clin Invest*. 2008;118(12):4036–4048.
17. De Santo C, et al. Invariant NKT cells modulate the suppressive activity of IL-10-secreting neutrophils differentiated with serum amyloid A. *Nat Immunol*. 2010;11(11):1039–1046.
18. O'Konek JJ, et al. Mouse and human iNKT cell agonist beta-mannosylceramide reveals a distinct mechanism of tumor immunity. *J Clin Invest*. 2011; 121(2):683–694.
19. Allavena P, Sica A, Solinas G, Porta C, Mantovani A. The inflammatory micro-environment in tumor progression: the role of tumor-associated macrophages. *Crit Rev Oncol Hematol*. 2008;66(1):1–9.
20. Mantovani A, Schioppa T, Porta C, Allavena P, Sica A. Role of tumor-associated macrophages in tumor progression and invasion. *Cancer Metastasis Rev*. 2006;25(3):315–322.
21. Grivennikov SI, Greten FR, Karin M. Immunity, inflammation, and cancer. *Cell*. 2010;140(6):883–899.
22. Kim CH, Johnston B, Butcher EC. Trafficking machinery of NKT cells: shared and differential chemokine receptor expression among Valpha24(+)Vbeta11(+) NKT cell subsets with distinct cytokine-producing capacity. *Blood*. 2002;100(1):11–16.
23. Kim CH, Butcher EC, Johnston B. Distinct subsets of human Valpha24-invariant NKT cells: cytokine responses and chemokine receptor expression. *Trends Immunol*. 2002;23(11):516–519.
24. Thomas SY, et al. CD1d-restricted NKT cells express a chemokine receptor profile indicative of Th1-type inflammatory homing cells. *J Immunol*. 2003;171(5):2571–2580.
25. Song L, et al. Oncogene MYCN regulates localiza-

tion of NKT cells to the site of disease in neuroblastoma. *J Clin Invest*. 2007;117(9):2702–2712.
26. Yahata T, et al. Functional human T lymphocyte development from cord blood CD34+ cells in nonobese diabetic/Shi-scid, IL-2 receptor gamma null mice. *J Immunol*. 2002;169(1):204–209.
27. Giassi LJ, et al. Expanded CD34+ human umbilical cord blood cells generate multiple lymphohematopoietic lineages in NOD-scid IL2rgamma(null) mice. *Exp Biol Med (Maywood)*. 2008;233(8):997–1012.
28. Battaglia F, et al. Hypoxia transcriptionally induces macrophage-inflammatory protein-3alpha/CCL-20 in primary human mononuclear phagocytes through nuclear factor (NF)-kappaB. *J Leukoc Biol*. 2008;83(3):648–662.
29. Goillot E, et al. Tumor necrosis factor as an autocrine growth factor for neuroblastoma. *Cancer Res*. 1992;52(11):3194–3200.
30. Seeger RC, Atkinson J, Reynolds CP. Neuroblastoma. In: Holland JF, Frei E III, Bast RC Jr, Kufe DW, Morton DL, Weichsenbaum RR, eds. *Cancer Medicine*. Philadelphia, Pennsylvania, USA: Lea and Febiger; 1996:2991–3020.
31. Facciabene A, et al. Tumour hypoxia promotes tolerance and angiogenesis via CCL28 and T(reg) cells. *Nature*. 2011;475(7355):226–230.
32. Roos D, Loos JA. Changes in the carbohydrate metabolism of mitogenically stimulated human peripheral lymphocytes. II. Relative importance of glycolysis and oxidative phosphorylation on phytohaemagglutinin stimulation. *Exp Cell Res*. 1973;77(1):127–135.
33. Krauss S, Brand MD, Buttgereit F. Signaling takes a breath--new quantitative perspectives on bioenergetics and signal transduction. *Immunity*. 2001; 15(4):497–502.
34. Frauwirth KA, et al. The CD28 signaling pathway regulates glucose metabolism. *Immunity*. 2002; 16(6):769–777.
35. Jones RG, Thompson CB. Revving the engine: signal transduction fuels T cell activation. *Immunity*. 2007;27(2):173–178.
36. Lappas CM, Day YJ, Marshall MA, Engelhard VH, Linden J. Adenosine A2A receptor activation reduces hepatic ischemia reperfusion injury by inhibiting CD1d-dependent NKT cell activation. *J Exp Med*. 2006;203(12):2639–2648.
37. Li L, et al. NKT cell activation mediates neutrophil IFN-gamma production and renal ischemia-reperfusion injury. *J Immunol*. 2007;178(9):5899–5911.
38. Wallace KL, et al. NKT cells mediate pulmonary inflammation and dysfunction in murine sickle cell disease through production of IFN-gamma and CXCR3 chemokines. *Blood*. 2009;114(3):667–676.
39. Wallace KL, Linden J. Adenosine A2A receptors induced on iNKT and NK cells reduce pulmonary inflammation and injury in mice with sickle cell disease. *Blood*. 2010;116(23):5010–5020.
40. Field JJ, Nathan DG, Linden J. Targeting iNKT cells for the treatment of sickle cell disease. *Clin Immunol*. 2011;140(2):177–183.
41. Baev DV, et al. Distinct homeostatic requirements of CD4+ and CD4- subsets of Valpha24-invariant natural killer T cells in humans. *Blood*. 2004; 104(13):4150–4156.
42. Matsuda JL, et al. Homeostasis of V alpha 14i NKT cells. *Nat Immunol*. 2002;3(10):966–974.
43. Gordy LE, et al. IL-15 regulates homeostasis and terminal maturation of NKT cells. *J Immunol*. 2011; 187(12):6335–6345.
44. Hsu C, et al. Cytokine-independent growth and clonal expansion of a primary human CD8+ T-cell clone following retroviral transduction with the IL-15 gene. *Blood*. 2007;109(12):5168–5177.
45. Pikarsky E, et al. NF-kappaB functions as a tumour promoter in inflammation-associated cancer. *Nature*. 2004;431(7007):461–466.
46. Greten FR, et al. IKKbeta links inflammation and tumorigenesis in a mouse model of colitis-associated cancer. *Cell*. 2004;118(3):285–296.
47. Szlosarek P, Charles KA, Balkwill FR. Tumour necrosis factor-alpha as a tumour promoter. *Eur J Cancer*. 2006;42(6):745–750.
48. Affara NI, Coussens LM. IKKalpha at the crossroads of inflammation and metastasis. *Cell*. 2007; 129(1):25–26.
49. Maris JM, Hogarty MD, Bagatell R, Cohn SL. Neuroblastoma. *Lancet*. 2007;369(9579):2106–2120.
50. Szlosarek PW, Balkwill FR. Tumour necrosis factor alpha: a potential target for the therapy of solid tumours. *Lancet Oncol*. 2003;4(9):565–573.
51. Brown ER, et al. A clinical study assessing the tolerability and biological effects of infliximab, a TNF-alpha inhibitor, in patients with advanced cancer. *Ann Oncol*. 2008;19(7):1340–1346.
52. Friedberg J, et al. Targeting the follicular lymphoma microenvironment through blockade of TNFalpha with etanercept. *Leuk Lymphoma*. 2008; 49(5):902–909.
53. Pietras A, et al. HIF-2alpha maintains an undifferentiated state in neural crest-like human neuroblastoma tumor-initiating cells. *Proc Natl Acad Sci U S A*. 2009;106(39):16805–16810.
54. Crowe NY, et al. Differential antitumor immunity mediated by NKT cell subsets in vivo. *J Exp Med*. 2005;202(9):1279–1288.
55. Waldmann TA. The biology of interleukin-2 and interleukin-15: implications for cancer therapy and vaccine design. *Nat Rev Immunol*. 2006;6(8):595–601.
56. Wuest TY, Willette-Brown J, Durum SK, Hurwitz AA. The influence of IL-2 family cytokines on activation and function of naturally occurring regulatory T cells. *J Leukoc Biol*. 2008;84(4):973–980.
57. La Cava A, Van Kaer L, Fu DS. CD4+CD25+ Tregs and NKT cells: regulators regulating regulators. *Trends Immunol*. 2006;27(7):322–327.
58. Straathof KC, et al. An inducible caspase 9 safety switch for T-cell therapy. *Blood*. 2005;105(11):4247–4254.
59. Tey SK, Dotti G, Rooney CM, Heslop HE, Brenner MK. Inducible caspase 9 suicide gene to improve the safety of allodepleted T cells after haploidentical stem cell transplantation. *Biol Blood Marrow Transplant*. 2007;13(8):913–924.
60. Quintarelli C, et al. Co-expression of cytokine and suicide genes to enhance the activity and safety of tumor-specific cytotoxic T lymphocytes. *Blood*. 2007;110(8):2793–2802.
61. Di Stasi A, et al. Inducible apoptosis as a safety switch for adoptive cell therapy. *N Engl J Med*. 2011; 365(18):1673–1683.
62. Reynolds CP, et al. Biological classification of cell lines derived from human extra-cranial neural tumors. *Prog Clin Biol Res*. 1988;271:291–306.
63. Kim ES, et al. Potent VEGF blockade causes regression of coopted vessels in a model of neuroblastoma. *Proc Natl Acad Sci U S A*. 2002;99(17):11399–11404.